



LUND UNIVERSITY

Probabilistic analysis of fire exposed steel structures

Magnusson, Sven Erik

1974

[Link to publication](#)

Citation for published version (APA):

Magnusson, S. E. (1974). *Probabilistic analysis of fire exposed steel structures*. (Bulletines of Division of Structural Mechanics and Concrete Construction, Bulletin 27; Vol. Bulletin 27). Lund Institute of Technology.

Total number of authors:

1

General rights

Unless other specific re-use rights are stated the following general rights apply:

Copyright and moral rights for the publications made accessible in the public portal are retained by the authors and/or other copyright owners and it is a condition of accessing publications that users recognise and abide by the legal requirements associated with these rights.

- Users may download and print one copy of any publication from the public portal for the purpose of private study or research.
- You may not further distribute the material or use it for any profit-making activity or commercial gain
- You may freely distribute the URL identifying the publication in the public portal

Read more about Creative commons licenses: <https://creativecommons.org/licenses/>

Take down policy

If you believe that this document breaches copyright please contact us providing details, and we will remove access to the work immediately and investigate your claim.

LUND UNIVERSITY

PO Box 117
221 00 Lund
+46 46-222 00 00

LUND INSTITUTE OF TECHNOLOGY · LUND · SWEDEN · 1974
DIVISION OF STRUCTURAL MECHANICS AND CONCRETE CONSTRUCTION · BULLETIN 27

SVEN ERIK MAGNUSSON

PROBABILISTIC ANALYSIS OF FIRE EXPOSED
STEEL STRUCTURES

LUND INSTITUTE OF TECHNOLOGY, LUND, SWEDEN 1974
DIVISION OF STRUCTURAL MECHANICS AND CONCRETE CONSTRUCTION

PROBABILISTIC ANALYSIS OF FIRE EXPOSED STEEL STRUCTURES

Sven-Erik Magnusson

LUND, NOV 1974

Acknowledgements

It is a pleasure to recall and publicly acknowledge a large number of stimulating and valuable discussions on the topic of this paper with the Head of the Department, Ove Pettersson. The author is indebted to all those colleagues and friends at The Division of Structural Mechanics and Concrete Construction and The Department of Structural Engineering who read the manuscript and made useful suggestions. In particular, I express my appreciation to Sture Åkerlund, who during the preparatory stages of this investigation kindly and patiently answered a lot of questions. I also wish to thank Bertil Fredlund for his help with the statistical evaluation of test results. To Margareta Persson, Lisbeth Henning, Eivor Nilsson and Ann Schollin I extend my warm thanks for their skill, efficiency and general helpfulness in transforming a bundle of disorganized notes into a ready publication.

The project has been financially sponsored by the National Swedish Council for Building Research (Statens Råd för Byggnadsforskning), and to this body I tender my cordial thanks.

Contents

Introduction

1. A structural fire design, based on the ventilation controlled natural fire process
 - 1.1 General background
 - 1.2 Temperature-time curve of fire process
 - 1.3 Maximum steel temperature
 - 1.4 Definition of limit state for fire-exposed steel beam
 - 1.5 Nominal loads and load factors in the differentiated design procedure
 - 1.5.1 Design fire load density
 - 1.5.2 Nominal values and load factors for dead and live load

2. Structural safety and probabilistic methods in general
 - 2.1 Calculation of probability of failure
 - 2.2 Safety margin R-S
 - 2.3 Safety factor R/S
 - 2.4 Outline of some probabilistic safety systems
 - 2.4.1 Classification of design formats
 - 2.4.2 Risk-based versus safety index-based design
 - 2.4.3 Formulation of design criteria in safety index formats
 - 2.4.4 Order of central moment employed
 - 2.4.5 Truncation of Taylor series expansion
 - 2.4.6 Analysis of uncertainty
 - 2.4.6.1 Resistance R
 - 2.4.6.2 Load induced effect S
 - 2.4.7 Evaluation of safety factors and load factors

3. Evaluation of uncertainty measures in the fire engineering design
 - 3.1 Uncertainty in fire load density statistics
 - 3.2 Variability of maximum steel temperature T_{\max}
 - 3.2.1 ΔT_1
 - 3.2.2 ΔT_2
 - 3.2.3 ΔT_3
 - 3.2.4 Equivalence between column and beam temperatures.
Choice of representative beam temperature

- 3.3 Uncertainty in load-carrying capacity φ
 - 3.3.1 Error term $\Delta\varphi_1$
 - 3.3.2 Error term $\Delta\varphi_2$
 - 3.3.3 Material variability term
- 3.4 Live and dead load characteristics
- 4. Numerical methods. Monte Carlo technique
 - 4.1 Basic numerical methods
 - 4.2 Monte Carlo technique
 - 4.2.1 Foundations
 - 4.2.2 Simulation procedure
 - 4.3 Results of Monte Carlo simulations
 - 4.3.1 Variation of β_C and β_{ER} with κ , $A\sqrt{h}/A_t$ and D_n/L_n
 - 4.3.2 Variation of β_C with uncertainty in fire load statistics Δq and uncertainty in insulation parameter κ
 - 4.3.3 Relevance of distribution-free design formats
 - 4.4 Confidence bounds of simulation statistics
- 5. Method of linear approximation
 - 5.1 Derivation of means and variances of R and S
 - 5.2 Analysis of system and component variance
- 6. Safety indices inherent in different design procedures
 - 6.1 Safety index β_C inherent in the differentiated design procedure
 - 6.2 Safety index β_C inherent in the standard design procedure
- 7. Evaluation of load factors in the differentiated design procedure
 - 7.1 Use of linearization function α
 - 7.2 Use of mathematical programming methods
- 8. Concluding remarks
 - 8.1 Validity of derived safety measures. Further studies
 - 8.2 Use of temperature criteria
 - 8.3 Consistent structural design
 - 8.3.1 Gross errors
 - 8.3.2 Passive and active fire protection

Summary

Tables

Notation

References

Probabilistic Analysis of Fire Exposed Steel Structures

Introduction

This paper may be seen as a completely revised sequence to earlier reports /1/, /2/.

An overall fire-safety analysis of a building or a number of buildings can be described in a very general way as a two-step procedure. First of all, the optimum level of fire protection must be determined in relation to the total resources allocated for the erection and maintenance of the building and its functions. The second step involves distributing the investment reserved for fire protective measures in such a way that both cost-effectiveness as well as the minimum public safety requirements are achieved.

The abovementioned multi-levelled socio-economic optimization can only succeed by the employment of a performance evaluation, which investigates the reliability of the different system components such as escape routes, control of smoke production and smoke movement, detection and extinguishing devices, integrity of the structural elements when exposed to fire. Comprehensive reviews of the present state-of-art of the overall fire-safety can be found in /3/ and /4/.

This paper will deal exclusively with the last component reliability, an assessment of the probability that a structural member will attain a certain limit state when under the influence of a fully developed fire. The problem is of varying importance depending on the type of building considered; for a majority of buildings an identification or rather, rational estimate, of the risk of structural collapse due to fire would mean a significant step towards the possibility of more consistent safety level decisions.

The value of a reliability analysis of fire exposed structures is emphasized by statistical investigations /4/. For the about 2000 buildings more or less seriously damaged in the Netherlands in 1967 the causes of damage were as follows:
in 20 cases a total or partial collapse was caused by local overloading;

in 50 cases total or partial collapses were caused by material defects and/or faulty design;
in 50 cases collisions occurred, where some moving vehicle or falling body struck a building and caused impact damage with more or less serious results;
in 200 cases explosions either inside or outside buildings caused structural damage;
in 200 cases wind loads caused severe structural damage.
in c:a 1500 cases exposure to accidental fire. (Of about 15000 fires, flash-over in at least one room occurred roughly in one case out of ten).

The last figure indicates the number of exceptional loadings due to fire in one country during one year. The economic consequences of these extreme loading situations must be put in relation to the costs of the fire-protective measures, which for an ordinary Swedish office steel building are in the range 20 - 30 per cent of the cost for the structural steel. Against this background, we are forced to acknowledge that until now we have had no possibility of determining the degree of unconservative or over-conservative design inherent in present building fire regulations. Moreover, we are faced with an unbalance in the present design procedure. Load-bearing structures are designed according to two separate functional demands, "normal" function (gravity loads, wind loading, earthquake loading, etc) and "fire resistance" function. This is done according to different building codes and quite different demands for accuracy. It must be recognized that the "out of service" probability for a building under non-fire conditions usually is unknown. Nevertheless, the safety margins are produced by a rational design based on scientific principles. For a fire exposed structure, on the other hand, the design has historically been added as an afterthought and in such a standardized manner that the relevance to the structural behaviour under real fire condition often has been questionable.

During the last decade, the understanding, both theoretical and experimental, of the fire process and its influence on building components has developed to a degree that the basis for a qualified structural fire engineering design exists. The perhaps most consistent and far-reaching application of this new research development can be found in a manual for the design of fire-exposed

steel structures that is to be published during autumn 1974 by the Swedish Institute of Steel Construction /5/. The purpose of the manual is to make possible the full use of the alternative design procedures offered by the Swedish Building Code. This code, written in 1967, explicitly permits as an alternative a fire structural design based, not on conventional classification requirements measured as endurance time in the standard fire test, but on a systematic theoretical approach.

The appearance of this manual brings into focus the problem of the reliability of fire-exposed building components. Examples of important, even critical, issues in this area are

- What are the safety levels in existing structures?
- How will these safety levels be affected by using the new differentiated design procedure, based on the effect of the natural fire process?
- The design values in /5/ of different types of loading, e.g. fire load density, live and dead load, had to be chosen on the combined basis of subjective judgement and the rather few statistical facts available. Are these values of nominal loads and load factors "optimal" or "consistent" (in a way to be defined later)? If not, can the modern theories of probabilistic analysis of structural safety be used to give us a more systematic choice of these parameters?

This paper is a first attempt of making a rational specification and assessment of the reliability of fire-exposed steel structures. Incomplete knowledge of the physical processes involved and lack of statistical data imply that all computed quantitative measures of structural safety are themselves to be considered as random variables. While there are methods (e.g. Bayesian statistics) to deal with this kind of uncertainty, it is important in this pilot study to minimize both the complexity of the problem and the variance of the structural safety parameters. The structure of the method presented for a systematized safety analysis is quite general and may be applied to a wide class of building components. In this paper, the approach will be exemplified for one kind of

structural element and building occupancy, a simply supported steel beam in office buildings. This is the case, where our information for the moment seems most complete, and which, with respect to the factors mentioned above, seems suitable for a first investigation.

The first part of the paper will summarize the development of the deterministic design model used in the manual /5/. Although the progress in the fire research area has been reported elsewhere, it is probably safe to assume that much of it is far from common knowledge among architects and structural engineers. For this reason a brief survey of the most relevant facts seems appropriate. Comprehensibility will be stressed, meaning that only facts relevant to the subsequent structural safety analysis will be included. A more extensive survey is given in /28/, where also further references can be found. It will be shown how the design procedure forms the framework, within which an application of the Monte Carlo method can be introduced to give a probabilistic analysis of structural fire safety. The results will be compared with those of an approximate, first order uncertainty analysis. Safety measures (safety indices) for the traditional and the new design method will be identified and appropriate load factors to use in the latter procedure derived. A first attempt will be made to decompose the system uncertainty or variance into a sum of clearly identified component variances, thus opening the way for a procedure to optimize the structural failure avoidance.

1. A Structural Fire Design, Based on the Ventilation Controlled Natural Fire Process

1.1 General Background

Traditionally, and mainly due to building code requirements, design of structural components exposed to fire has not been integrated in the ordinary structural analysis procedure. To make possible a more competent and efficient design, a reassessment of existing methods of predicting the behaviour of fire-exposed structural members is at this time being made in several countries. The reconsideration applies to the whole domain of structural fire engineering design, i.e. both to the process of fire development and to the fire behaviour of the structure.

A great many experimental fires, carefully executed, have demonstrated that a rational prediction of the fire resistance of a structural element only can be done by taking into consideration factors, hitherto not represented in the conventional design procedures of most countries. Fundamentally important in this design is the correct determination of the temperature-time curve of the fully-developed fire. The standard temperature-time curve used in most countries at best covers only a limited range of possible conditions regarding the detail characteristics of the fire load, the ventilation of the fire compartment and the thermal properties of the surrounding structures of this compartment. No account is taken of the fact that the cooling down period of the fire must be included. Examples of the deficiency of the standard curve are given by Figure 1.1a /6/. The full line curves are experimental with the fire load density given as MJ/m^2 of total surrounding surfaces of the fire compartment A_t (= sum of walls, floor and ceiling) and the ventilation opening given by the quantity $A\sqrt{h}/A_t$, where A denotes the opening area (windows and doors) in m^2 and h is an averaged value of the height in m of these openings. The dotted curve is the ISO standard curve for the furnace temperature. As a consequence of the inadvertency illustrated by Figure 1.1a, it is now being generally accepted that only the complete temperature-time curve of the actual fire can serve as a basis for an accurate analysis of the fire severity.

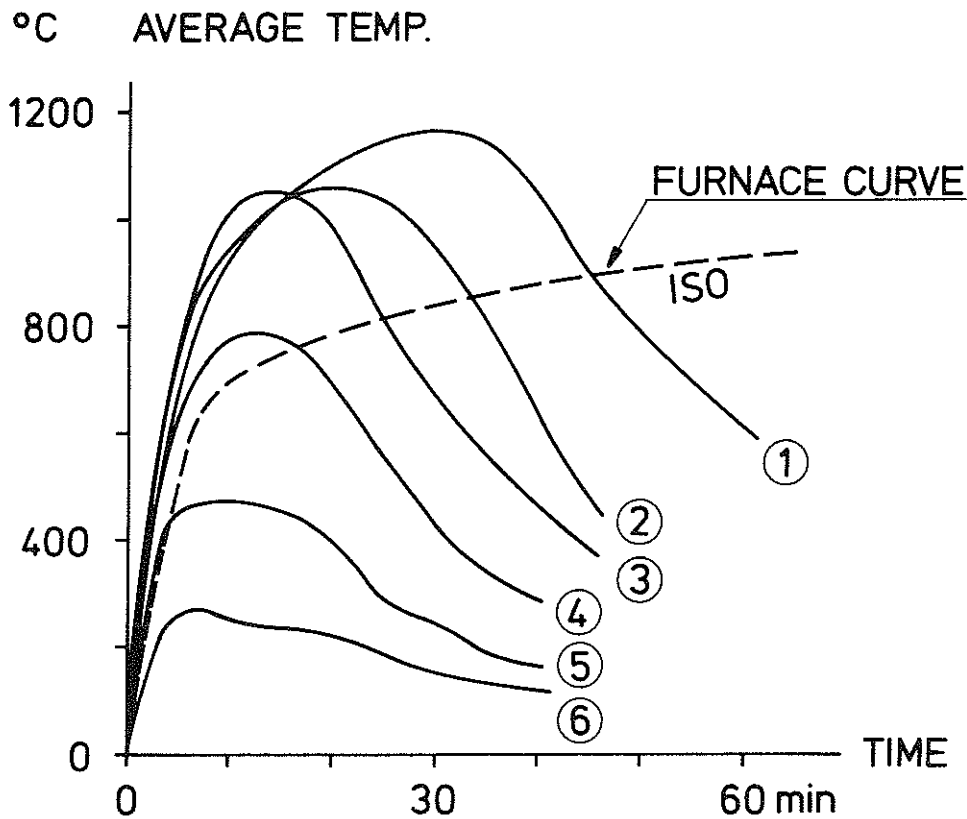


Figure 1.1a Comparison of standard test furnace curve and natural fire processes /6/ with different values of q and $A\sqrt{h}/A_t$ /6/.

Curve No. 1	$q = 251 \text{ MJ/m}^2$	$A\sqrt{h}/A_t = 0.06 \text{ m}^{1/2}$
Curve No. 2	$q = 251 \text{ MJ/m}^2$	$A\sqrt{h}/A_t = 0.12 \text{ m}^{1/2}$
Curve No. 3	$q = 126 \text{ MJ/m}^2$	$A\sqrt{h}/A_t = 0.06 \text{ m}^{1/2}$
Curve No. 4	$q = 126 \text{ MJ/m}^2$	$A\sqrt{h}/A_t = 0.12 \text{ m}^{1/2}$
Curve No. 5	$q = 63 \text{ MJ/m}^2$	$A\sqrt{h}/A_t = 0.12 \text{ m}^{1/2}$
Curve No. 6	$q = 31 \text{ MJ/m}^2$	$A\sqrt{h}/A_t = 0.12 \text{ m}^{1/2}$

Several design methods have been presented to meet this requirement. Broadly, they can be grouped in two categories. In the first, varying characteristics of the natural fire process such as amount of combustible material, available air supply, are accounted for by translating the natural fire severity into an equivalent time of exposure to the standard fire endurance test. The second, alternative course is to base the fire structural design directly on the gastemperature-time curve of the individual fire process. The two approaches have been described and compared in /7/.

The probabilistic analysis of structural fire safety presented in this paper uses the second design method as starting point. When using this approach, the fire exposure is regarded as any other cause of exceptional loading. The procedure is based on the complete fire process, the decay period included. It is up to the designer to demonstrate that the structural component, under relevant load, survives a burn-out. Stipulated design fire load densities are given by the code. The combination of ventilation openings, thermal characteristics of the fire compartment and design fire load determines the design fire process. The verification of the load-bearing capacity can be made experimentally, if new and untested design features are involved, or analytically. Assumptions regarding the thermal characteristics, such as heat capacity, heat conductivity, creep, cracking, thermal elongation, shrinkage, etc., must be proved by material tests. Essential steps in the design are illustrated by Figure 1.1b /15/.

Contrasted to the traditional method, outlined in Figure 1.1c, a summary of the advantages are: a correspondencé with the actual physical processes taking place, capability of being systematically improved as knowledge increases and an ambition towards more performance-oriented design procedures.

The remaining parts of chapter 1 will provide the background material for the design curves of the manual /5/ and serve as an introduction to the deterministic basis of the subsequent safety analysis.

1.2 Temperature-Time Curve of Fire Process

The whole design procedure is based on the possibility of computing the gastemperature-time curve of the fire process with a degree of precision sufficient for structural design purposes. Therefore, the way of solving this unwieldy problem will be accounted for in some detail. There are three main parameters governing the behaviour of the natural compartment fire: Amount of combustible material, the fire exposure geometry, mainly porosity and specific surface area, of this material and the size of the ventilation openings. The interaction between these variables can somewhat

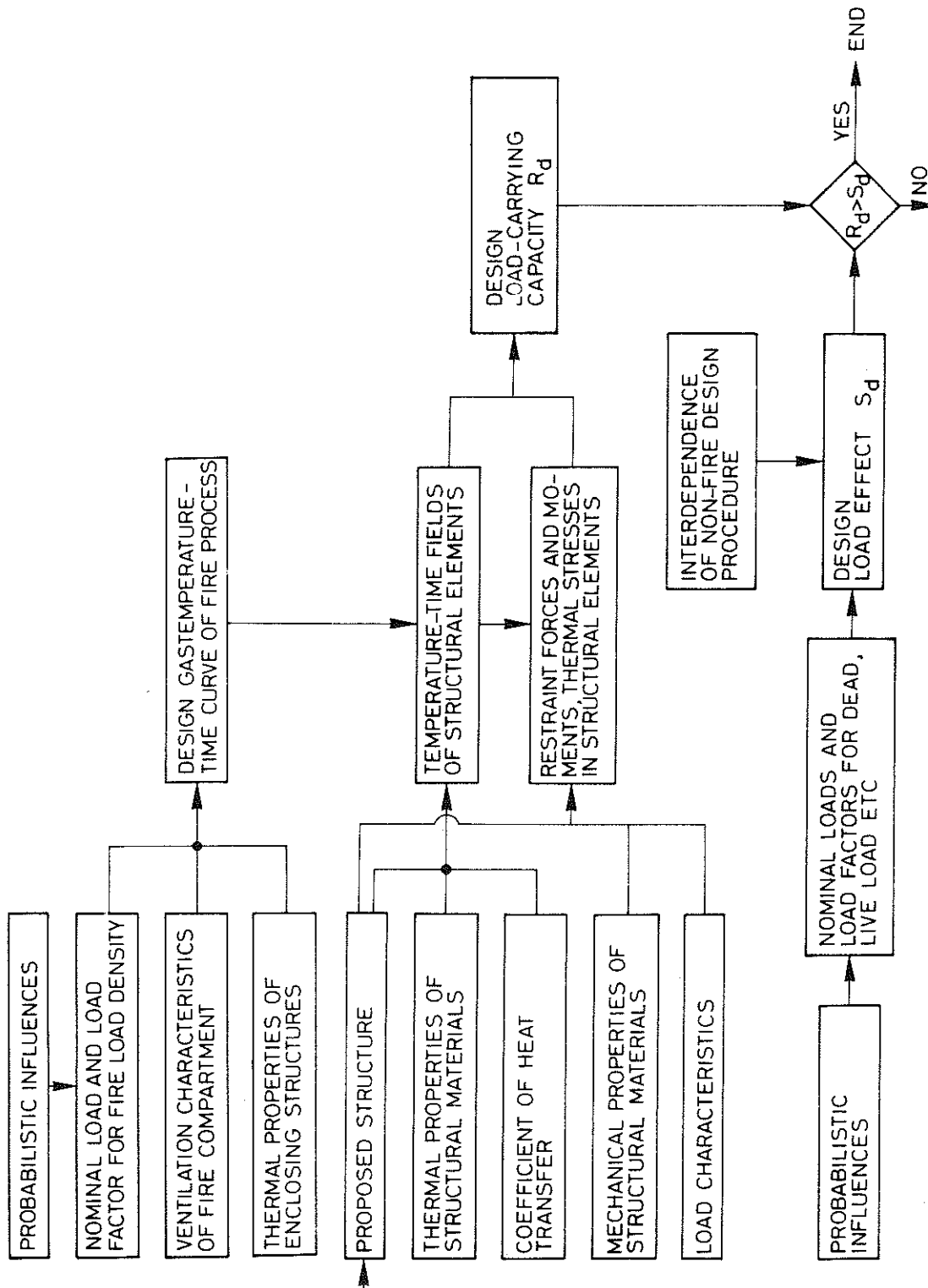


Figure 1.1b Flow diagram of design procedure used in /5/.

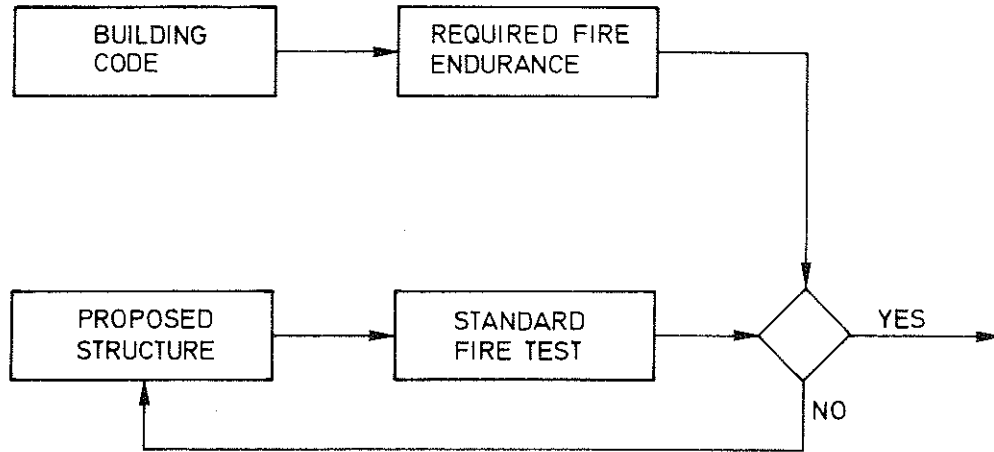


Figure 1.1c Flow diagram of standard design procedure.

simplified be described in the following way /8/, /9/, /10/, /11/, /38/. The air supplied by the ventilation openings can be shown to be proportional to the factor $AV\bar{h}$. This implies the existence of an upper bound for the rate of burning R , or more exact, rate of heat release I_C . For sufficiently small values of the ventilation factor $AV\bar{h}$ combined with high values of the fire load, or rather fire exposed surface area A_F of the fuel, very extensive test series have shown that the maximum rate of burning R_{\max} is approximately given by the formula

$$R_{\max} = kAV\bar{h} \text{ kg/min} \quad (1.2a)$$

irrespective of total quantity and surface area of fuel. For a fire process with wood as fuel, a representative value of k is $5 - 6 \text{ kg/min} \cdot \text{m}^{5/2}$. Approximately, the same value is obtained by a theoretical combustion analysis. The process is called "ventilation-controlled". For larger values of the ratio $AV\bar{h}/A_F$, where the available air supply is no longer the limiting factor, the rate of energy release will be determined by the specific inter-related fuel bed properties such as average thickness, particle size and porosity. In this "fuel bed controlled" regime, the maximum rate of energy release during a fire process can vary from almost zero up to the value given by Eq. 1.2a.

The theoretical analysis of natural fires are based on the following two energy conservation equations.

$$I_C = I_L + I_W + I_R \quad (1.2b)$$

$$\int_0^{\infty} I_C dt = M \cdot W \quad (1.2c)$$

Eq. 1.2b expresses the instantaneous energy balance. The meaning of the different terms, illustrated in Figure 1.2a, are

I_C = rate of heat release by combustion,

I_L = rate of heat loss by convection in the openings,

I_W = rate of heat loss through bounding walls, floor and ceiling,

I_R = rate of heat loss by radiation through the openings.

When expressions for all terms in the above equation are known it is possible to compute the temperature of the gases in the compartment. Equation 1.2c, where the product $M \cdot W$ stands for the original energy content of the fuel, states the energy equilibrium of the total fire process.

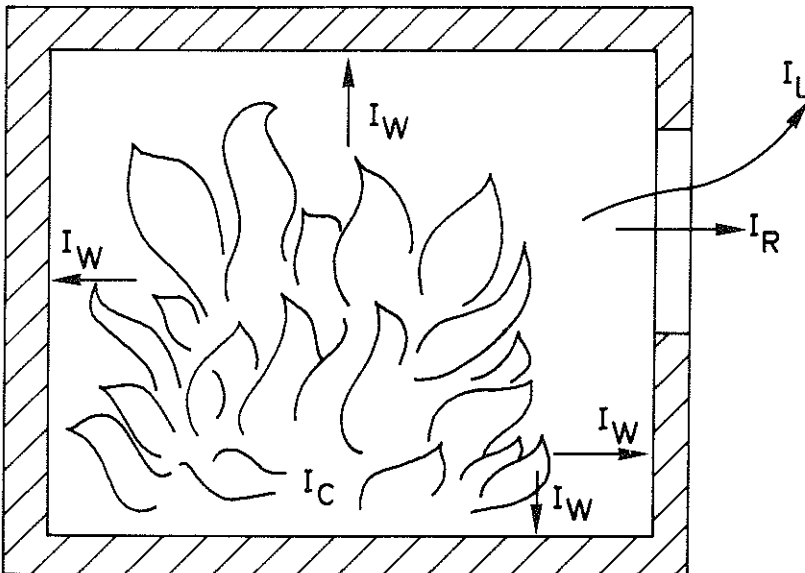


Figure 1.2a Illustration of the heat balance equation.

As noted, an advance knowledge of the $t-I_C$ curve for a fire process in the fuel bed controlled regime is as a rule not obtainable. The same is valid for the ignition and decay or cooling down periods of the ventilation controlled process.

An empirical way of obtaining the unknown parts of the $t-I_C$ -curve for an experimental fire is now to compute, with Eq. 1.2b as a basis, the gastemperature-time curve for a specified $t-I_C$ -curve, and then use Eq. 1.2c combined with such experimental verifications as the measured gastemperature-time curves, measured heat flow into walls, measured radiation, to indicate the accuracy of the chosen $t-I_C$ -curve. In this way a large number of fullscale burn-out tests have been analyzed, and proved the relevance of this simulation technique to natural fire situations /40/, /9/, /11/. One example of these simulations is given in Figures 1.2b - c. As a result of these comparative analyses, the $t-I_C$ -curve for the complete fire process can be assumed to be known for ventilation controlled wood fuel fires.

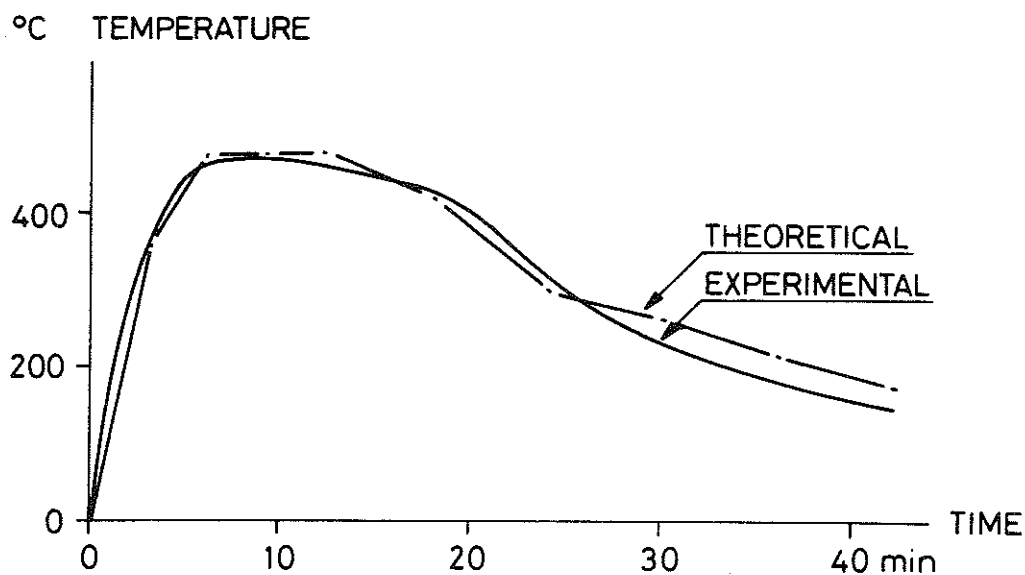


Figure 1.2b Comparison between experimental and theoretical gastemperature-time of natural fire process, curve No. 5 in Figure 1.1a.

RATE OF ENERGY TRANSFER
IN COMPARTMENT REFERRED
TO BOUNDING SURF. AREA

$10^4 \cdot W/m^2$

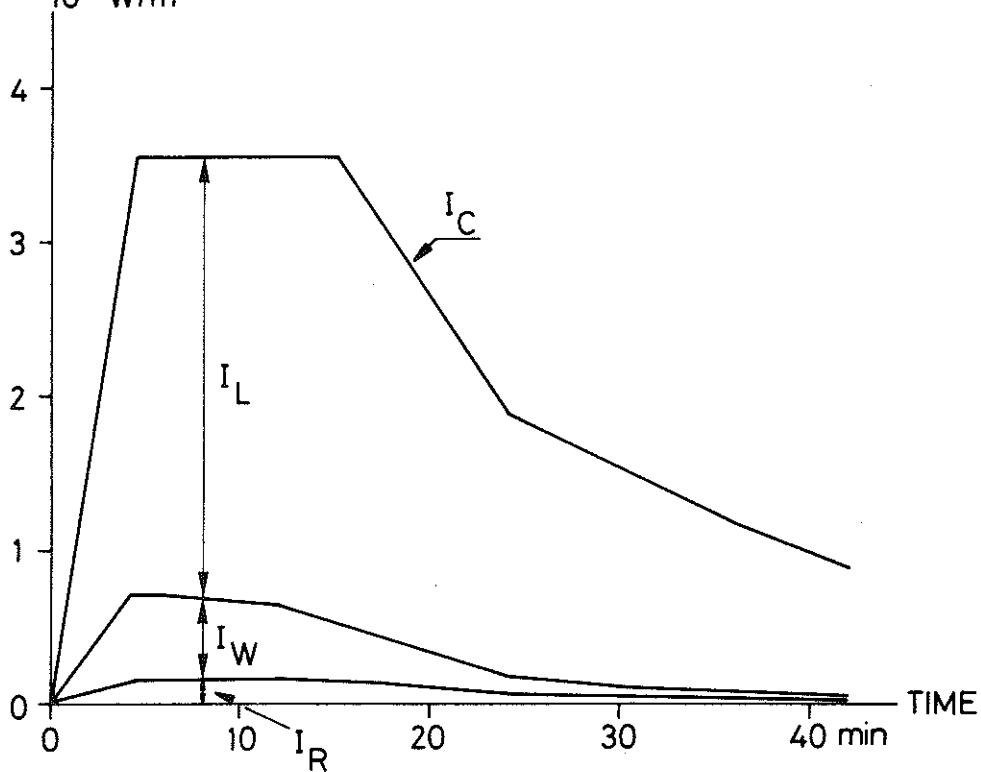


Figure 1.2c The variation with time of the different terms in heat balance equation for curve No. 5 in Figure 1.1a.

This means that the complete fire development now can be computed for different fire load densities q , ventilation openings or opening factors $A\sqrt{h}/A_t$ of the compartment and thermal properties of surrounding structures. Examples of these computations are given by Figure 1.2d.

Statistical surveys of fire load densities and ventilation openings indicate /10/ that a large portion of natural fires in office buildings might not be ventilation-controlled. Considering this, an investigation of the uncertainty inherent in these gastemperature-time curves must be a vital part of a reliability analysis of any design procedure, based on these curves.

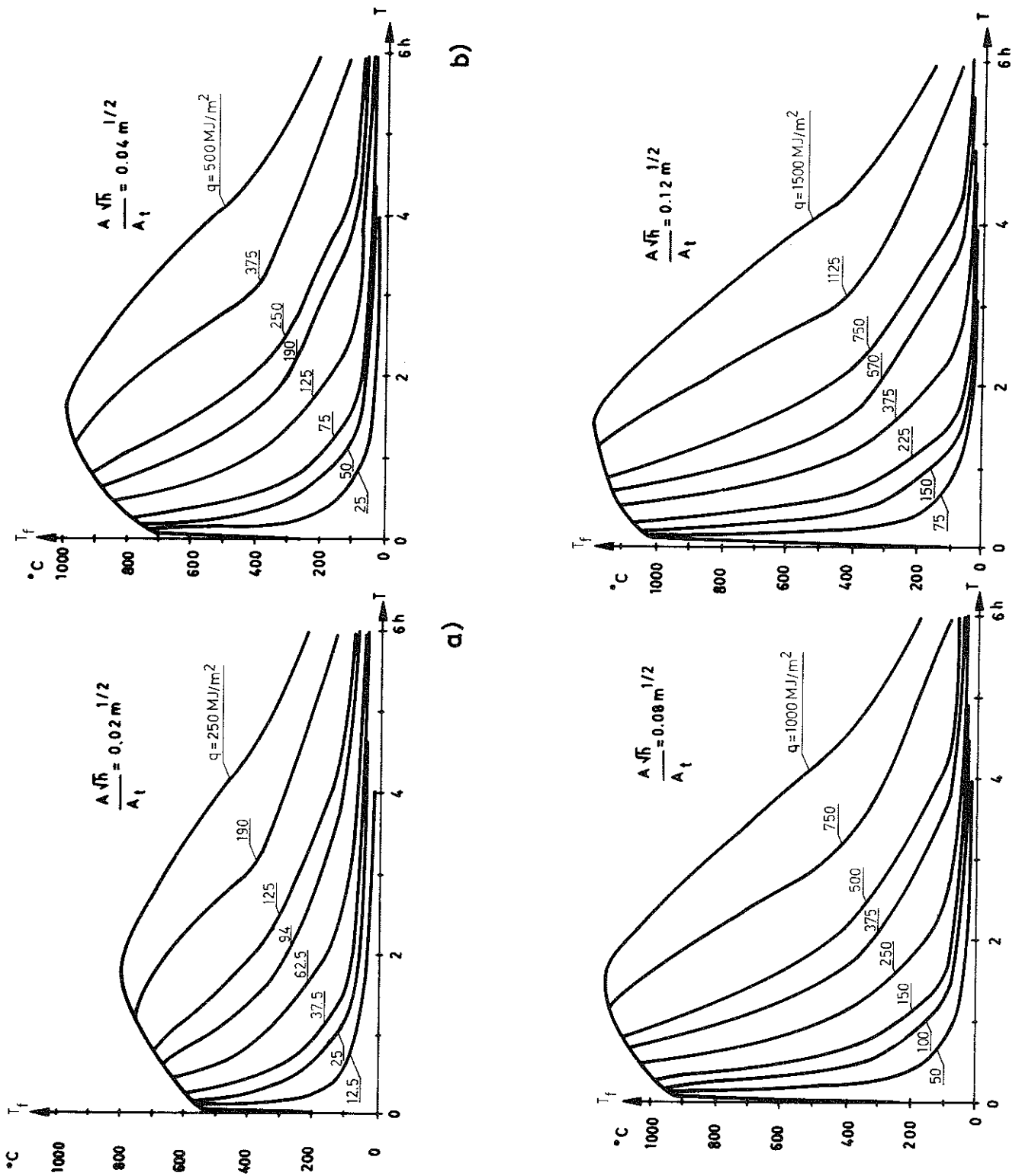


Figure 1.2d Computed gastemperature-time curves for the ventilation-controlled fire process (design curves) /40/.

1.3 Maximum Steel Temperature

The study concerns a type of building component indicated in Figure 1.3a, a protected structural steel beam supporting a floor, roof or ceiling system. When exposed to fire, e.g. the design gas-temperature-time curves given in Figure 1.2d, a non-stationary temperature field will be produced, changing the load-carrying capacity of the beam. In the manual /5/, the heat flow analysis is made on two different levels of sophistication. The first, more accurate method requires specific knowledge of the temperature-dependence of all relevant thermal material properties.

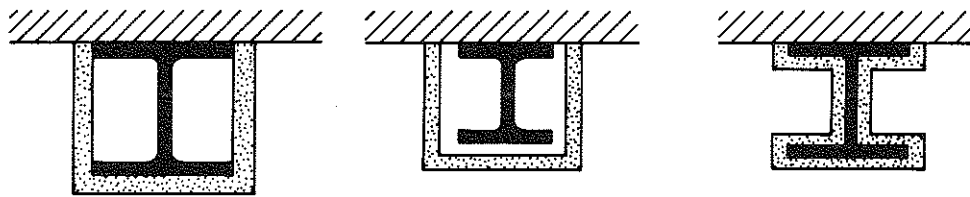


Figure 1.3a Structural component studied in this paper.

In the second method, the main simplifications are (most of them apply to the first method as well)

- the thermal conductivity of the insulation material is regarded as a constant = λ_i
- the heat capacity of insulation material is neglected
- the heat-flow is one-dimensional
- the temperature variation over the cross-section neglected
- in the case of steel beam supporting a slab system, no heat flow occurs across the interface between beam and slab.

To take the temperature-dependence of λ_i into account, the value chosen must be representative for the relevant temperature range. Based on comparisons between theoretical results and experiments, the manual suggests that the value of λ_i is chosen with the time

average insulation temperature taken equal to the maximum steel temperature.

The temperature-time curve of the steel T will be determined by the relationship

$$\frac{\Delta T}{\Delta t} = \frac{A_i}{V_s (1/\alpha + d_i/\lambda_i) \gamma_s c_{ps}} (T_f - T) \quad (1.3a)$$

where

- ΔT = increase in steel temperature T ($^{\circ}\text{C}$) during time step Δt (h)
- A_i = fire-exposed area of steel element (m^2/m)
- V_s = volume of steel (m^3/m)
- α = temperature dependent heat transfer coefficient ($\text{W}/\text{m}^2 \text{ }^{\circ}\text{C}$)
- d_i = insulation thickness (m)
- λ_i = thermal conductivity of insulation material ($\text{W}/\text{m }^{\circ}\text{C}$)
- γ_s = density of steel (kg/m^3)
- c_{ps} = temperature-dependent specific heat capacity of steel ($\text{J}/\text{kg }^{\circ}\text{C}$)
- T_f = instantaneous gas temperature ($^{\circ}\text{C}$)

As final results, the manual gives the nominal or design maximum steel temperature T_n ,

$$T_n = T_n (q_n, \sqrt{A_t}/A_t, k_f, A_i/V_s, d_i/\lambda_i) \quad (1.3b)$$

where k_f is a non-dimensional translation factor describing the influence on the gastemperature-time curve of varying thermal properties of walls, floor and ceiling. The factor k_f is tabulated in the manual for different enclosure material combinations, and should properly be treated as stochastic variable. The inaccuracy introduced by giving k_f a deterministic value is negligible. In the present context k_f has been chosen = 1, implying compartments with enclosing structures consisting of materials of comparatively high density and thermal conductivity (brick, concrete).

As a rule, the value of $1/\alpha$ in Eq. 1.3a is small compared with the value of d_i/λ_i , implying that the presentation can be further condensed by combining the A_i/V_s - and d_i/λ_i -values into one parameter κ , to be denoted insulation parameter

$$\kappa = \frac{A_i \lambda_i}{V_s d_i} \text{ (W/m}^3 \text{ }^\circ\text{C)} \quad (1.3c)$$

Figure 1.3b gives for opening factor $A\sqrt{h}/A_t = 0.04 \text{ m}^{1/2}$ the value of T_n as a function of the design fire load density q_n for different values of A_i/V_s and d_i/λ_i .

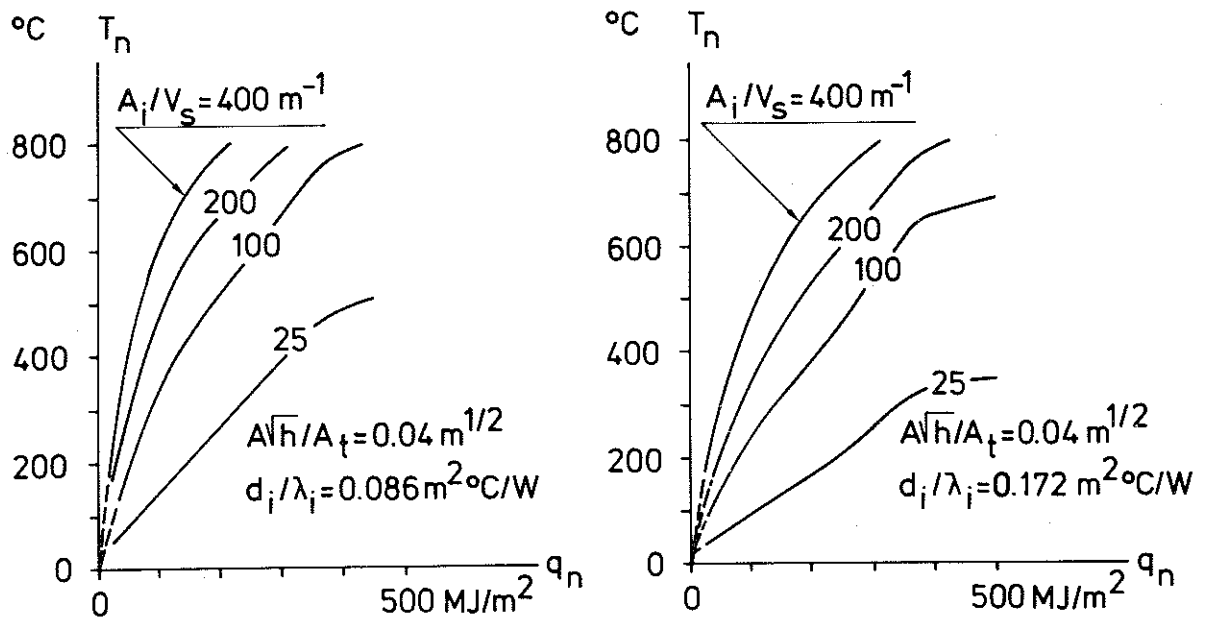


Figure 1.3b Design maximum steel temperature as a function of fire load density q , A_i/V_s and d_i/λ_i for $A\sqrt{h}/A_t = 0.04 \text{ m}^{1/2}$.

1.4 Definition of Limit State for Fire-Exposed Steel Beam

A reliability study of a structural element requires that a clear definition is established of a relevant reference state, in relation to which a desired safety margin can be ensured. For most structural elements, general limit or reference states can be defined /12/: e.g. the limit state of unserviceability (excessive deformations) or the ultimate limit state (capacity of cross section exceeded, instability). Much research is at the moment in progress in order to define these limit states and show the most appropriate criteria of calculation and verification for each of them. With respect to the deformation behaviour and load-carrying capacity of fire-exposed steel beams, the manual design diagrams

are taken from /13/, where a computational model for a deformation analysis is presented. Based on a combination of the actual stress-strain curves and the creep characteristics of steel at elevated temperatures, the model describes the bending process under transient heating conditions with consideration taken of relevant parameters, e.g. loading level, rate of heating, different temperature distributions and restraint conditions. As a final result, design diagrams are presented, giving the load-carrying capacity as a function of the maximum steel temperature for different types of steel material, cross section, loading and restraint condition. The influence of creep is accounted for by differentiating the curves with respect to specific rates of heating. These curves are derived from a deformation limit state, meaning that failure or out of service condition is supposed to have been reached when the maximum beam deformation f_{\max} for a complete fire process, the decay or cooling down phase included, satisfies the inequality

$$f_{\max} \geq \frac{l^2}{800 h} \quad (1.4a)$$

where

l = length of beam (cm)

h = depth of beam (cm)

The relation between this failure criterion and the actual collapse state is discussed in /13/.

An example of the design diagrams is presented in Fig. 1.4a, valid for a simply supported steel I-beam with uniformly distributed load. The critical load is expressed by the coefficient ψ , where $\psi = 1$ corresponds to the uniformly distributed load L_e defining the elastic limit load of the beam

$$L_e = \frac{8W F_y}{l^2} \psi \quad (1.4b)$$

where

L_e = load intensity (kN/m)

W = elastic modulus (m³)

F_y = yield stress of steel at room temperature (MPa)

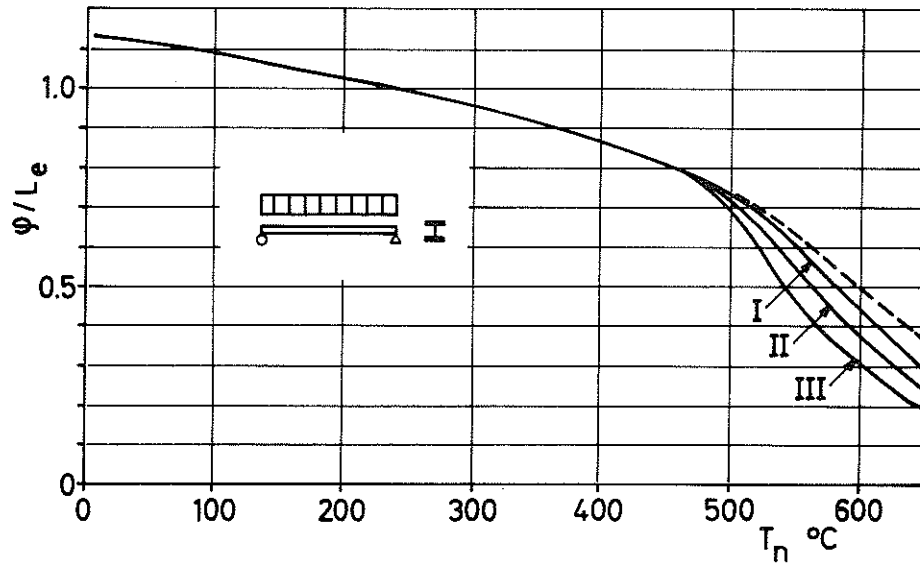


Figure 1.4a The critical load, expressed as ψ/L_e according to Eq. 1.4b, for a simply supported I-section beam of carbon steel with a uniformly distributed load, as a function of the maximum steel temperature T_n for three different rates of heating and cooling (I, II, III). The value of ψ/L_e for infinitely fast rates of heating and cooling is also given for purposes of comparison.

<u>Curve</u>	<u>Rate of heating ($^{\circ}\text{C}/\text{min}$)</u>	<u>Rate of cooling ($^{\circ}\text{C}/\text{min}$)</u>
I	100	33.3
II	20	6.67
III	4	1.33

It is assumed that the temperature is constant over the beam and that there is no restraint on longitudinal expansion of the beam /13/.

1.5 Nominal Loads and Load Factors in the Differentiated Design Procedure

The design procedure, outlined in proceeding sections, will be demonstrated for the structural element studied, a simply supported steel beam in an office building.

1.5.1 Design Fire Load Density

For those types of building occupancies where a representative fire load survey has been made, the manual stipulates that the nominal value of fire load density q_n = the value signifying the 80 per cent level of the corresponding cumulative distribution function. (In all cases, a subscript n denotes a nominal value).

$$q_n = F_q^{-1}(0.8) \quad (1.5.1a)$$

To this value of q_n must be added the heat contents q_o of combustible material in the structural elements and of any combustible finishing material like wall-to-wall carpeting etc. which are not included in the statistical survey. The load factor applied on the nominal fire load density = 1. The cumulative distribution curve of fire load densities for offices, as measured in a survey reported in /14/, is given in Figure 1.5.1a. Assuming that the heat contents q_o of the structural fire load is negligible, Eq. 1.5.1a gives

$$q_n = 138.2 \text{ MJ/m}^2 \quad (1.5.1b)$$

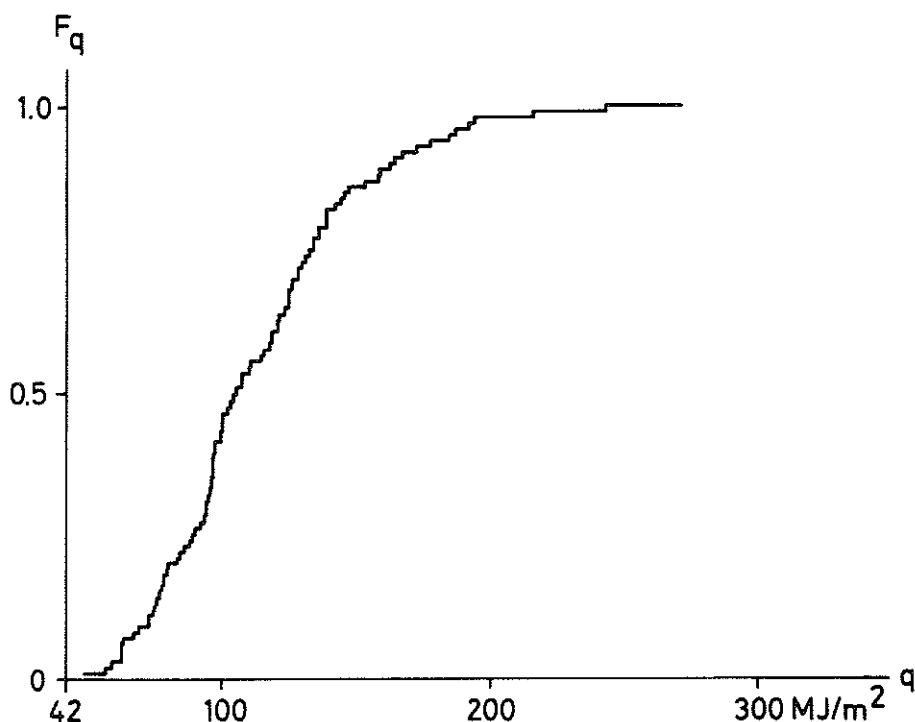


Figure 1.5.1a Cumulative distribution function for fire load density from a statistical survey of 101 office rooms in Stockholm /14/.

1.5.2 Nominal Value and Load Factor for Dead and Live Load

The general design inequality can be written

$$R_{n,f} \geq \gamma_{D,f} D_{n,f} + \gamma_{L,f} L_{n,f} \quad (1.5.2a)$$

where

$R_{n,f}$ = nominal or design value of minimum resistance (load-carrying capacity) during fire exposure

$D_{n,f}$, $L_{n,f}$ = nominal values of dead and live load respectively

$\gamma_{D,f}$, $\gamma_{L,f}$ = load factors, to be applied to the nominal loads

For office buildings, the manual specifies the following values for nominal live load $L_{n,f}$ and load factors $\gamma_{D,f}$, $\gamma_{L,f}$.

Nominal values of live load		Load factors	
Not moveable	Moveable	$\gamma_{D,f}$	$\gamma_{L,f}$
0.35 kN/m ²	1.00 kN/m ²	1	1.4

These figures for $L_{n,f}$ apply to the case where a complete evacuation of personnel during a fire can not be anticipated. The nominal value of the dead load $D_{n,f}$ is to be put equal to the mean dead load \bar{D} .

Clearly, some assumptions must be made regarding the design procedure used in the normal non-fire case of loading. For simplicity and in accordance with normal Swedish practice, it is assumed that the beam is designed using the concept of allowable stress and with an overall safety factor γ_o (strength factor) = 1.5. For offices, the present Swedish codes prescribe a value of the nominal live load $L_n = 2.0 \text{ kN/m}^2$ floor area, irrespective of tributary area. The not moveable part of $L_n = 0.5 \text{ kN/m}^2$ and the moveable part = 1.5 kN/m^2 . The nominal dead load D_n is to be put equal to mean dead load.

Measuring $R_{n,f}$ in L_e -units, according to Eq. 1.4b, the design inequality 1.5.2a can now be written

$$R_{n,f} \geq \frac{\gamma_{D,f} D_{n,f} + \gamma_{L,f} L_{n,f}}{\gamma_o (L_n + D_n)} \quad (1.5.2b)$$

Using the nominal loads, load factors and overall strength factor given earlier, the design working stress level during a fire-exposure will be, expressed in L_e -units, (see Eq. 1.4b) 0.658, 0.648 and 0.64 for $D_{n,f}/L_n = D_n/L_n = 3,1$ and $1/3$ respectively. This implies, see Figure 1.4a, that the design maximum steel temperature will be independent of the D_n/L_n -ratio and equal to $510^\circ\text{C} - 530^\circ\text{C}$, varying with the rate of heating. Assuming the rate of heating to be equal to that corresponding to curve II in Figure 1.4a, the design critical steel temperature will be $\approx 520^\circ\text{C}$. Taking the value of q_n from Eq. 1.5.1b and given the amount of combustible material q_o not included in Figure 1.5.1a, the required value of the insulation parameter κ is found from the manual /5/ by interpolation of A_i/V_s and d_i/λ_i in tables. Values that must be specified as input are q_n , $A\sqrt{h}/A_t$ and k_f .

2. Structural Safety and Probabilistic Methods in General

Chapter 2 presents a condensed and incomplete summary of the general probabilistic structural safety methods discussed today. Only main characteristics, necessary later in this paper to the analysis of fire-exposed structures, will be mentioned. Detailed references can be found e.g. in /16/, /17/.

2.1 Calculation of Probability of Failure

In structural safety analysis, the general assumption is that the resistance R and load or load effect S are random variables, characterized by their probability density functions f_S and f_R . Risk or probability of failure P_f in the sense of the realization of a specified limit state, can then be expressed in different ways, e.g.

$$P_f = P(R < S) \quad (2.1a)$$

$$P_f = P(R/S < 1) \quad (2.1b)$$

$$P_f = P(\ln R/S < 0) \quad (2.1c)$$

In the expression

$$P_f = P(Y < 0)$$

Y is called the formulation variable.

In classical reliability analysis P_f is obtained from

$$P_f = \int_0^{\infty} \int_0^s f_S(s) f_R(r) ds dr = \int_0^{\infty} F_R(s) f_S(s) ds \quad (2.1d)$$

where F_R denotes the probability distribution function of R .

Equation 2.1d is derived assuming that R and S are independent and presupposes that the exact shapes of the distribution functions are known. In practical cases, knowledge of f_R and f_S (or F_R and F_S) is limited to a severe degree. In favourable circum-

stances, the first two central moments of the distribution functions are available and then with a sampling or prediction error that has to be estimated by statistical methods in each individual case. The precise form of the distribution functions, especially in areas more than a few number of standard deviations from the mean, is unknown. As has been demonstrated by a number of authors, the value of P_f evaluated using Eq. 2.1d is in general structural safety analysis (with $P_f \leq 10^{-5}$) highly dependent on the choice of distribution functions for the random variables involved. See e.g. /18/. As a consequence, considerable effort has been made to find alternative and more consistent systems to define structural reliability and its incorporation into design format. We will first consider new ways to re-formulate the (random) safety margin R-S and the (random) safety factor R/S used in Eqs. 2.1a-c.

2.2 Safety Margin R-S

Returning to Eq. 2.1a

$$P_f = P(R-S \leq 0)$$

this relation may be rewritten /20/.

Consider the random variable

$$U = \frac{[(R-S) - (\overline{R-S})]}{\sqrt{\sigma_R^2 + \sigma_S^2}} \quad (2.2a)$$

Mean values are denoted by a bar.

By definition, U is a standardized or normalized, i.e. with $\overline{U} = 0$ and $\sigma_U = 1$, measure of the safety margin (R-S). Now

$$\begin{aligned} P_f = P(R-S \leq 0) &= P \left[\frac{(R-S) - (\overline{R-S})}{\sqrt{\sigma_R^2 + \sigma_S^2}} \leq - \frac{(\overline{R-S})}{\sqrt{\sigma_R^2 + \sigma_S^2}} \right] = \\ &= P \left[U \leq - \frac{1}{V_{R-S}} \right] = F_U(-\beta_C) \end{aligned} \quad (2.2b)$$

where F_U designates an unspecified, though in principle derivable, cumulative distribution function and β_C , or the reciprocal of the coefficient of variation of the safety margin, is a so called "safety index", defining the reliability.

2.3 Safety Factor R/S

Defining the probability of failure P_f by Eq. 2.1c and using the standardized variate /21/

$$Z = \frac{\ln(R/S) - \overline{\ln(R/S)}}{\sigma_{\ln R/S}} \quad (2.3a)$$

we get in a similar way

$$\begin{aligned} P_f &= P \left[\ln(R/S) < 0 \right] = P \left[Z < \frac{-\overline{\ln(R/S)}}{\sigma_{\ln R/S}} \right] = F_Z \left(\frac{-\overline{\ln(R/S)}}{\sigma_{\ln(R/S)}} \right) = \\ &= F_Z (-\beta_{ER}) \end{aligned} \quad (2.3b)$$

Apparently the two quantities β_C and β_{ER} are of significance in any probabilistic analysis of structural safety. During the last decade, a number of reliability-based design rationales have appeared. In almost all of them, the factors β_C or β_{ER} or other formulations of a safety-index are incorporated. Examples of how this is being done will be given in section 2.4.

2.4 Outline of Some Probabilistic Safety Systems

2.4.1 Classification of Design Formats

Any attempt to give a survey of this rapidly developing area is likely to be both incomplete and obsolete. Nevertheless, a classification of the different design formats according to the following characteristics may give an insight into the more salient features.

- Design based on safety indices or explicit risk
- Methods of expressing the design criteria in terms of the value

of the safety measure β

- Order of statistical moment employed in the formulation variable
- Order of terms in Taylor series expansion of formulation variable into basic variables
- Methods of uncertainty assessment
- Evaluation of safety factors
- Invariance properties (See /22/ and /23/.)

2.4.2 Risk-Based Versus Safety Index-Based Design

In most cases, the probability of failure enters the evaluation of safety only in indirect way. An exception is the format proposed in /19/, where design equations are based on the evaluated risk. As an example, using the formulation variable $Y = R-S$, the general design equation in this format becomes

$$\bar{R} \geq \bar{S} - F_U^{-1}(P_{f,0}) \cdot \sqrt{\sigma_R^2 + \sigma_S^2} \quad (2.4.2a)$$

where $P_{f,0}$ is the predetermined value of probability of failure and F_U^{-1} is the inverse of F_U .

2.4.3 Formulation of Design Criteria in Safety Index Formats

The basic idea in these code formats is that the reliability is approximately constant over a specified data domain if the c.o.v., coefficient of variation, of the formulation variable Y is kept constant $= 1/\beta$. In the Cornell format, where $Y = R-S$, the design equation becomes /20/ for a specified value of β_C

$$\bar{R} \geq \bar{S} + \beta_C \sqrt{\sigma_R^2 + \sigma_S^2} \quad (2.4.3a)$$

The corresponding value of central safety factor θ is

$$\theta = \frac{1 + \beta_C (V_R^2 + V_S^2 - \beta_C^2 V_R^2 V_S^2)^{1/2}}{1 - \beta_C^2 V_R^2} \quad (2.4.3b)$$

As can be seen, a high variability in R implies values of θ that may be unrealistically large. As an alternative, Esteva and Rosenblueth put forward a design format /21/ based on the formulation variable $Y = \ln(R/S)$, leading to the requirement that

$$\theta = \frac{\bar{R}}{\bar{S}} \geq e^{\beta_{ER} (V_R^2 + V_S^2)^{1/2}} \quad (2.4.3c)$$

The relation between β_C or β_{ER} on one hand and the central safety factor β on the other has been studied for different assumptions regarding the shape of probability density functions of R and S and values of V_R and V_S by a number of authors.

Other design format formulations exist, notably those of Ditlevsen /22/ (a partial coefficient format) and Hasofer - Lind /23/.

2.4.4 Order of Central Moment Employed

The precise mathematical form of the probability distribution curve of the formulation variable Y is in practical cases unknown. An alternate way of describing a distribution is by supplying information about the central moments up to an order j. By choosing the value of j large enough, accuracy to any preselected level of tolerance is achieved /24/. As an example, knowledge of the first four moments (mean, variance, skewness and peakedness) permits an accurate estimation of percentiles of the approximating Pearson distribution. In structural safety analysis, moments up to an order two are usually employed.

2.4.5 Truncation of Taylor Series Expansion

The random variables R and S are invariably functions of other, more basic variables. The problem is to derive the means and variances of R and S from the first and second moments of the basic variables. Exact calculation is only possible when the

functional relationship between the two sets of variables is a linear transformation. In all other cases, approximate methods must be used. A convenient method is to make a Taylor expansion of R and S with the derivatives evaluated at the mean values and truncate the expansion at the linear terms. Assuming that the resistance R is a function of n independent stochastic variables $X_1 \dots X_n$;

$$R = R(X_1, X_2 \dots X_j \dots X_n)$$

The first-order approximate values of \bar{R} and σ_R will then be given by

$$\bar{R} = R(\bar{X}_1, \bar{X}_2 \dots \bar{X}_j \dots \bar{X}_n) \quad (2.4.5a)$$

$$\sigma_R^2 = \sum_{j=1}^n \left(\frac{\partial R}{\partial X_j} \right)_o^2 \sigma_{X_j}^2 \quad (2.4.5b)$$

The subscript o denotes in this case evaluation at mean values. We may use these relations to simplify the expression for β_{ER} , Eq. 2.3b,

$$\beta_{ER} = \frac{\overline{\ln(R/S)}}{\sigma_{\ln(R/S)}} \quad (2.4.5c)$$

The first order theory yields

$$\overline{\ln(R/S)} = \overline{\ln R - \ln S} \approx \overline{\ln R} - \overline{\ln S} \approx \ln \bar{R} - \ln \bar{S} = \ln (\bar{R}/\bar{S}) \quad (2.4.5d)$$

$$\begin{aligned} \sigma_{\ln(R/S)}^2 &\approx \left(\frac{\partial \ln(R/S)}{\partial R} \right)_o^2 \sigma_R^2 + \left(\frac{\partial \ln(R/S)}{\partial S} \right)_o^2 \sigma_S^2 = \frac{\sigma_R^2}{R^2} + \frac{\sigma_S^2}{S^2} = \\ &= V_R^2 + V_S^2 \end{aligned} \quad (2.4.5e)$$

$$\beta_{ER} \approx \frac{\ln(\bar{R}/\bar{S})}{(V_R^2 + V_S^2)^{1/2}} \quad (2.4.5f)$$

The formulas must be used with discrimination. A necessary condition for passable precision is that the functions R, S etc. are approximately linear in the region close to \bar{X}_j , $j=1\dots n$, simultaneously as the majority of the mass of the density function lies in this area. In more complicated cases, the required central moments must be derived by a Monte Carlo simulation.

2.4.6 Analysis of Uncertainty

2.4.6.1 Resistance R

The problem of assessing and reporting uncertainties is of fundamental importance in any structural safety analysis. In /25/ the basic concepts in this area are reported. The incorporation of the uncertainty information into the design equation differs from one format to another. In the first published second moment code format /20/, the resistance R is expressed as a function of three random parameters M, P and F

$$R = R(M, P, F)$$

where M is material strength, P is a variable reflecting uncertainties in strength calculations and F is a geometrical property of the structure, such as cross-sectional area or section modulus. There is no a priori given relationship between R and the variables M, F and P, but for ordinary design a product form is functionally justified

$$R = M \cdot F \cdot P \tag{2.4.6.1a}$$

Coefficients entering the formula may be incorporated in either M, P or F.

In e.g. /26/, R is written

$$R = M \cdot F \cdot P \cdot \bar{R} \tag{2.4.6.1b}$$

with \bar{R} evaluated from the identity

$$\bar{R} = \frac{\bar{R}}{\bar{R}'} \cdot \frac{\bar{R}'}{R_n} \cdot R_n \quad (2.4.6.1c)$$

where

R_n = nominal value of capacity according to theory
 R' = value of capacity obtained by laboratory tests
 R = true capacity in real service conditions

As a result of this decomposition, only the ratio \bar{R}/\bar{R}' has to be judged subjectively.

In the extended reliability model reported in /19/, total uncertainty is evaluated directly from the structural analysis formulas, using Eq. 2.4.5a-b. Each basic variable X_j is assigned two uncertainty measures: one corresponding to objective variability and one, of Bayesian character, describing the accuracy of this measured variability. To the total resulting uncertainty is added an algorithm error term.

2.4.6.2 Load Induced Effect S

Uncertainty in load effect S is expressed by writing

$$S = E \cdot (L + D) \quad (2.4.6.2a)$$

(in the case of live and dead load effects only) where E is a random variable expressing the dispersion in load effect prediction and L and D describe the basic variability of the live and dead load respectively.

If the variables L and D are taken from load survey statistics assuming a uniformly distributed load, they should include the increased variance resulting from the load concentration effects appearing in real situations. The factor E is in princip derivable by comparing experimental member forces (for a well-defined loading situation) with the theoretical values. Both the variance in load effect prediction and the variance due to professional load idealizations tend to be of minor importance compared with the

basic variability in S given by load surveys. Reference is once again made to /19/, /20/, /26/.

2.4.7 Evaluation of Safety Factors and Load Factors

The Cornell code format results primarily in the following design equations for a predetermined value of β_C

$$\bar{R} \geq \bar{S} + \beta_C (\sigma_R^2 + \sigma_S^2)^{1/2} \quad (2.4.7a)$$

or

$$\bar{R} \geq \theta \bar{S} \quad (2.4.7b)$$

with central safety factor θ given by Eq. 2.4.3b. It is professionally desirable to connect this equation with the traditional code specifications using stress reducing coefficients, load factors or partial (split) coefficients, exemplified with the following relations

$$\phi R_n \geq \gamma S_n \quad (2.4.7c)$$

$$\phi R_n \geq \gamma_D D_n + \gamma_L L_n \quad (2.4.7d)$$

$$R_n = R_n \left(\frac{X_1}{\gamma_1}, \dots, \frac{X_K}{\gamma_K} \right) \geq \gamma_D D_n + \gamma_L L_n \quad (2.4.7e)$$

where all factors or coefficients depend only on the variance of the corresponding random variable and on the value of β_C . This separation of the uncertainty into smaller, identifiable parts will here be illustrated only for the load factor format. Papers dealing with this problem are e.g. /24/, /27/.

Using the separation function /27/

$$(X_1^2 + X_2^2 + \dots)^{1/2} \approx \alpha_{X_1 X_2 \dots} (X_1 + X_2 + \dots) \quad (2.4.7f)$$

twice, the inequality 2.4.7a can be rewritten

$$\bar{R} \geq \bar{S} + \beta \alpha_{RS} (\sigma_R + \sigma_S) \quad (2.4.7g)$$

$$\bar{R}(1 - \beta \alpha_{RS} V_R) \geq \bar{L} + \bar{D} + \beta \alpha_{RS} \alpha_{DL} (\sigma_D + \sigma_L) \quad (2.4.7h)$$

$$\bar{R}(1 - \beta \alpha_{RS} V_R) \geq \bar{L}(1 + \alpha_{RS} \alpha_{DL} \beta V_L) + \bar{D}(1 + \alpha_{RS} \alpha_{DL} \beta V_D) \quad (2.4.7i)$$

Identifying with inequality 2.4.7d or 1.5.2a, the central safety factor has been decomposed into three parts

$$\phi = (1 - \alpha_{RS} \beta V_R) \frac{\bar{R}}{R_n} \quad (2.4.7j)$$

$$\gamma_D = (1 + \alpha_{RS} \alpha_{DL} \beta V_D) \frac{\bar{D}}{D_n} \quad (2.4.7k)$$

$$\gamma_L = (1 + \alpha_{RS} \alpha_{DL} \beta V_L) \frac{\bar{L}}{L_n} \quad (2.4.7l)$$

The factors ϕ , γ_D , γ_L are based on mean values, but could just as well have been evaluated on the basis of characteristic values (nominal values) and Cornell's code format could have been replaced with the Esteva-Rosenblueth format or with Ang's on the prescribed distribution risk-based format.

3. Evaluation of Uncertainty Measures in the Fire Engineering Design

In determining the reliability of a specified design procedure, a rational uncertainty analysis is of basic importance. A dependable assessment of the total uncertainty requires primarily that

- all physical variables affecting the reliability are identified
- probability distributions, or at least means and variances (first and second moments), are assigned to relevant variables
- uncertainty of specific parameters are combined in such a way that a comparison with test data becomes possible
- test data are collected and evaluated whenever possible

The reliability of the design process studied in this paper is affected by a great number of random variables. This makes it necessary to divide the safety analysis into a number of steps, where each step produces an uncertainty measure, that can either be directly compared to test data or assigned statistic parameters in a consistent way. Clearly, the uncertainty analysis described in section 2.4.6 must be changed to fit the new physical situation.

The remaining sections of this chapter will deal with the evaluation procedure that has been used to estimate the total uncertainty of a fire-exposed steel beam.

3.1 Uncertainty in Fire Load Density Statistics

Figure 1.5.1a gives the cumulative distribution function of fire load densities in 101 office rooms in Stockholm. A great deal of the fire load consists of packed paper, sometimes enclosed in steel furniture. The degree of contribution of a fire load of this type to a fully-developed fire is still far from known.

On the other hand, consideration must be taken of the fact that the fire load survey reported in Figure 1.5.1a excluded combustible material in structural members. The influence of these two factors is investigated in some detail in a recently published report /39/. The results of a statistical survey are published in form of histograms

and sample mean and standard deviation for the fire load density (measured in equivalent kg of wood per m² floor area) of 500 fire compartments in office buildings. For the total population, mean and standard deviation of the moveable fire load are 24.5 and 19.9 kg/m². For the structural (immobile) fire load, the corresponding figures are 37.2 and 10.0 for rooms with built-in cupboards and in the case of rooms without built-in cupboards 9.2 and 5.3 kg/m² respectively. For the total number of rooms, the sample mean and standard deviation of the immobile fire load are 16.1 and 13.8 kg/m². The sample mean and standard deviation \bar{q} and σ_q of the distribution given by Figure 1.5.1a are (expressed in MJ per m² total surface area of the fire compartment)

$$\bar{q} = 114.3 \text{ MJ/m}^2 \quad (3.1a)$$

$$\sigma_q = 39.4 \text{ MJ/M}^2 \quad (3.1b)$$

As a rough approximation, the values in /39/ have to be multiplied with 4 to be expressed in the units of Eqs. 3.1a-b. It is thus seen that the mean value and standard deviation of the total fire load given in /39/ are somewhat higher than the corresponding values of the Swedish investigation comprising only the moveable part of the total fire load. Regarding the problem of the actual calorific contribution of packed paper to the fire development, two reduction coefficients are introduced in /39/. The first describes the weight percentage of the paper taking part in the combustion process, and the second coefficient gives the effective calorific or heat value of that percentage. The two reduction coefficients are dependent on the actual gastemperature-time curve. The report treats only the case of the gastemperature being lower or equal to the standardized ISO-curve used in the endurance test and may for this reason give biased values. It is tentatively concluded that the distribution function of the energy contents actually contributing to the fire process (including both moveable and structural fire load) may be represented by Figure 1.5.1a. To be able to estimate the variation in the final reliability levels arising from our incomplete knowledge of the energy actually released, the effective fire load q_{eff} will be written

$$q_{\text{eff}} = \Delta q \cdot q \quad (3.1c)$$

where

q is the stochastic variable represented by Figure 1.5.1a

Δq is an error factor with chosen mean and variance.

3.2 Variability of Maximum Steel Temperature T_{\max}

Regarding the computational basis for the value T_n , see section 1.3. The randomness in the maximal steel temperature T_{\max} will here be divided into three parts ΔT_j , $j = 1, 2, 3$. An additive form rather than multiplicative of these terms is preferred from a functional point of view due to the great range of the nominal value T_n . The correction term ΔT_2 is approximately independent of the value of T_n , and a multiplicative form would have indicated the necessity of a random correction factor ΔT_2 with a temperature-dependent c.o.v. The additive form implies that the stochastic variable T_{\max} is written

$$T_{\max} = T_n + \Delta T_1 + \Delta T_2 + \Delta T_3 \quad (3.2a)$$

where

T_n = deterministic value, given by design curves for nominal values of q , $AV\sqrt{h}/A_t$, k_f and κ

ΔT_1 = uncertainty due to variation in the κ -value

ΔT_2 = uncertainty reflecting the prediction error in the theory of compartment fires and heat flow analysis

ΔT_3 = correction term reflecting the difference between a natural fire in a laboratory and under real life service conditions.

Eq. 3.2a exemplifies the approach to the uncertainty assessment: the total uncertainty is differentiated into components, which have to be specified in such a way that a statistically correct comparison between the employed design theory and experiment becomes possible. The design theory is the "skeleton", in relation to which all information must be evaluated. The words "statistically correct" above imply that care must be taken to minimize the stochastic interdependence of the different component uncertainties. This in turn implies a design theory where the specific elements as closely as possible emulate the physical reality.

3.2.1 ΔT_1

As described earlier, the κ -value consists of four factors:

$\kappa = (A_i/V_s) \cdot (\lambda_i/d_i)$. If the variability in A_i/V_s can be neglected, it remains to assess the uncertainty in d_i and λ_i . The scatter in d_i depends e.g. on whether the insulation material is sprayed or prefabricated as board and must take into account the risk that mechanical damage may decrease the nominal value. The dependence of λ_i on the temperature is usually evaluated using heat flow meters and may differ from the actual curve under fire exposure (cracking phenomena, etc). Changes in the density of the insulating material may also influence the value of λ_i . The λ_i -value may furthermore change with time (ageing). As there is scant data for a proper evaluation, the statistic parameters describing d_i and λ_i must be based on subjective judgement.

As an average for the statistical population, the mean of ratios $\frac{d_i}{d_{i,n}}$ and $\frac{\lambda_i}{\lambda_{i,n}}$ are both chosen to be 1.0 with a standard deviation = 0.2. The influence of changes in the statistic parameters representing these ratios will be investigated. Writing the random variable κ_{eff} as

$$\kappa_{\text{eff}} = \frac{A_i \lambda_i}{V_s d_i} \quad (3.2.1a)$$

and the constant value κ_n as

$$\kappa_n = \frac{A_i \lambda_{i,n}}{V_s d_{i,n}} \quad (3.2.1b)$$

the random variable ΔT_1 will be given by

$$\Delta T_1 = T_n(\kappa_{\text{eff}}) - T_n(\kappa_n) \quad (3.2.1c)$$

Investigations have shown that fire-related structural failures in several cases have been caused by the undesigned removal of the fire protection from some part of the structural member. The proposed statistics of the parameter κ do not cover this situation. The reason is that the deterministic one-dimensional model of the heat flow into the steel cross section, Eq. 1.3a, is inadequate in this case. As soon as results from more accurate temperature-field com-

putations and statistical survey data are available, this important practical situation may be analyzed, defining the economically optimum level of control and inspection.

3.2.2 ΔT_2

ΔT_2 is the error term describing the difference between the design value T_n , and the maximum steel temperature as given by laboratory tests. For a comparison to be meaningful within the context of Eq. 3.2a some assumptions must be fulfilled

- the relative frequency distribution of the parameters determining the compartment fire development in the tests, mainly size of fire load, fire load surface and ventilation factor, must match the corresponding distribution curves met in real conditions
- the κ -value of the insulation in the laboratory tests must be known with sufficient degree of accuracy.

Information from systematic investigations of steel beam elements exposed to natural fires is scarce and, as a rule, difficult to evaluate. On the other hand, for steel columns there exists a comprehensive tests series from Fire Research Station, Boreham Wood, England /6/, /29/, intended to provide information about temperatures attained in building fires involving various fire loads and ventilation factors. In 22 burn-out tests, 83 internal, free standing and insulated columns were exposed to fire and the temperature-rise carefully recorded with four thermo-couples in each column. In nearly all cases, the protection was 13 mm mineral wool, for a few columns changed to 19 mm asbestos insulating board.

As the statistical parameters representing ΔT_2 describe the perhaps most disputable and critical link in the design procedure, the basic data in the derivation of ΔT_2 will be accounted for in some detail.

The cumulative distribution function for the fire load densities in the experiments is compared with the data from the fire load survey in Figure 3.2.2a. The two sample mean values are nearly equal (114 MJ/m² compared with 106 MJ/m²) while the distribution scatter is

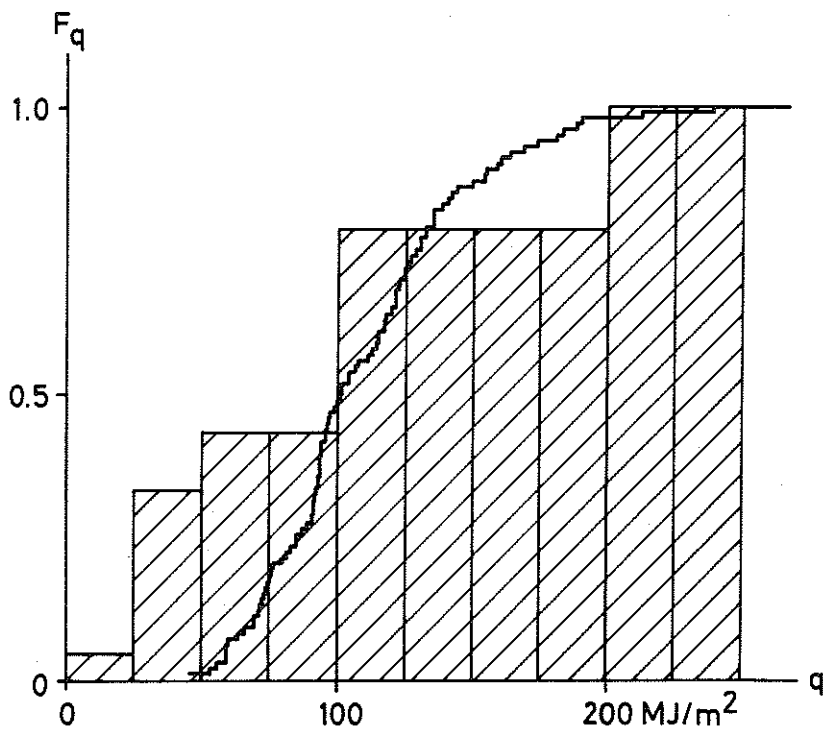


Figure 3.2.2a The cumulative distribution function of the fire load density in the JFRO-test series, compared with the distribution function in Figure 1.5.1a.

considerably larger for the burn-out tests (the sample standard deviation is 82 and 39 MJ/m² respectively). From Figure 3.2.2a it can be seen that the burn-out test series comprised some tests with lower fire load density than can be found in real life thus lowering the average maximum steel temperature. On the other hand, it may be surmised that the average ventilation factor was somewhat lower in the tests than in the buildings surveyed, thus increasing the fire severity.

The values of A_1 , V_1 and d_1 were taken equal to the nominal ones, the graph representing the temperature-dependence of λ_1 was determined by computing the temperature-time curve of a steel column with the actual fire process temperature as a basis /11/, see Figure 3.2.2b. The data for the asbestos board were chosen the same as for the corresponding Swedish protection material. Included in the comparison sample were also the results from 14 column temperature-time curves obtained from

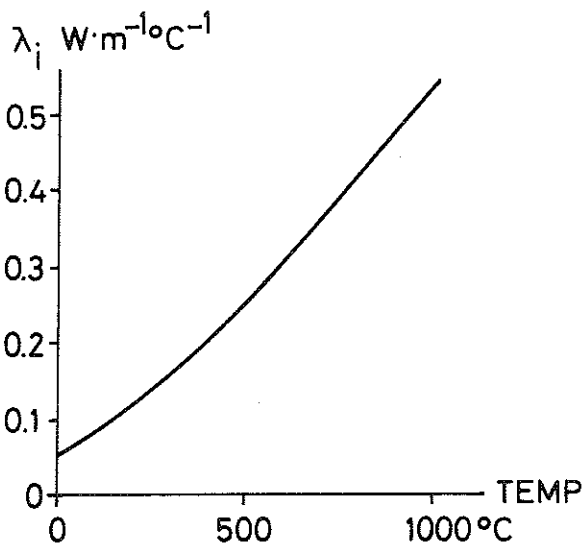
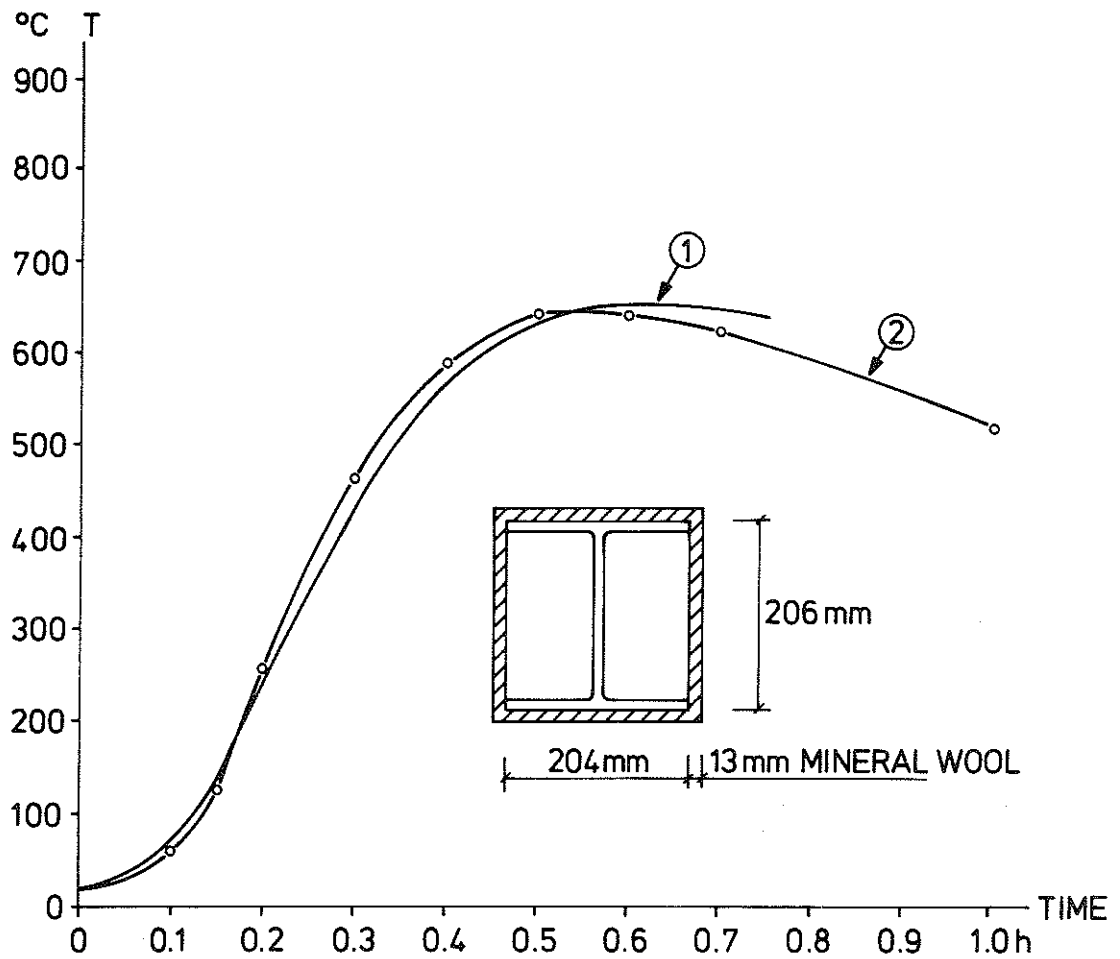


Figure 3.2.2b Actual ① and calculated steel temperature-time curve ② from the JFRO-test series. Relation between thermal conductivity and the average temperature of the mineral wool insulation, used in the calculation.

burn-out tests performed at the Division of Structural Mechanics, Lund Institute of Technology, in connection with an investigation of fire spread risk in low rise housing developments.

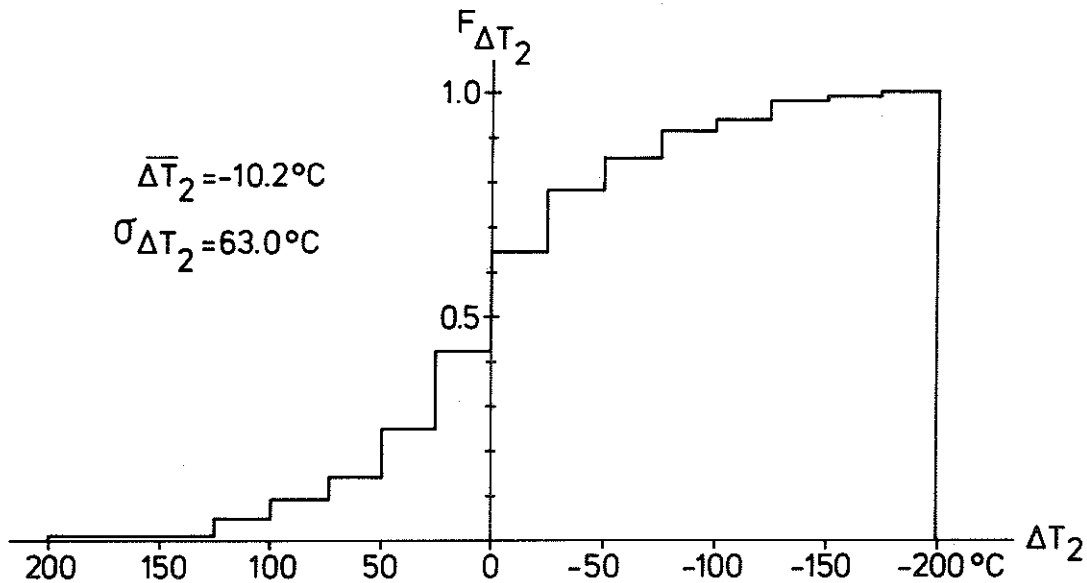


Figure 3.2.2c Cumulative distribution curve of error term ΔT_2 , describing the prediction error in compartment fire theory and heat transfer analysis.

Figure 3.2.2c gives the cumulative distribution function of the error term ΔT_2 , evaluated from 97 column tests. The sample mean and standard deviation were found to be

$$\overline{\Delta T_2} = -10^\circ\text{C} \quad (3.2.2a)$$

$$\sigma_{\Delta T_2} = 63^\circ\text{C} \quad (3.2.2b)$$

Of the 83 JFRO-columns, 41 were tested in a fire compartment with $A\sqrt{h}/A_t \approx 0.06 \text{ m}^{1/2}$, 38 were tested with $A\sqrt{h}/A_t \approx 0.12 \text{ m}^{1/2}$. Studying the variation of ΔT_2 with opening factor $A\sqrt{h}/A_t$ it was found that for $A\sqrt{h}/A_t = 0.06 \text{ m}^{1/2}$

$$\overline{\Delta T_2} = -23^\circ\text{C} \quad (3.2.2c)$$

$$\sigma_{\Delta T_2} = 66^\circ\text{C} \quad (3.2.2d)$$

and for $A\sqrt{h}/A_t = 0.12 \text{ m}^{1/2}$

$$\overline{\Delta T_2} = -4^\circ\text{C} \quad (3.2.2e)$$

$$\sigma_{\Delta T_2} = 63^\circ\text{C} \quad (3.2.2f)$$

As can be seen, the variance of ΔT_2 is nearly independent of $A\sqrt{h}/A_t$, and the variation of $\overline{\Delta T_2}$ with $A\sqrt{h}/A_t$ is of small practical importance. For these reasons, the statistics of ΔT_2 given by Eqs. 3.2.2a-b have been chosen representative for all $A\sqrt{h}/A_t$ -values.

There are reasons to believe that the variance of ΔT_2 given by Eq. 3.2.2b may be on the conservative side

- to get decisive steel temperature levels in the JFRO-tests, the thickness of the insulation d_i was chosen smaller than in practical cases, increasing the risk of scatter in insulation properties
- the extremely small value of d_i had as a consequence that the design temperature T_n in some cases could only be obtained by unreliable extrapolation.

The term ΔT_2 could have been further differentiated by breaking it into two parts: the first describing the divergence between design gastemperature-time curve and actual fire process and the second defining inaccuracy in the heat flow analysis translating the fire process into a maximum steel temperature. The added insight does not seem to justify the computational effort necessary for this further decomposition.

Summing up, it is concluded that the statistical parameters characterizing the fire load densities and ventilation openings in the burn-out tests have been chosen in such a way that a significant basis for a comparison between predicted and real life maximum steel temperature exists.

Moreover, it seems reasonable to assume that additional information

will not significantly change the values of $\overline{\Delta T}_2$ and $\sigma_{\Delta T_2}$ given in Eqs. 3.2.2a-b.

3.2.3 ΔT_3

The error term ΔT_3 is intended to cover the transition from laboratory tests to real life situation, and should incorporate influences due to factors like

- design value of $A\sqrt{h}/A_t$ differs from the real one
- geometric dimensions of the room
- change of specific fuel bed properties e.g. fuel surface area
- the influence of outer wind on fire process.

The error term ΔT_3 has been assigned the following statistics

$$\overline{\Delta T}_3 = 0 \quad (3.2.3a)$$

$$\sigma_{\Delta T_3} = 25^\circ\text{C} \quad (3.2.3b)$$

The reasons for choosing the variance of ΔT_3 relatively small are taken from /11/, where it is shown that for a given effective fire load q_{eff} (see Eq. 3.1c) and a given ventilation factor, the resulting maximum temperature of an insulated steel member will be nearly independent of whether the fire process is ventilation-controlled or not. A change from the experimental type of fire load (wood crib) to a more realistic exposure geometry of the fuel may change the time-curve of the effective heat release I_C , but the overall effect on the maximum temperature of the steel structure will be small.

3.2.4 Equivalence between Column and Beam Temperatures. Choice of Representative Beam Temperature

Due to lack of experimental data, the uncertainty term ΔT_2 in the maximum steel temperature had to be evaluated with laboratory tests of insulated, fire-exposed steel columns as a basis. For such columns,

fire-exposed on all sides, the instantaneous temperature over the cross-section will not vary significantly, and the choice of correlation temperature presents no difficulties. For a typical beam floor assembly, on the other hand, the temperature distribution over the cross-section at an arbitrary moment will be in the range 50 - 200°C, /13/, /30/. Experimental and theoretical experience suggest that for a fire-exposed steel column and steel beam with the same effective κ -value, there will be close agreement between the average maximum steel temperature T_{ac} of the column and the average T_{afw} of the maximum lower flange and web temperatures of the beam. No actual measurements for beams and columns with identical κ -values exposed to the same natural fire process exist. The hypothesis is based on the fact that the heat flow analysis, as used in the manual, gives correspondence between computed and experimental T_{ac} -values (see Figure 3.2.4a) and between computed and experimental T_{afw} -curves (see Figure 3.2.4b).

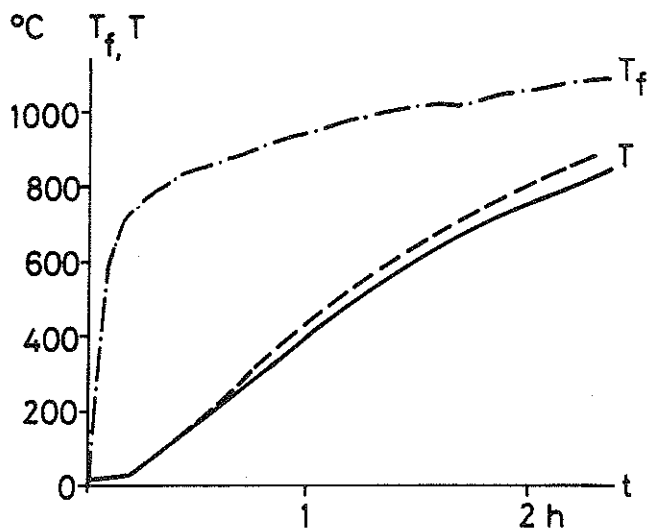


Figure 3.2.4a Measured (—) and calculated (----) average time curve of fire exposed steel column /5/. -·-·- denotes the gastemperature-time curve /5/.

3.3 Uncertainty in load-carrying capacity ψ

As described in section 1.4, the predicted design capacity ψ_n of a simply supported fire-exposed girder is given by Figure 1.4a for a known maximum steel temperature and rate of heating. The true resistance R of the beam is here expressed in the following form

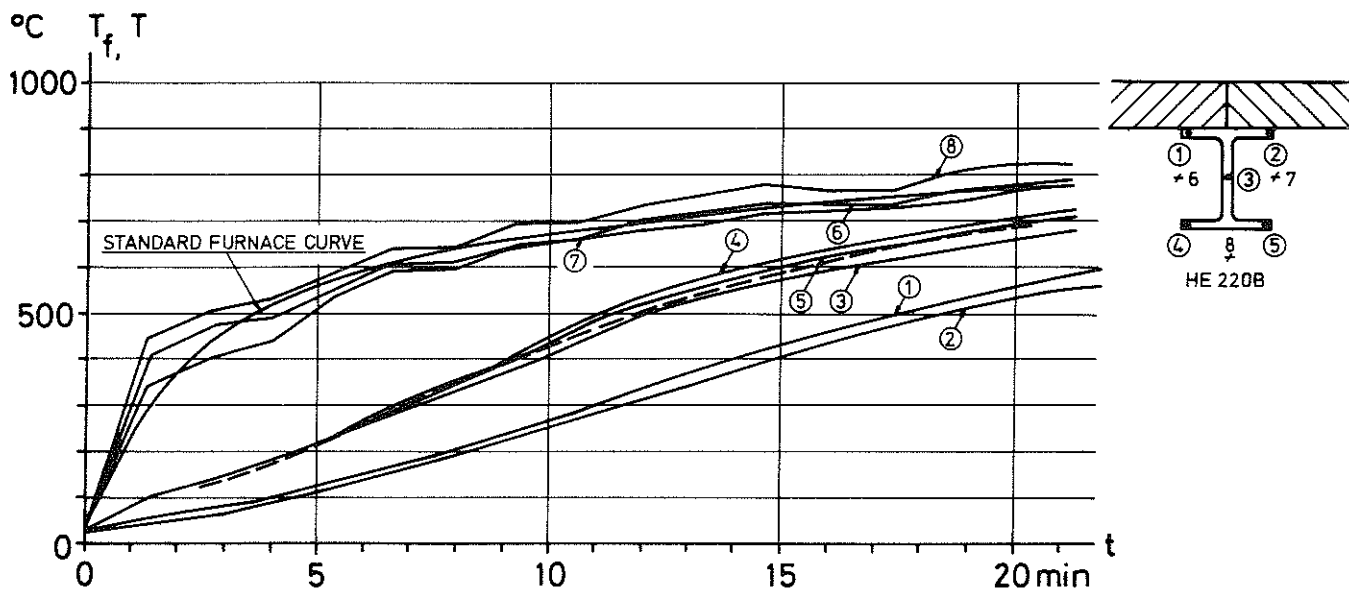


Figure 3.2.4b Measured and calculated (-----) steel temperature-time curves for fire exposed steel beam /5/.

$$R = (\varphi_n + \Delta\varphi_1 + \Delta\varphi_2) \cdot M \quad (3.3a)$$

where

$\Delta\varphi_1$ = the uncertainty measured by a comparison between the theoretical value φ_n and laboratory tests. $\Delta\varphi_1$ is based on known values of yield strength at room temperature, but includes scatter due to variability of material properties at elevated temperature, creep parameters etc.

$\Delta\varphi_2$ = the uncertainty due to the difference between laboratory tests and "in situ" fire exposure.

M = random factor, expressing uncertainty in material strength, expressed as yield strength at room temperature.

The reasons for choosing a mainly additive rather than multiplicative form are the same as in section 3.2. Eq. 3.3a implies that the proportional dependence of capacity on yield strength will be independent of temperature.

3.3.1 Error Term $\Delta\psi_1$

The randomness in the true resistance may be evaluated from experimental tests. Usually these investigations are not performed as natural fire tests but take place in a testing furnace, heated according to some predetermined temperature-time curve. As basis for the evaluation of the scatter in the n -values given by Eq. 1.4a, 41 tests performed under the auspices of CECM at "Institut für Baustoffkunde und Stahlbetonbau der Technischen Universität" at Braunschweig, Germany and "Station Experimentale d'Essais au Feu", Maizières-lès-Metz (France), /31/, were evaluated. The steel quality was Fe 37 (E 24) and E 36, with the real yield strength at room temperature determined with test pieces taken from each tested beam. The beams had I-cross-sections with the form factor determined in each individual case. The failure or critical temperature was determined with reference to three different limit states (c.f. Eq. 1.4a)

$$\frac{\Delta f}{\Delta t} = \frac{l^2}{9000 h} \quad (3.3.1a)$$

$$f = l/30 \quad (3.3.1b)$$

$$\frac{\Delta f}{\Delta t} \rightarrow \infty \quad (3.3.1c)$$

The second and third criteria yielded nearly identical critical temperatures. All three criteria define an ultimate limit state. Figure 3.3.1a gives the cumulative distribution of $\Delta\psi_1$ evaluated with respect to the limit states defined by Eqs. 3.3.1b-c (curve 1) and Eq. 3.3.1a (curve 2). For curve 1, sample mean and standard deviation are

$$\overline{\Delta\psi_1} = 0.143 L_e \quad (3.3.1d)$$

$$\sigma_{\Delta\psi_1} = 0.091 L_e \quad (3.3.1e)$$

These values are based on the assumption, earlier motivated, of equivalence between column steel temperatures and the average of the lower web and flange steel beam temperatures. The relatively large difference between design and experimental load-carrying capacity is explained by the computational assumptions made in the design case. The design

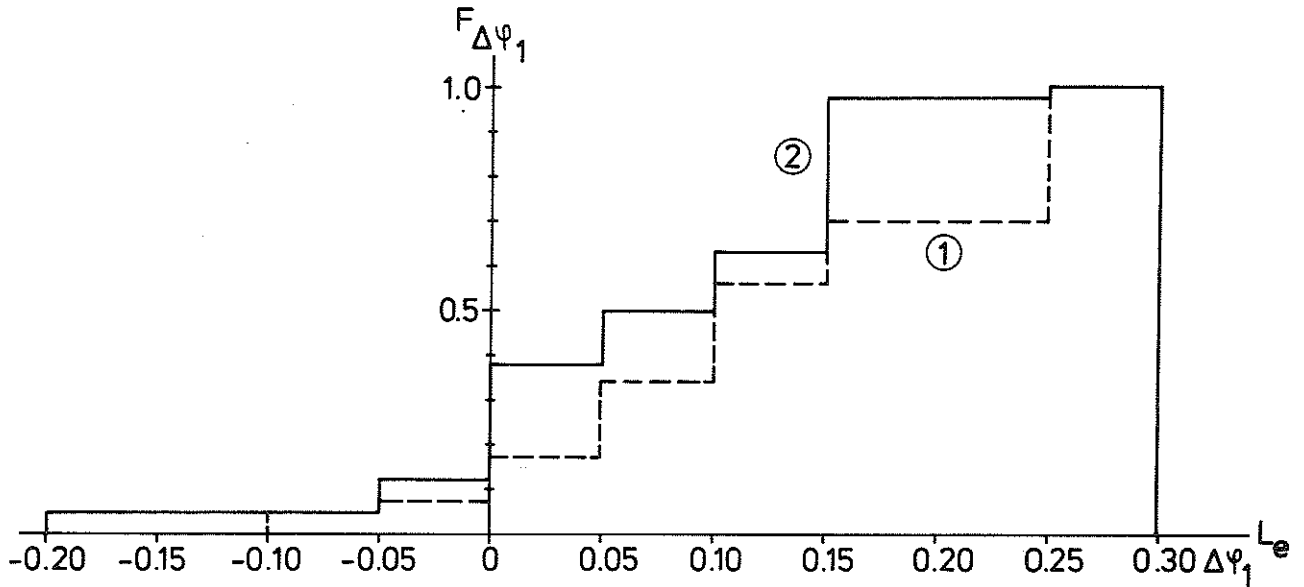


Figure 3.3.1a Cumulative distribution function for the uncertainty term $\Delta\psi_1$. Curve ① refers to an ultimate limit state according to Eqs. 3.3.1b-c and curve ② to a limit state defined by Eq. 3.3.1a.

curves are valid for a complete fire process, the decay period included, while in the experiments the furnace temperature was kept rising until failure occurred. The ψ_n -values presuppose that the failure condition is expressed by Eq. 1.4a and that steel temperature is constant longitudinally and over the cross section. The influences of a variation of these conditions have been investigated in /13/ and are not at odds with the $F_{\Delta\psi_1}$ -curves given in Figure 3.3.1a.

The statistics of $\Delta\psi_1$ expressed by Eqs. 3.3.1d-e are valid within a temperature range of 500 - 600°C. Using these values unchanged for lower temperatures leads to estimates of load-carrying capacities R at room temperature which are too high. Taking the small prediction error valid for simple bending failures of I-cross sections at room temperatures into account, the random variable $\Delta\psi_1$ has been multiplied by a temperature-dependent random factor $C_{\Delta\psi_1}$ where

$$C_{\Delta\psi_1} = T_{\max}/550 \quad (3.3.1f)$$

to get the effective error term $\Delta\varphi_{1,eff}$

$$\Delta\varphi_{1,eff} = C_{\Delta\varphi_1} \cdot \Delta\varphi_1 \quad (3.3.1g)$$

3.3.2 Error Term $\Delta\varphi_2$

The term $\Delta\varphi_2$ should cover uncertainties created by the transition from test condition to actual service condition. The difference can be attributed to the change taking place unintentionally in loading and restraint characteristics. In practice, the beam is invariably a substructural element in a floor or roof assembly. The assembly, e.g. a beam-concrete slab construction, can be designed for composite or non-composite load-carrying function. Even in the non-composite case, i.e. when the beam is assumed to provide the resistance to applied bending moments without assistance from the concrete slab, friction and mechanical fastening device between beam and slab provide for an interaction, what is called a pseudo-composite beam-slab /30/. It was shown in /30/ that for floor-systems constructed truly without any end-restraints (moments and axial forces) brought in during fire exposure, the fire resistance rating, i.e. the value of the critical steel temperatures, were nearly identical in the three (non-composite, pseudo-composite and composite) cases for loading levels producing design allowable stresses. This implies that if the restraint forces brought into a simply-supported beam-slab assembly during the fire exposure are negligible, no added uncertainty will be created due to different design specification for the beam-slab interaction.

It remains to investigate the case when accidental restraint forces are brought into the structural system, in some cases producing local instability phenomena, in other cases actually increasing the fire endurance /13/. The relative frequency of the occurrence as well as the magnitude of unintentional restraint forces remains unknown. For an evaluation of the influence on the critical temperature or critical loading level of specified restraint forces, the investigations in /13/ and /30/ provide a good insight. Based on these works, the sample mean and standard deviation of the uncertainty term $\Delta\varphi_2$ has been subjectively given the following values

$$\overline{\Delta\psi}_2 = 0 \quad (3.3.2a)$$

$$\sigma_{\Delta\psi}_2 = 0.10 L_e \quad (3.3.2b)$$

3.3.3 Material Variability Term M

Extensive investigations have been made regarding the scatter in yield strength of mild structural steel at room temperature. Based on literature reports /36/, the following statistics have been chosen for M

$$\overline{M} = 1.1 \quad (3.3.3a)$$

$$\sigma_M = 0.1 \quad (3.3.3b)$$

3.4 Live and Dead Load Characteristics

In /32/ are listed some important load combinations

1. Dead load + lifetime maximum live load
2. Dead load + arbitrary-point-in-time sustained live load + lifetime maximum wind load
3. Dead load + lifetime maximum live load + daily maximum wind load
4. Dead load + arbitrary-point-in-time sustained live load + lifetime maximum snow load + annual (or seasonal) maximum wind load
5. Dead load + arbitrary-point-in-time sustained live load + annual maximum snow load + lifetime maximum wind load.

To this list one may add a load combination expressing the loading conditions at fire outbreak

6. Dead load + arbitrary-point-in-time sustained live load + daily maximum wind load + annual maximum snow load.

Live load statistics are taken from /33/. Table 3.4a expresses the dependence of the average live load on the tributary area. These values include loads due to personnel. During a fire outbreak, it

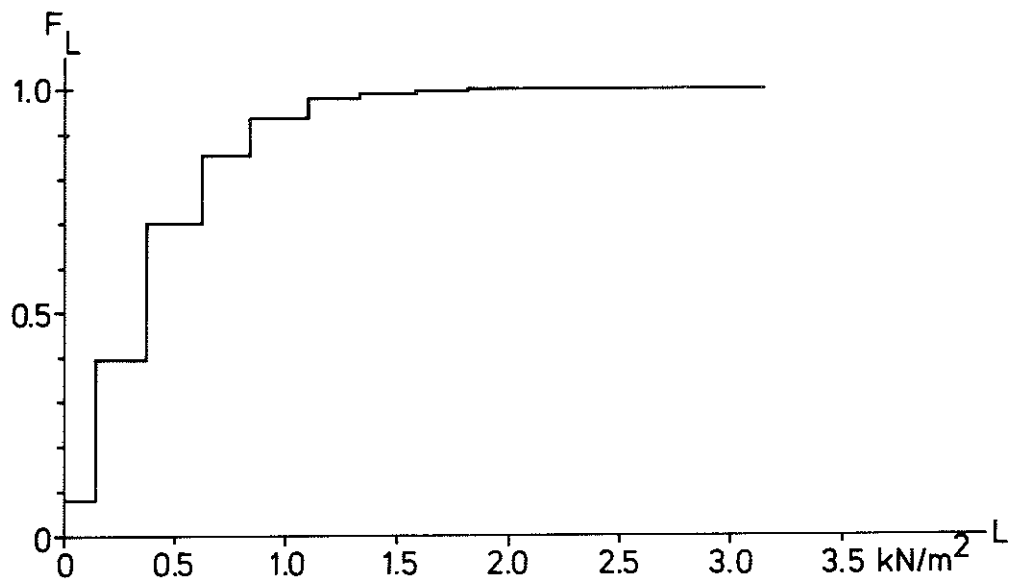


Figure 3.4a Cumulative distribution function of live load in office building /33/, valid at fire out-break. Mean bay area = 31.2 m².

seems reasonable to assume that people will move from those parts of the building in direct contact with the fire. In this paper, the live load statistics will be valid for a mean bay area = 31.2 m². Figure 3.4a gives the cumulative distribution curve of the live load for this bay size group, assuming that 5 people of mean weight 662 N are working in such an area. The average live load \bar{L} and the coefficient of variation V_L will then be, assuming that σ_L in Table 3.4a is unchanged

$$\bar{L} = 0.507 \text{ kN/m}^2 \quad (3.4a)$$

$$V_L = 0.68 \quad (3.4b)$$

The load effect S is written as

$$S = S_D + S_L = E(L + D) \quad (3.4c)$$

Taking the values given in /26/, it may be assumed that the mean

and coefficient of variation (c.o.v.) of the live and dead load effect are

$$\bar{E} = 1.0 \quad (3.4d)$$

$$V_E = 0.1 \quad (3.4e)$$

The random variable E accounts for both uncertainty due to load concentration effects and the dispersion in load effect prediction, assuming uniformly distributed load.

For the random variable D, the following values have been estimated
/26/

$$\bar{D} = D_n \quad (3.4f)$$

$$V_D = 0.04 \quad (3.4g)$$

4. Numerical Methods. Monte Carlo Technique

4.1 Basic Numerical Methods

The preceding sections have provided the basic data necessary for a safety analysis. It remains to find a suitable numerical solution method. Realizing that exact mathematical analysis in closed form is not possible, there seems to be two possible ways open

- Observing that the $q_n - T_n$ and $T_n - \varphi_n$ -curves are rather "flat" functions, the first order uncertainty analysis, described in section 2.4.5, may give results of required accuracy.
- Prescribe distribution functions for those stochastic parameters where statistical information is lacking and evaluate the multi-dimensional integral Eq. 2.1d with aid of Monte Carlo sampling technique.

The advantages with the Monte Carlo method are several:

- the method has intuitive appeal and is easy to understand
- it can easily be adapted to changing problem formulations
- it gives in its basic or crude application few programming problems
- it leaves as final result both probability density functions of R and S and the value of P_f .

Among the disadvantages are:

- the method requires a computer and a great deal of computer time at a considerable cost
- the final output, i.e. the probability density functions of R and S, does not give any systematic indication of how the system uncertainty depends on the uncertainty in the different components such as ΔT_1 , ΔT_2 , ΔT_3 , $\Delta \varphi_1$, $\Delta \varphi_2$, etc
- the accuracy is difficult to check.

For these reasons it is generally advised to use the method only as a last resort when more elegant methods fail to produce results.

In this case, use of Monte Carlo procedures seems inevitable since there is no other way of checking more approximate methods. The remaining part of this section will be used to specify the formation of a suitable Monte Carlo simulation model. The Taylor-expansion analysis will be illustrated in section 5.

4.2 Monte Carlo Technique

4.2.1 Foundations

As used in this paper, the Monte Carlo method will involve a large number of simulations of the real physical process, with each step in the sampling model matching the circumstances envisioned in the original problem. Each step or trial in the Monte Carlo implies a random drawing from a specified probability distribution. A convenient and most commonly used procedure is to draw a uniformly distributed pseudorandom number d_u

$$F_{d_u}(d_u) = \begin{cases} 0, & d_u < 0 \\ d_u, & 0 \leq d_u \leq 1 \\ 1, & d_u > 1 \end{cases} \quad (4.2.1a)$$

using any of the well-established methods generating numbers that pass reasonable statistical tests of randomness. To transform the value d_u to a value X with the required cumulative distribution function $F_X(X)$, we have to solve the equation

$$d_u = F_X(X) \quad (4.2.1b)$$

which also can be written

$$X = F_X^{-1}(d_u) \quad (4.2.1c)$$

where F_X^{-1} is the inverse of F_X .

The solution of Eq. 4.2.1b is graphically illustrated by Figure 4.2.1a.

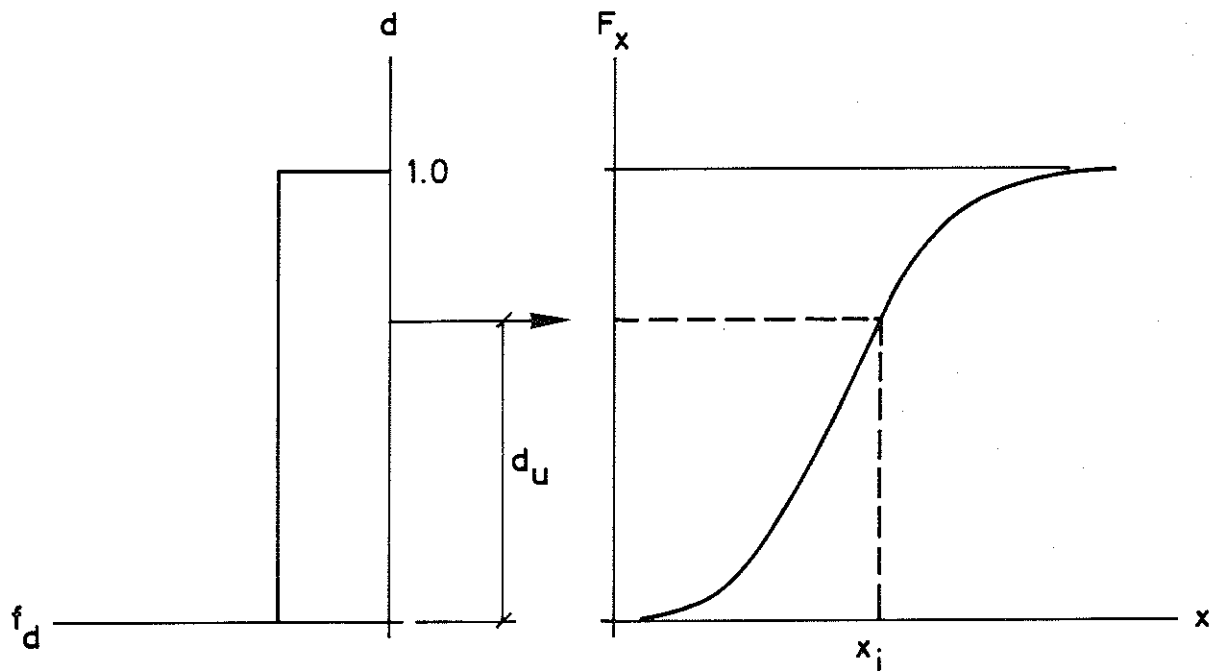


Figure 4.2.1a Sampling procedure

4.2.2 Simulation procedure

The simulation procedure is outlined in Figure 4.2.2a. Because of the close identification between the different steps in the simulation play and the actual physical process, the flow chart should be largely self-explanatory. Each circle denotes a random drawing from the cumulative distribution function specified. The following is an enumeration of the equations referred to in the flow chart, valid for the k :th play of a game.

$$q_{\text{eff}}^{(k)} = q^{(k)} \Delta q^{(k)} \quad (4.2.2a)$$

$$T_{\kappa_n}^{(k)} = T_n(q_{\text{eff}}^{(k)}, A\sqrt{h}/A_t, k_f, \kappa_n) \quad (4.2.2b)$$

$$\kappa_{\text{eff}}^{(k)} = \frac{A_i}{V_s} \cdot \frac{\lambda_i^{(k)}}{d_i^{(k)}} \quad (4.2.2c)$$

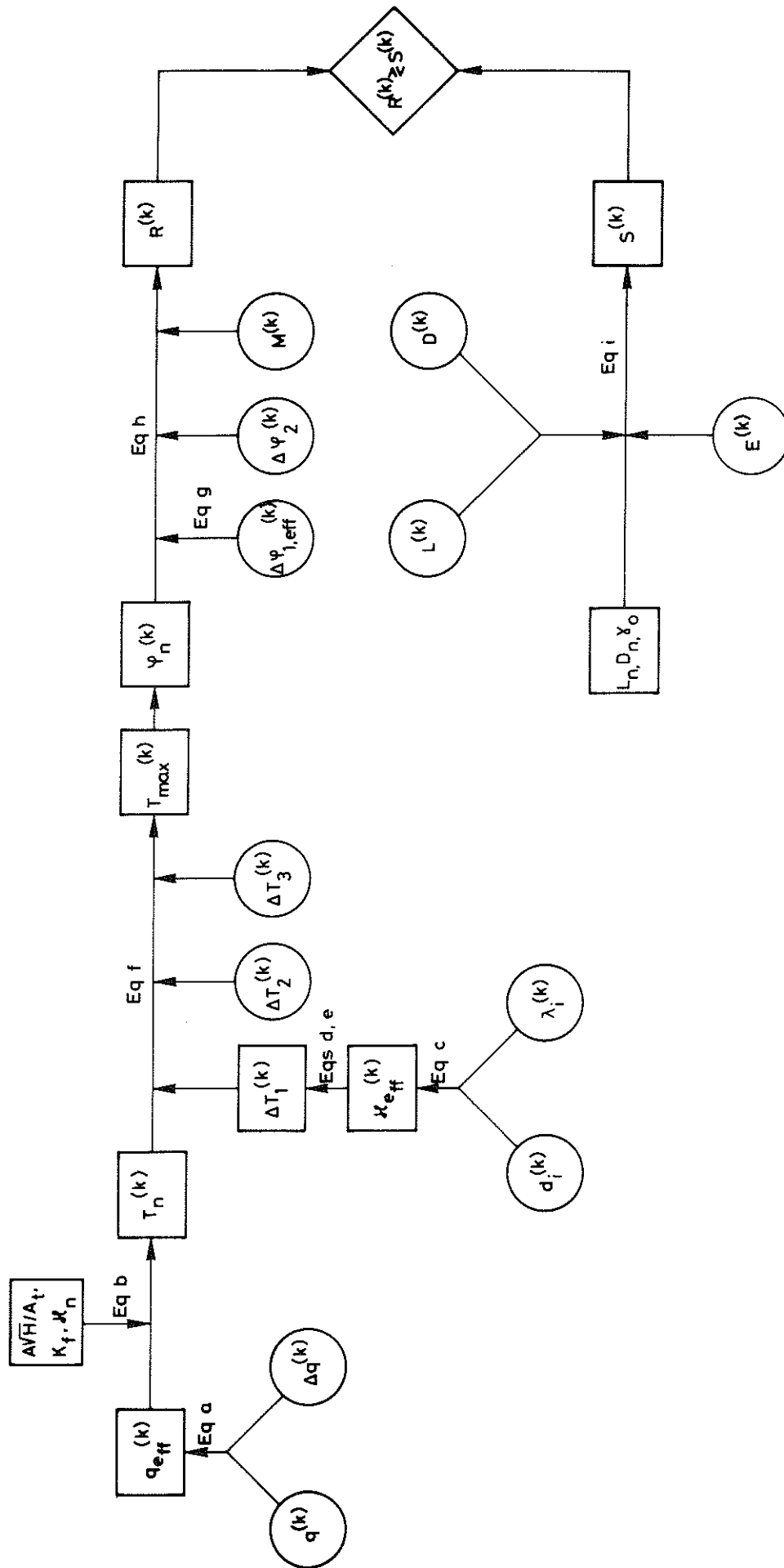


Figure 4.2.2a Simulation procedure. Each circle denotes a random sampling. Eq. a corresponds to Eq. 4.2.2a, etc.

$$T_{\kappa_{\text{eff}}}^{(k)} = T_n(q_{\text{eff}}^{(k)}, A\sqrt{h}/A_t, k_f, \kappa_{\text{eff}}^{(k)}) \quad (4.2.2d)$$

$$\Delta T_1^{(k)} = T_{\kappa_{\text{eff}}}^{(k)} - T_{\kappa_n}^{(k)} \quad (4.2.2e)$$

$$T_{\text{max}}^{(k)} = T_{\kappa_n}^{(k)} + \Delta T_1^{(k)} + \Delta T_2^{(k)} + \Delta T_3^{(k)} \quad (4.2.2f)$$

$$\Delta \varphi_{1,\text{eff}}^{(k)} = T_{\text{max}}/550 \Delta \varphi_1^{(k)} \quad (4.2.2g)$$

$$R^{(k)} = (\varphi_n^{(k)} + \Delta \varphi_{1,\text{eff}}^{(k)} + \Delta \varphi_2^{(k)}) M^{(k)} \quad (4.2.2h)$$

$$S^{(k)} = \frac{E^{(k)} \cdot (L^{(k)} + D^{(k)})}{\gamma_o (L_n + D_n)} \quad (4.2.2i)$$

4.3 Results of Monte Carlo Simulation

The simulation procedure described in section 4.2.2 has been programmed and run on a Univac 1108-computer. In general, each simulation game has consisted of 5000 plays. In each game, a seven-digit number has been used to denote the specific parameter combination for that particular game. Digit No. 1 denotes value of insulation parameter κ

1	means $\kappa_n =$	290 W/m ³ °C (250 kcal/m ³ h °C)
2	" $\kappa_n =$	580 W/m ³ °C (500 kcal/m ³ h °C)
3	" $\kappa_n =$	1160 W/m ³ °C (1000 kcal/m ³ h °C)
4	" $\kappa_n =$	2320 W/m ³ °C (2000 kcal/m ³ h °C)
5	" $\kappa_n =$	4640 W/m ³ °C (4000 kcal/m ³ h °C)
6	" $\kappa_n =$	9320 W/m ³ °C (8000 kcal/m ³ h °C)

Digit No. 2 denotes value of opening factor $A\sqrt{h}/A_t$

1	means $A\sqrt{h}/A_t =$	0.04 m ^{1/2}
2	" $A\sqrt{h}/A_t =$	0.08 m ^{1/2}

3 means $A\sqrt{h}/A_t = 0.12 \text{ m}^{1/2}$

Digit No. 3 denotes combination of means and c.o.v. for effective value of d_i and λ_i compared with design values

1 means $(d_i ; \lambda_i) = (1.0, 0.0)d_{i,n} ; (1.0, 0.0)\lambda_{i,n}$

2 " $(d_i ; \lambda_i) = (1.0, 0.1)d_{i,n} ; (1.0, 0.1)\lambda_{i,n}$

3 " $(d_i ; \lambda_i) = (1.0, 0.2)d_{i,n} ; (1.0, 0.2)\lambda_{i,n}$

4 " $(d_i ; \lambda_i) = (1.0, 0.0)d_{i,n} ; (1.0, 0.2)\lambda_{i,n}$

Digit No. 4 denotes mean value and standard deviation of random variable Δq

1 means $\Delta q = (1.0, 0.0)$

2 " $\Delta q = (0.70, 0.15)$

Digit No. 5 denotes choice of limit state

1 means that $F_{\Delta R_1}$ is represented by curve 1 in Figure 3.3.1a

2 " that $F_{\Delta R_1}$ is represented by curve 2 in Figure 3.3.1a

Digit No. 6 denotes ratio design dead load / design live load in the allowable stress design for non-fire load combination. 1 means $D_n/L_n = 1/3$, 2 means $D_n/L_n = 1$, 3 means $D_n/L_n = 3$.

Digit No. 7 used as reserve.

The following variables have been the same throughout all simulations

- cumulative distribution curve of fire load density, see Figure 1.5.1a
- the correction term ΔT_2 , see Figure 3.2.2c
- the correction term $\Delta \psi_1$, see Figure 3.3.1a
- cumulative distribution curve of live load acting at an arbitrary moment in time; see Figure 3.4a
- the c.o.v. V_E of the live load and dead load effect prediction (equation error term) is assumed to be 0.10 in both cases. C.f.

Eq. 3.4e

- the mean dead load is taken equal to the design value with the c.o.v. $V_D = 0.04$, see Eq. 3.4f-g
- in all cases where a distribution function has not been measured or otherwise prescribed, the random variable has been assumed to be normally distributed.

Tables 4.3a, 4.3c will provide the basic, stochastically important parameters resulting from a Monte Carlo simulation game.

4.3.1 Variation of β_C and β_{ER} with κ , $A\sqrt{h}/A_t$ and D_n/L_n

The variation of the safety-index β_{ER} with the nominal value of the insulation parameter κ is given in Figure 4.3.1a for three different values of the opening factor. In all cases $D_n/L_n = 3$. Figures 4.3.1b-d show how the safety-index β_C varies with the ratio D_n/L_n for $A\sqrt{h}/A_t$ again = 0.04, 0.08 and 0.12 $m^{1/2}$ respectively. Figure 4.3.1e illustrates the dependence of the f_R - and f_S -curves, i.e. the relative frequency distribution curves of R and S, on the D_n/L_n -ratio and the κ_n -value. The $A\sqrt{h}/A_t$ -value = 0.08 $m^{1/2}$. Some tentative conclusions may be drawn from Tables 4.3a-c and Figures 4.3.1a-e

- the ratio D_n/L_n will quite unintentionally be a factor of basic importance in determining the safety level
- the influence of the size of ventilation factor cannot be ignored in a proper design procedure

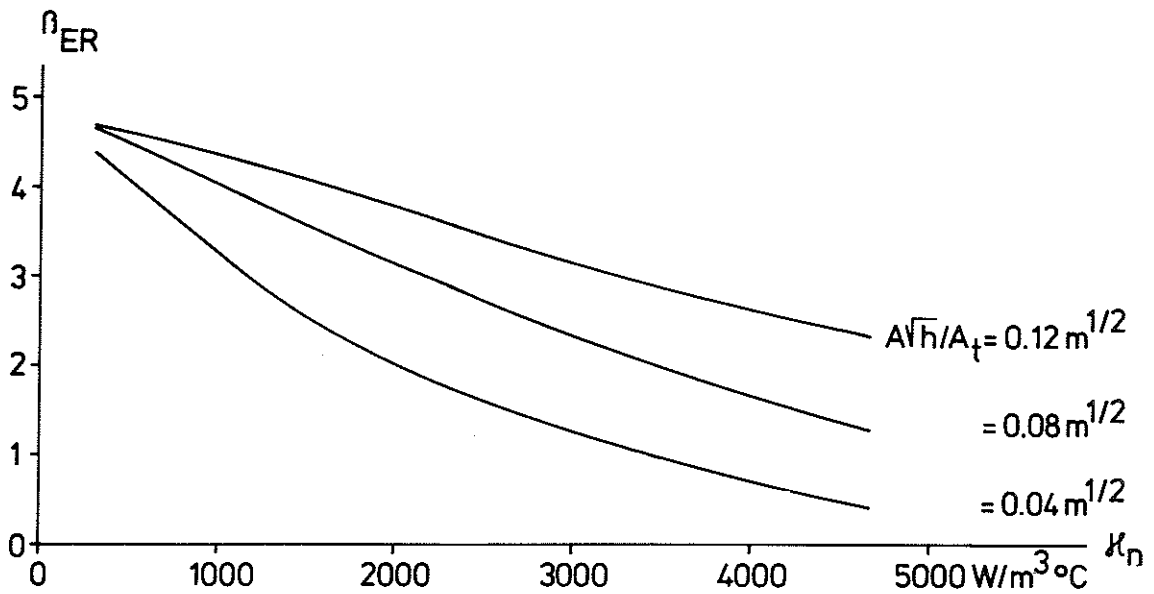


Figure 4.3.1a The variation of safety index β_{ER} with insulation parameter κ and opening factor $A\sqrt{h}/A_t$. $D_n = 6.0 kN/m^2$, i.e. $D_n/L_n = 3$

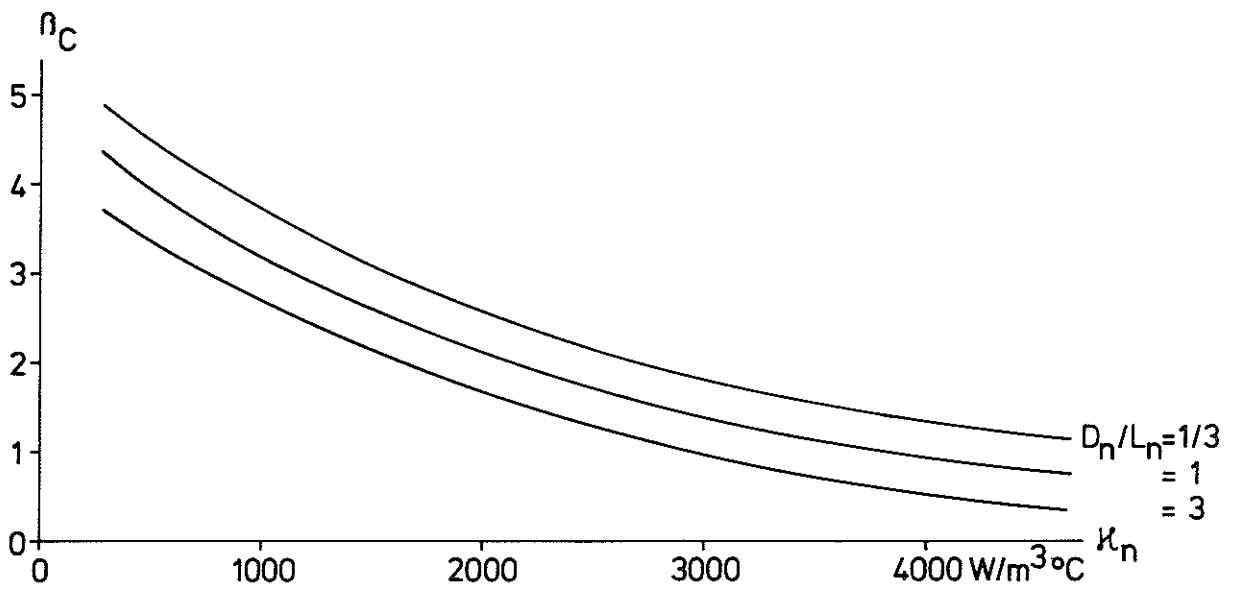


Figure 4.3.1b The variation of safety index β_C with insulation parameter κ and ratio D_n/L_n for opening factor $A\sqrt{h}/A_t = 0.04 m^{1/2}$.

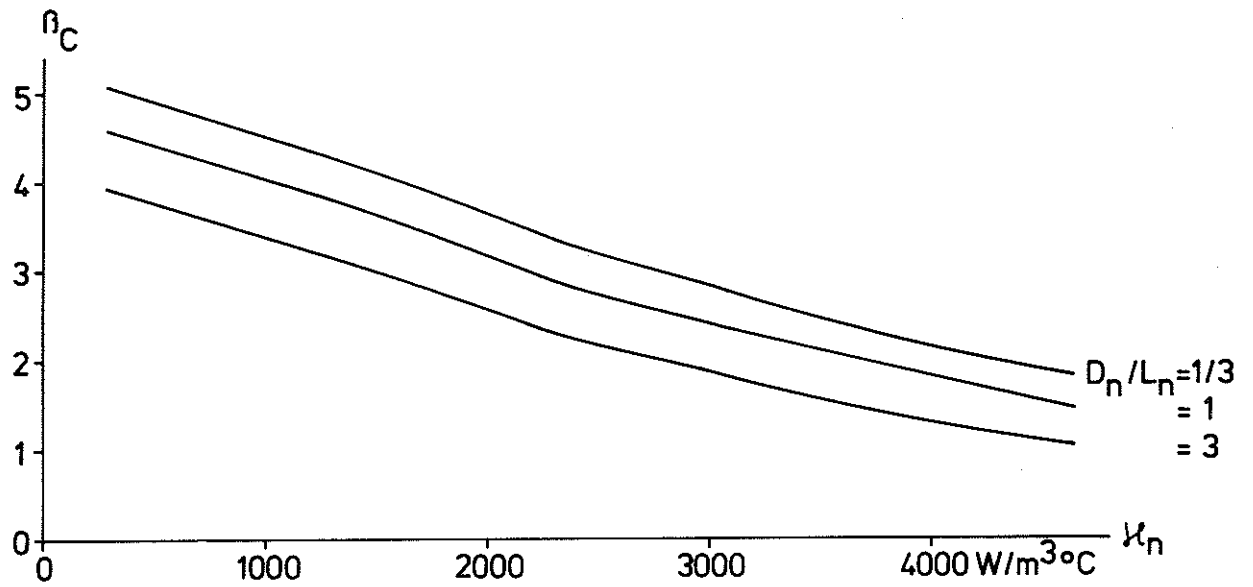


Figure 4.3.1c The variation of safety index β_C with insultaion parameter κ and ratio D_n/L_n for opening factor $A\sqrt{h}/A_t = 0.08 \text{ m}^{1/2}$

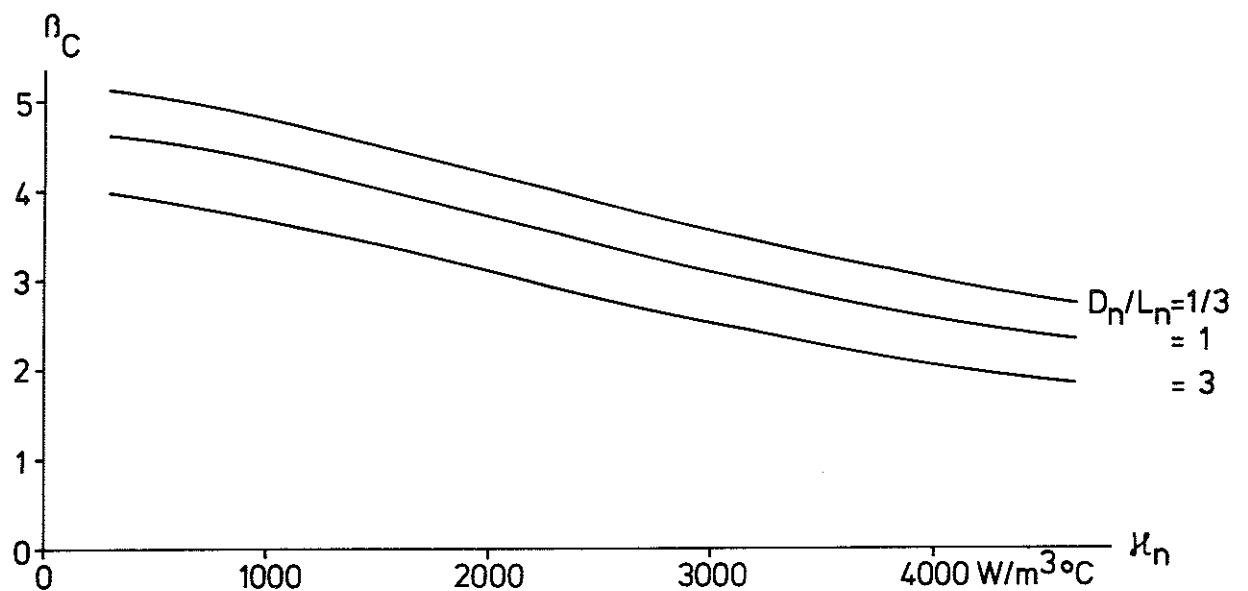


Figure 4.3.1d The variation of safety index β_C with insulation parameter κ and ratio D_n/L_n for opening factor $A\sqrt{h}/A_t = 0.12 \text{ m}^{1/2}$

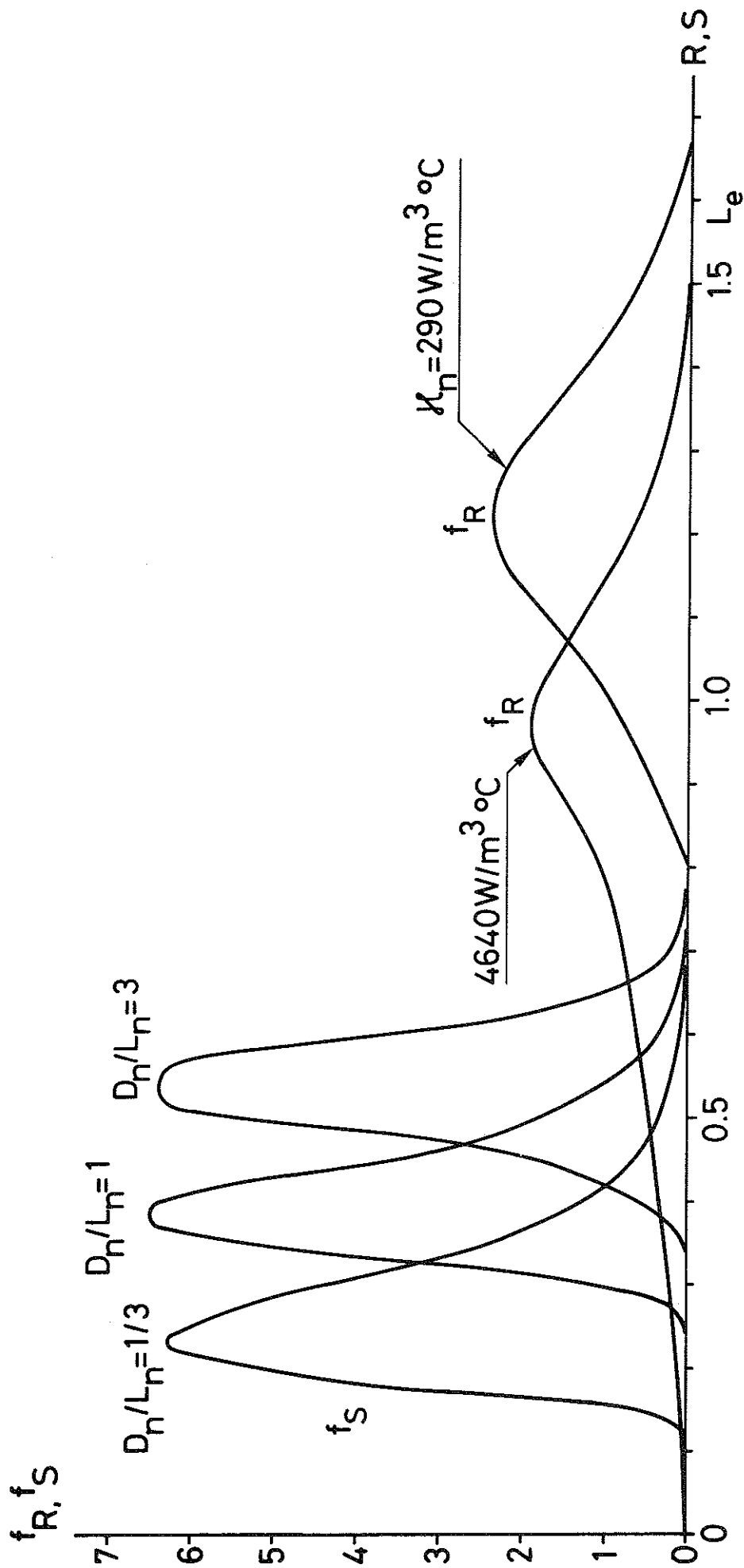


Figure 4.3.1e Relative frequency distribution functions f_R and f_S obtained by simulation.
 Opening factor $A\sqrt{h}/A_t = 0.08 \text{ m}^{1/2}$

4.3.2 Variation of β_C with Uncertainty in Fire Load Statistics q and Uncertainty in Insulation Parameter κ

Some random parameters in the simulation procedure had to be estimated subjectively, notably the d_i - and λ_i -variables of the κ -value and the variable Δq in Eq. 3.1c, describing uncertainty in fire load statistics. A measure of how the final safety level is affected by a change in these estimates is given by the curves in Figure 4.3.2a.

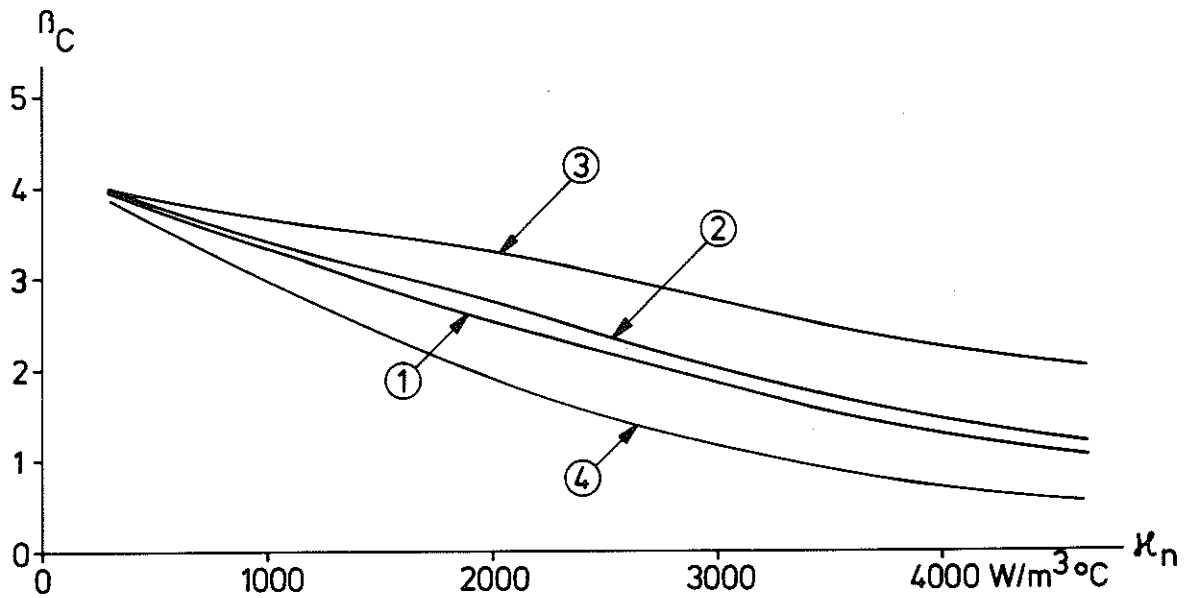


Figure 4.3.2a Variation of safety index β_C with insulation parameter κ_n as a function of variability in κ_n -value and Δq (uncertainty of fire load statistics)

Curve 1: is taken from Table 4.3b

Curve 2: the same input as curve 1 with one exception, the random variable κ_{eff} has mean and variance = $(\kappa_n, 0)$

Curve 3: the same input as curve 2, but with the mean and standard deviation of Δq changed to

$$\overline{\Delta q} = 0.7 \quad (4.3.2a)$$

$$\sigma_{\Delta q} = 0.15 \quad (4.3.2b)$$

Curve 4: the same input as curve 3, but with mean and standard deviation of Δq changed to

$$\overline{\Delta q} = 1.3 \quad (4.3.2c)$$

$$\sigma_{\Delta q} = 0.3 \quad (4.3.2d)$$

The D_n/L_n -values for all curves = 3.

The four curves of Figure 4.3.2a indicate that minor variations in the characteristics of the fire protective material are tolerable and that an accurate specification of the combustion characteristics of different authentic fire load exposures is of vital interest in assessing the probability of failure level.

4.3.3 Relevance of Distribution-Free Design Formats

The three right columns in Tables 4.3a-c give values of P_f computed in three different ways: the percentage of simulation plays for which $S^{(k)} > R^{(k)}$, c.f. Eqs 4.2.2h-i, by assuming that the random variable $R-S$ is normally distributed and using Eq. 2.2b and, finally, by taking $\ln(R/S)$ to be a normally distributed variate and applying Eq. 2.3b. We define $P_{f,c}$ and $P_{f,ER}$ by

$$P_{f,c} = \Phi(-\beta_C) \quad (4.3.3a)$$

$$P_{f,ER} = \Phi(-\beta_{ER}) \quad (4.3.3b)$$

where $\Phi(\)$ denotes the cumulative distribution function of a standard normal variate.

Visual inspection of Figure 4.3.1e gives the impression that the central parts of the frequency function of R is not far from normal, justifying use of Eq. 2.2b, except that the long left hand tail of f_R will substantially increase the actual value of P_f . Thus it is only natural that evaluating P_f by stipulating that $R-S$ is a normal variate will lead to values on the unsafe side. Tables 4.3a-c confirm this conclusion.

Equation 4.3.3a has been evaluated neglecting the fact that functionally the value of R cannot be < 0 .

Regarding the Esteva-Rosenblueth format, the general form of the log-normal distribution with a long righthand tail makes it likely that there will be a significant difference between P_f -values obtained by simulation and the corresponding $P_{f,ER}$ -values. From Tables 4.3a-c it can further be deduced that a higher D_n/L_n -ratio implies an increase in the actual P_f -value. Logically, the corresponding values of safety index should decrease. Also for this reason, use of the second moment reliability format according to Cornell seems in this special case to be more functionally justified. As a consequence, a formulation of the safety index according to Eq. 2.4.3a will be preferred for the rest of the paper.

The difference or inconsistency between simulated P_f on one hand and $P_{f,ER}$ and $P_{f,C}$ on the other illuminates the uncertainty introduced in a design format based on distribution-free methods.

Probability of failure is the quantitative measure of risk and thus the fundamental parameter. For this reason, it may be appropriate to try to preserve the conciseness and elegance of the safety-index formulation and at the same time adjust the value of β_C obtained for example in a first-order second moment analysis with regard to the actual form of the distribution function F_U in Eq. 2.2b. For economic reasons, this should preferably be done without recourse to a full-size Monte Carlo simulation game. Future optimization studies will, to be effective, probably require the development of approximate methods to be used in this connection.

4.4 Confidence Bounds of Simulation Statistics

Sampling theory studies the relationships existing between a population and samples taken from that population. The theory can be used to estimate unknown population parameters (mean, standard deviation) from the corresponding sample quantities. The latter are often called sample statistics or just statistics.

The pseudo-random numbers used in the simulation procedure are generated recursively through an arithmetic process. A random number H_{n+1} is given through the formula

$$H_{n+1} = H_n(2^{18} + 3) \bmod 2^{35} \quad (4.4a)$$

The procedure is called the multiplicative congruence method. A sequence is uniquely determined by the initial value H_0 . Every simulation game described in this paper has used the same starting value H_0 . If for a given physical situation (identification number in Tables 4.3a-c) M different simulation games had been performed, each with a new value of H_0 , the produced estimates \bar{R}^* , σ_R^* etc. of the true parameters \bar{R} , σ_R would have changed from one game to another. In other words, each sample statistic will have a distribution which is called the sampling distribution of the statistic.

Intuitively, the variance of this distribution will decrease with increasing N. We analyze the sample statistic \bar{R} first. The central limit theorem states that for reasonable large values of N the sampling distribution of the sample mean \bar{R}^* is approximately normal (see e.g. /34/) with

$$E(\bar{R}^*) = \bar{R} \quad (4.4b)$$

where $E(\)$ denotes the expected value.

$$\text{Var}(\bar{R}^*) = \sigma_R^2/N \quad (4.4c)$$

The quantity $\text{Var}(\bar{R}^*)$ is the uncertainty inherent in the sampling procedure. The literature describes a number of variance-reducing sampling methods (correlated sampling, importance sampling, stratified sampling etc.) as opposed to the "crude" or "naive" sampling technique employed here.

With $N = 5000$, the assumption of a normally distributed sample mean is certainly valid, implying that interval estimates of the parameter \bar{R} are easily and accurately made. If

$1 - \alpha =$ chosen confidence interval

$Z_{1-\alpha/2}$ = the $(1 - \alpha/2) \cdot 100$ per cent point of the standard probability distribution

a confidence bound for \bar{R} is given by

$$\bar{R}^* - Z_{1-\alpha/2} \frac{\sigma_R^*}{\sqrt{N}} \leq \bar{R} \leq \bar{R}^* + Z_{1-\alpha/2} \frac{\sigma_R^*}{\sqrt{N}} \quad (4.4d)$$

with \bar{R}^* , \bar{R} and σ_R^* expressed in L_e -units.

An example: For game No. 4131110 we can state (somewhat imprecisely) that \bar{R} is between $(0.922 \pm 1.96 \frac{0.268}{\sqrt{5000}})$, i.e. (0.922 ± 0.007) , with a confidence level of 95 per cent. For a 99.9 per cent confidence level, the corresponding estimate band would be

$$(0.922 \pm 3.29 \frac{0.268}{\sqrt{5000}}), \text{ i.e. } (0.922 \pm 0.012)$$

The procedure may be reversed to determine the number of plays necessary for a certain confidence interval. Denoting the maximum allowable error in \bar{R} by δ , we have

$$N = \left(\frac{Z_{1-\alpha/2} \cdot \sigma_R^*}{\delta} \right)^2 \quad (4.4e)$$

If $\delta = 0.01$ (L_e -units) and the confidence level 99.9 per cent, $N = \left(\frac{3.29 \cdot 0.268}{0.01} \right)^2 \approx 7800$. The precision of Eq. 4.4e is dependent on the accuracy of the initial estimate σ_R^* of σ_R .

Similarly, statistical theory shows that for large N

$$E(\sigma_R^*) \approx \sigma_R \quad (4.4f)$$

$$\text{Var}(\sigma_R^*) \approx \frac{\sigma_R^2}{2N} \quad (4.4g)$$

Using Eqs. 2.4.5a-b, it is now possible to approximatively compute the sampling variance of the safety index values listed in Tables 4.3a-c as a function of N . For $N = 5000$ the variability in β_C or β_{ER} due to sampling error may be considered negligible.

The next problem will be to give confidence intervals for the failure probability P_f . The basic statistical distribution function used in this connection is the binominal probability density function

$f_b(x, p, N)$, which gives the probability of exactly x successes, $x = 0, 1, 2 \dots N$, in N independent trials if the probability of success in a single play is p .

$$f_b(x, p, N) = \binom{N}{x} p^x (1-p)^{N-x} \quad (4.4h)$$

The probability of k or fewer successes in N trials is given by the cumulative distribution function $F_b(k, p, N)$

$$F_b(k, p, N) = \sum_{x=0}^k \binom{N}{x} p^x (1-p)^{N-x} \quad (4.4i)$$

It follows that the problem of estimating the accuracy (as measured by its standard error) of the estimate of the probability of failure P_f , given by a Monte Carlo simulation of N plays, is the same as estimating the value of the parameter p of a binominal distribution.

A more convenient way is to use the fact that for large values of N the probability density function f_b is approximated by the normal probability density function with the mean μ and variance σ^2 given by

$$\mu = Np \quad (4.4j)$$

$$\sigma^2 = Np(1-p) \quad (4.4k)$$

provided that Np and $N(1-p)$ both are > 5 . When the normal distribution approximation is not adequate, one can sometimes use a Poisson approximation instead.

The sample statistics given by Eqs. 4.4j-k may be used to give confidence bounds on P_f and the number of plays necessary to ensure a certain degree of accuracy in the value of P_f , see Eqs. 4.4d and 4.4e.

5. Method of Linear Approximation

This section will illustrate how the method of truncated Taylor series expansion, Eqs. 2.4.5a-b, can be employed to give an approximate measure of means and variance of R and S. It will be shown how the mathematical model describing the system variance facilitates the break-down of the total uncertainty into smaller, component variances and makes it possible, for the first time, to identify the critical parts of the design procedure.

5.1 Derivation of Means and Variances of R and S

As is readily understood, the method of partial derivatives will require a re-organization of the computational model. In the first step, all input curves read into the computer in the simulation model must be replaced with analytical expressions. These approximate representations should simultaneously fulfill several conditions: give a maximum good fit, be easy to differentiate, be accurately approximated (at least in some regions) by a low degree Taylor expansion. In the present context there has been no attempt whatsoever to give an optimized choice of representation functions.

A look at the design q_n - T_n -diagrams, see Figure 1.3b, suggests that the curves are similar in shape to the non-linear stress-strain relationship of several metals. The implication is that analytical expressions used to describe stress-strain data, such as

$$q_n = T_n / C_1 + C_2 \cdot T_n^{C_3} \quad (5.1a)$$

with C_1 , C_2 and C_3 evaluated constants, may be applicable and give an accurate condensation of a design data base otherwise difficult to handle. The approach may be of value in future optimization studies but will not be covered any further here. For the present purpose, a simple linear expression has been used

$$T_{k_{eff}} = C_o + q_{eff} (C_T + C_{\Delta k} \Delta k) \quad (5.1b)$$

where C_o , C_T and $C_{\Delta\kappa}$ are deterministic constants to be evaluated from the diagrams, q_{eff} is a stochastic variable representing the effective fire load density

$$q_{\text{eff}} = \Delta q \cdot q \quad (5.1c)$$

where the random variable Δq describes the uncertainty in the fire load statistics represented by the cumulative distribution function in Figure 1.5.1a. $\Delta\kappa$ is a random variable describing the variability in insulation factor κ ;

$$\Delta\kappa = (\overline{\Delta\kappa}, \sigma_{\Delta\kappa}) \quad (5.1d)$$

$\overline{\Delta\kappa}$ and $\sigma_{\Delta\kappa}$ are evaluated from input values of $\lambda_{o,i}$ and $d_{o,i}$; $\lambda_{o,i} = (\overline{\lambda_{o,i}}, \sigma_{\lambda_{o,i}})$, $d_{o,i} = (\overline{d_{o,i}}, \sigma_{d_{o,i}})$. $d_{o,i}$ and $\lambda_{o,i}$ are both dimensionless, expressing the ratio between actual and nominal values. First order approximation gives

$$\overline{\Delta\kappa} = \kappa_n \cdot \frac{\overline{\lambda_{o,i}}}{\overline{d_{o,i}}} - \kappa_n \quad (5.1e)$$

$$\sigma_{\Delta\kappa} = \left[\left(\frac{\sigma_{\lambda_{o,i}}}{\overline{\lambda_{o,i}}} \right)^2 + \left(\frac{\sigma_{d_{o,i}}}{\overline{d_{o,i}}} \right)^2 \right]^{1/2} \cdot \frac{\overline{\lambda_{o,i}} \cdot \kappa_n}{\overline{d_{o,i}}} \quad (5.1f)$$

The final maximum steel temperature T is given by

$$T_{\text{max}} = T_{\kappa_{\text{eff}}} + \Delta T_2 + \Delta T_3 \quad (5.1g)$$

with ΔT_2 and ΔT_3 taken from Eqs. 3.2.2a-b, 3.2.3a-b.

Regarding the load-carrying capacity φ a rough description of the $T_n - \varphi_n$ -relations in Figure 1.4a is given by

$$\varphi_n = \left(\frac{700 - T_n}{700} \right)^{0.4} \cdot 1.13 \quad (5.1h)$$

The final value of φ (or R), expressed L_e -units, will be

$$R = \left[\left(\frac{700 - T_{\text{max}}}{700} \right)^{0.4} \cdot 1.13 + \Delta\varphi_{1,\text{eff}} + \Delta\varphi_2 \right] \cdot M \quad (5.1i)$$

Application of Eqs 2.4.5a-b gives for the mean \bar{T}_{\max} and standard deviation $\sigma_{T_{\max}}$ of T_{\max}

$$\bar{T}_{\max} = C_o + \overline{\Delta q} \cdot \bar{q} \cdot (C_T + C_{\Delta\kappa} \overline{\Delta\kappa}) + \overline{\Delta T}_2 + \overline{\Delta T}_3 \quad (5.1j)$$

$$\begin{aligned} \sigma_{T_{\max}}^2 &= \left(\frac{\partial T_{\max}}{\partial (\Delta q)} \right)^2 \sigma_{\Delta q}^2 + \left(\frac{\partial T_{\max}}{\partial q} \right)^2 \sigma_q^2 + \left(\frac{\partial T_{\max}}{\partial (\Delta\kappa)} \right)^2 \sigma_{\Delta\kappa}^2 + \\ &+ \left(\frac{\partial T_{\max}}{\partial (\Delta T_2)} \right)^2 \sigma_{\Delta T_2}^2 + \left(\frac{\partial T_{\max}}{\partial (\Delta T_3)} \right)^2 \sigma_{\Delta T_3}^2 \end{aligned} \quad (5.1k)$$

$$\begin{aligned} \sigma_{T_{\max}}^2 &= \bar{q}^2 (C_T + C_{\Delta\kappa} \overline{\Delta\kappa})^2 \sigma_{\Delta q}^2 + \overline{\Delta q}^2 (C_T + C_{\Delta\kappa} \overline{\Delta\kappa})^2 \sigma_q^2 + \\ &+ (\overline{\Delta q} \cdot \bar{q} \cdot C_{\Delta\kappa})^2 \sigma_{\Delta\kappa}^2 + \sigma_{T_1}^2 + \sigma_{T_2}^2 \end{aligned} \quad (5.1l)$$

With known values of \bar{T}_{\max} and $\sigma_{T_{\max}}$, \bar{R} and σ_R can be evaluated

$$\bar{R} = \left[\left(\frac{700 - \bar{T}_{\max}}{700} \right)^{0.4} \cdot 1.13 + \overline{\Delta\psi}_{1,\text{eff}} + \overline{\Delta\psi}_2 \right] \cdot \bar{M} \quad (5.1m),$$

$$\begin{aligned} \sigma_R^2 &= \left[\left(\bar{T}_{\max} \right)^{0.4} \cdot 1.13 + \overline{\Delta\psi}_{1,\text{eff}} + \overline{\Delta\psi}_2 \right]^2 \cdot \sigma_M^2 + \\ &+ \bar{M}^2 \left[\left(-\frac{1.13}{700} \cdot 0.4 \cdot \left(\frac{700 - \bar{T}_{\max}}{700} \right)^{-0.6} \right)^2 \sigma_{T_{\max}}^2 + \right. \\ &\left. + \sigma_{\Delta\psi_{1,\text{eff}}}^2 + \sigma_{\Delta\psi_2}^2 \right] \end{aligned} \quad (5.1n)$$

In Eqs. 5.1m-n, c.f. Eqs. 3.3.1d-e and Eq. 3.3.1g,

$$\overline{\Delta\psi}_{1,\text{eff}} = \bar{T}_{\max}/550 \cdot \overline{\Delta\psi}_1 \quad (5.1o)$$

$$\begin{aligned} \sigma_{\Delta\psi_{1,\text{eff}}}^2 &= (\bar{T}_{\max}/550)^2 \sigma_{\Delta\psi_1}^2 + (\overline{\Delta\psi}_1/550)^2 \cdot \sigma_{T_{\max}}^2 = \\ &\approx (\bar{T}_{\max}/550)^2 \sigma_{\Delta\psi_1}^2 \end{aligned} \quad (5.1p)$$

An important qualification for the derivations above is that all variables have been considered statistically independent.

For the load effect S, the following relations are valid

$$\bar{S} = \frac{\bar{E}(\bar{L} + \bar{D})}{\gamma_o(L_n + D_n)} \quad (5.1q)$$

$$\sigma_s^2 = \left(\frac{(\bar{L} + \bar{D})^2}{\gamma_o(L_n + D_n)} \right)^2 \sigma_E^2 + \left(\frac{\bar{E}}{\gamma_o(L_n + D_n)} \right)^2 (\sigma_L^2 + \sigma_D^2) \quad (5.1r)$$

Using the following values, see Table 5.1a, of C_o , C_T and $C_{\Delta k}$, Eqs. 5.1b-r have been used to compute the relevant parameters of the uncertainty analysis. The values have been chosen with simple eye inspection, with no attempt to get optimal fit by numerical methods. All values refer to a fire compartment with opening factor $A\sqrt{h}/A_t = 0.08 \text{ m}^{1/2}$. The evaluation has been made for values of $\kappa_n = 1160, 2320$ and $4640 \text{ W/m}^3 \text{ }^\circ\text{C}$. The results appear in Table 5.1b, together with corresponding results from the Monte Carlo simulation.

The conclusion that can be drawn from Table 5.1b is that in this situation the method of evaluating system moments from the moments of the basic components or variables by truncating the Taylor series' expansion after the linear terms is in general successful. For the two lower values of κ_n with both $q-T_n$ and $T_{\max} - \varphi_n$ -curves nearly linear in relevant regions, the omission of partial derivatives of higher order should reasonably be of little consequence. Increasing the insulation parameter κ to $\kappa_n = 4640 \text{ W/m}^3 \text{ }^\circ\text{C}$ (decreasing the insulation capacity) implies that corresponding steel temperature- and strength-curves exhibit a more non-linear behaviour. Consequently the divergence between the two methods becomes somewhat larger but is still within acceptable limits. What percentage of the difference that depends on the fact that the chosen values of C_o , C_T and $C_{\Delta k}$ are approximate is unknown. This could have been investigated by changing the simulation computer program to fit exactly the computational procedure used in the linearized analysis.

5.2 Analysis of System and Component Variance

In a Monte Carlo simulation, if no special steps are taken, the final output describing the system performance will contain little information about the importance of specific variables and of their possible interrelations. One salient feature of the Taylor series expansion method is that the different terms in the relations describing the system moments as functions of the moments of the basic components give an easily available and direct measure of the variance arising from different sources.

This characteristic of the partial derivatives method has been used to analyze the components of the uncertainty in the load-carrying capacity R . We first turn our attention to Eq. 5.1k, describing the variance in the maximum steel temperature. Assuming $\overline{\Delta q} = 1$ and $\sigma_{\Delta q} = 0$, i.e. in all cases complete combustion, with the effective calorific content given by Figure 1.5.1a, this relation can be rewritten in a figurative way as

$$\text{Var}(T_{\max}) = \text{Var}(q) + \text{Var}(\kappa) + \text{Var}(\Delta T_2) + \text{Var}(\Delta T_3) \quad (5.2a)$$

where

$$\text{Var}(T_{\max}) = \sigma_{T_{\max}}^2$$

$$\text{Var}(q) = (C_T + C_{\Delta k} \overline{\Delta k})^2 \sigma_q^2 = \text{the basic and unavoidable variability in } T_{\max} \text{ due to the stochastic character of the parameter } q$$

$$\text{Var}(\kappa) = (\overline{q} \cdot C_{\Delta k})^2 \sigma_{\Delta k}^2 = \text{variance due to variability in the insulation parameter}$$

$$\text{Var}(\Delta T_2) = \sigma_{\Delta T_2}^2 \text{ describes variance due to uncertainty in the theory laying the basis for the design curves of the maximal steel temperature. As described earlier, the term } \Delta T_2 \text{ gives the error introduced both in the theory of compartment fires and in the heat transfer calculations producing steel temperature values}$$

$$\text{Var}(\Delta T_3) = \sigma_{\Delta T_3}^2 = \text{variance due to influences introduced in the}$$

transformation from laboratory conditions to real life service

Figure 5.2a gives a description of how the relative percentage values of these four variances vary with κ_n for $A\sqrt{h}/A_t = 0.08 \text{ m}^{1/2}$.

The corresponding figures for the resistance R are given by Figure 5.2b. The percentages have been evaluated using Eq. 5.1n, which can symbolically be formulated

$$\text{Var}(R) = \text{Var}(M) + \text{Var}(T_{\max}) + \text{Var}(\Delta\varphi_{1,\text{eff}}) + \text{Var}(\Delta\varphi_2) \quad (5.2b)$$

If compared with Eq. 5.1n, the interpretation of each term is obvious.

Figures 5.2a-b make one example of how probabilistic methods can be used to identify possible sources of uncertainty and the variation of these uncertainties with relevant design parameters. Information of the type outlined in Figures 5.2a-b will be necessary for the formulation of a strategy, aiming at an economically optimal structure failure avoidance.

Regarding Figure 5.2b, lack of data implies that some caution is justified when using the figure to estimate uncertainty due to different sources. The proportion of variance due to the error term $\Delta\varphi_2$ is quite arbitrary, as mean and variance according to Eq. 3.3.2a-b is

$$\overline{\Delta\varphi_2} = 0.0 \quad (3.3.2a)$$

$$\sigma_{\Delta\varphi_2} = 0.10 \text{ (L}_e\text{-units)} \quad (3.3.2b)$$

irrespective of the failure temperature level. As long as more reliable figures are not available, subjective judgement will have to do. More accurate statistics of the parameter $\Delta\varphi_2$ may be obtained by a Monte Carlo simulation, using the available strength theory /13/ coupled with a statistical description of the restraint conditions and lack-of-fit found in real service.

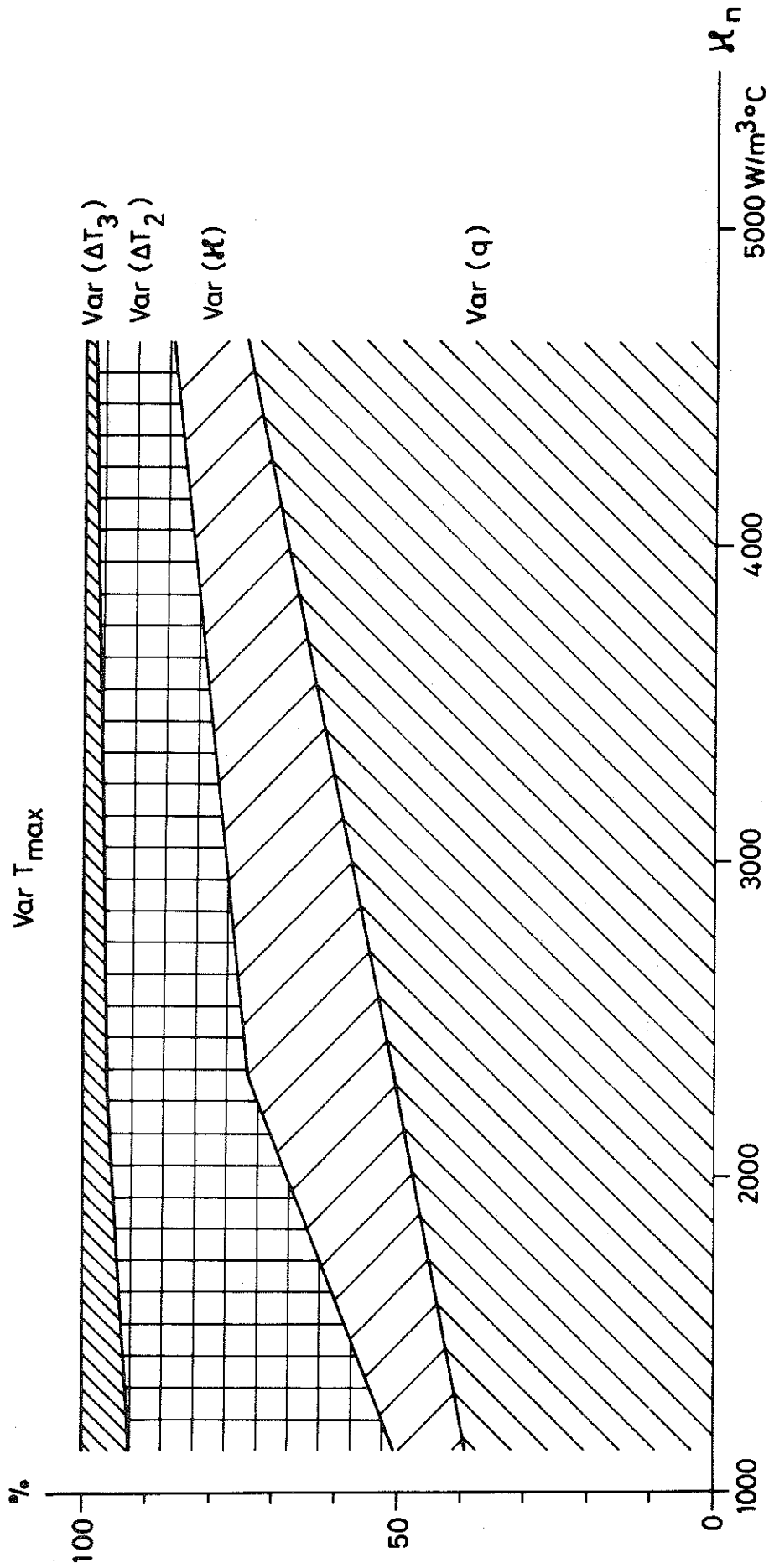


Figure 5.2a. Decomposition of total variance in T_{max} into component variances as a function of insulation parameter k_n

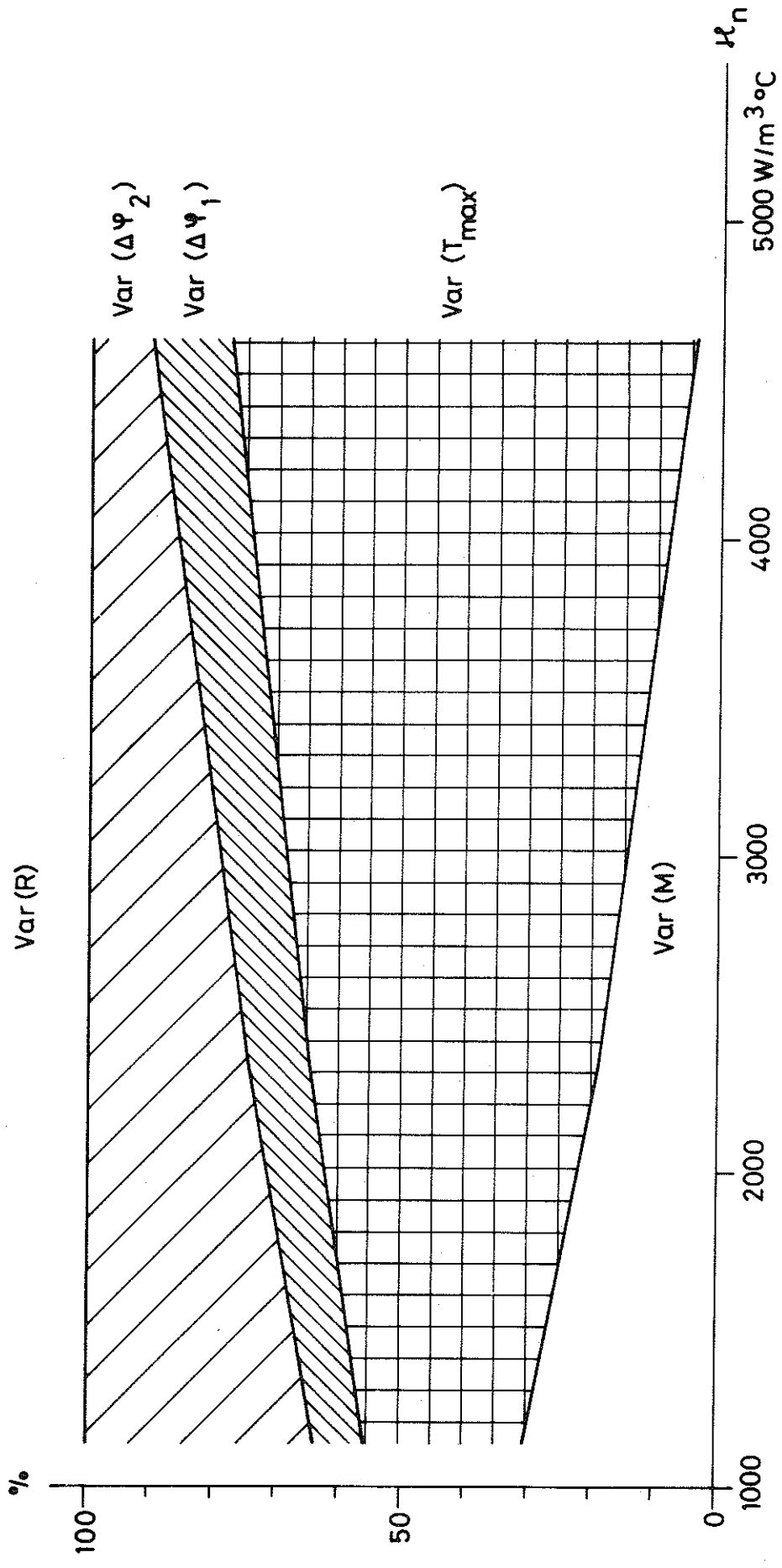


Figure 5.2b Decomposition of total variance in load-carrying capacity R into component variances as a function of insulation parameter κ_n

Having the arbitrariness of $\text{Var}(\Delta\psi_2)$ in mind, useful qualitative and quantitative conclusions can still be drawn from Figures 5.2a-b. As will be shown, later in section 6.1, the design value of κ for $A\sqrt{h}/A_t = 0.08 \text{ m}^{1/2}$ according to the differentiated design method will be

$$\kappa_n = 3380 \text{ W/m}^3 \text{ }^\circ\text{C}$$

Table 5.2a gives, for $\kappa_n = 3380 \text{ W/m}^3 \text{ }^\circ\text{C}$, the breakdown of the total variance into a sum of component variances. Still using symbolic notation, we find that

$$\text{Var}(\Delta T_2) \approx 0.10 \cdot \text{Var}(R) \quad (5.2c)$$

That is, even totally "perfect" theories concerning compartment fires and the heat transfer analysis, i.e. $\text{Var}(\Delta T_2) = 0$, would not decrease the variance in R with more than 10 per cent. (The change in \bar{R} would be still much less, corresponding to $\overline{\Delta T_2} = -10^\circ\text{C}$).

Taking the values of \bar{R} , \bar{S} , $\text{Var}(R)$ and $\text{Var}(S)$ from Table 4.3b it can be concluded that the value of β_C would not increase more than a few per cent. Compared with the variation in β_C caused by e.g. changing the D_n/L_n -ratio, the uncertainty due to the approximate theory of compartment fires is of minor importance.

In a further development towards a probability-based partial-coefficient format, the coefficients to the individual basic variables (q , d_i , λ_i , L , D etc) must be computed with the respective component mean and variance as a starting point. Generally speaking, a systematic sensitivity analysis of the system variance in R following the outlines presented in chapter 4 and 5 is of fundamental importance for a proper understanding of the structural fire safety problem.

6. Safety Indices Inherent in Different Design Procedures

One of the main aims of this paper is to investigate the reliability inherent in different design procedures. Of the various definitions of a safety index existing, the formulation given by Cornell /20/, Eq. 2.4.3a

$$\beta_C = (\bar{R} - \bar{S}) / \sqrt{\sigma_R^2 + \sigma_S^2} \quad (6a)$$

will be used. Two design procedures will be investigated, the differentiated Swedish method /5/ and the traditional method based on fire endurance in a standard furnace test.

6.1 Safety Index β_C in the Differentiated Design Procedure

By the design procedure outlined in section 1.5, the required value of κ_n in $W/m^3 \text{ } ^\circ C$ necessary for a design maximum steel temperature = $520^\circ C$ will be for different ventilation or opening factor $A\sqrt{h}/A_t$

q_n (MJ/m ²)	$A\sqrt{h}/A_t$ (m ^{1/2})		
	0.04	0.08	0.12
138.2	2020	3380	4420
193.0	1265	2190	3050

The lower line gives the values for κ_n if the nominal fire load density had been chosen equal to a characteristic value

$$q_n = \bar{q} + 2 \sigma_q = 193.0 \text{ MJ/m}^2 \quad (6.1a)$$

The original building code formulation from 1967 prescribed q_n according to Eq. 6.1a. Later discussions led to the conclusion that a somewhat less conservative value, see Eqs 1.5.1a-b, was permissible. This decision was primarily based on the fact that fire exposure must be regarded as an exceptional case of loading.

From Table 4.3a-c or Figures 4.3.1b-d, the values of safety in-

index β_C implied in the discussed design procedure is listed in Table 6.1a. Examples of safety index values inherent in present non-fire design codes are found e.g. in /26/

6.2 Safety Index Inherent in Standard Design Procedure

Swedish building code prescribes that during a traditional standard fire endurance test, the load applied upon the test specimen shall be equal to the design load. Measured in L_e -units, this corresponds to

$$\psi = 0.67 L_e \quad (6.2a)$$

Of the CECM-tests /31/ of fire-exposed simply supported steel beams used earlier in the uncertainty analysis, 31 had loading conditions corresponding to this ψ -value. We compute the sample mean and standard deviation of these 31 failure temperatures T_{fail} and find

$$\bar{T}_{fail} = 552^\circ\text{C} \quad (6.2b)$$

$$\sigma_{T_{fail}} = 29^\circ\text{C} \quad (6.2c)$$

In this temperature range, $\sigma_{T_{fail}} = 29^\circ\text{C}$ corresponds to a standard deviation in load-carrying capacity $\approx 0.10 L_e$ -units (see Figure 1.4a) which is the uncertainty of the standard endurance test in one test series, where two furnaces have been used. To get the total uncertainty in the method itself, the further main factors to consider are

- varying heat transmission characteristics in the furnace population
- the difference between gastemperature-time curves in the real exposure and in the furnace (rate of heating, absence of decay period)

If these influences are assumed to increase the scatter by a standard deviation $= 0.10 L_e$, the combined uncertainty, measured as a standard deviation, in the traditional standard test method would be $\approx 0.14 L_e$ -units.

The difference between this derivation and the procedure used to evaluate $\Delta\varphi_1$ should be observed. In the latter case, the load-carrying capacity was computed for each test specimen with regard taken of individual form factors, yield strengths at room temperature and rates of heating. The temperature measurements are relatively reliable and the difference $\Delta\varphi_1$ between theory and experiment could thus be attributed to an imperfect member performance prediction. On the other hand, in deriving $\sigma_{T_{fail}}$ we are comparing failure temperatures for beams loaded to a certain per cent of the elastic limit load, using nominal values of yield strength at room temperature.

The design method uncertainty of a protected steel beam just passing an endurance test of 30, 60, 90, etc minutes has thus been estimated. To at least some part, this uncertainty must be compensated by a systematic increase in the average resistance, due to the fact that a beam assembly fullfilling e.g. the 90-minute requirement as a rule survives the exposure for an additional and unspecified number of minutes. Total lack of data forces us to neglect this influence.

Figures 6.2a-c show the influence on the safety index β_C of the added uncertainty in R , arising from the variability in the outcome of standard fire endurance tests. For comparison, the corresponding curves from Figures 4.3b-d are shown.

Figure 6.2d gives the average time-steeltemperature curve for a protected structural member exposed to standard furnace test for varying degrees of insulation, using the heat flow computational procedure described in section 1.3. For a critical temperature of 550°C a fire resistance rating of 30, 60, 90 and 120 minutes requires values κ_{st} of the insulation parameter according to Table 6.2a. The different values in Figure 6.2d for $\kappa = 1160 \text{ W/m}^3 \text{ }^\circ\text{C}$ illustrate the variation introduced by neglecting $1/\alpha$ in Eq. 1.3a.

Table 6.2a indicates, for given fire resistance ratings, the range of variation of β_C that will be encountered under real service conditions if the range of $A\sqrt{h}/A_t$ is limited to 0.04 - 0.12 $\text{m}^{1/2}$ and that of the ratio D_n/L_n to 1/3 - 3. A fire resistance rating of 60 minutes results in β_C -values varying from 1.77 to 3.69, a variation of two units. Compared with the uncertainty in

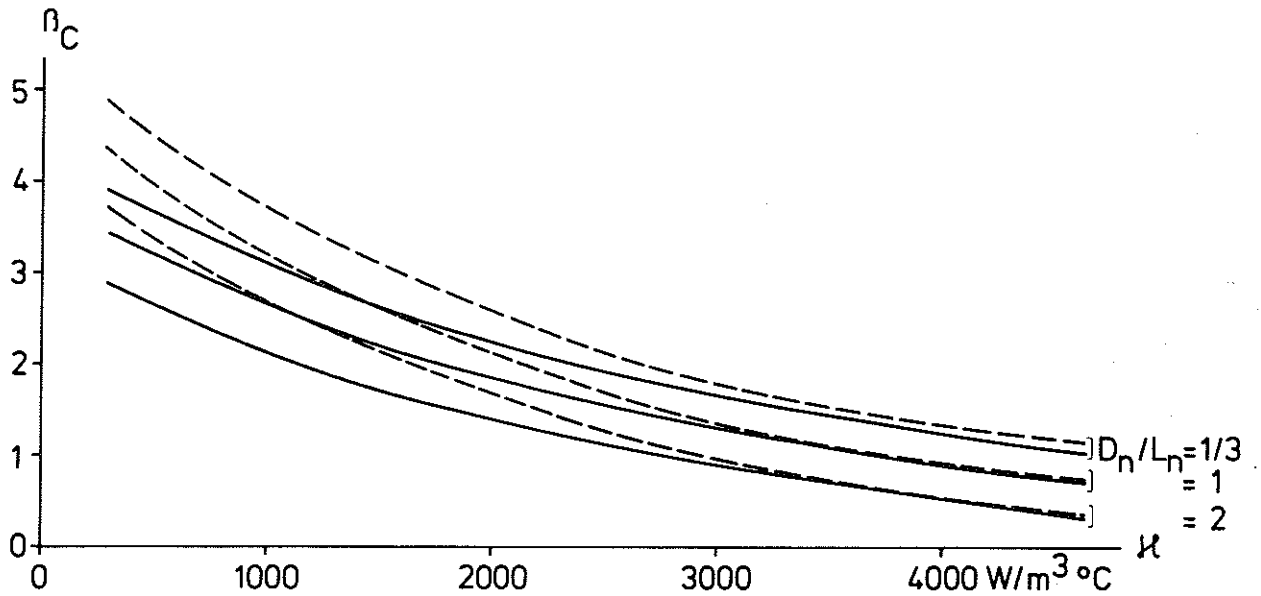


Figure 6.2a Variation of safety index β_C with insulation parameter κ_n and ratios D_n/L_n for a steel beam designed according to a standard fire endurance test. For comparison, the corresponding curves from Figure 4.3b are shown (-----). $A\sqrt{h}/A_t = 0.04 \text{ m}^{1/2}$

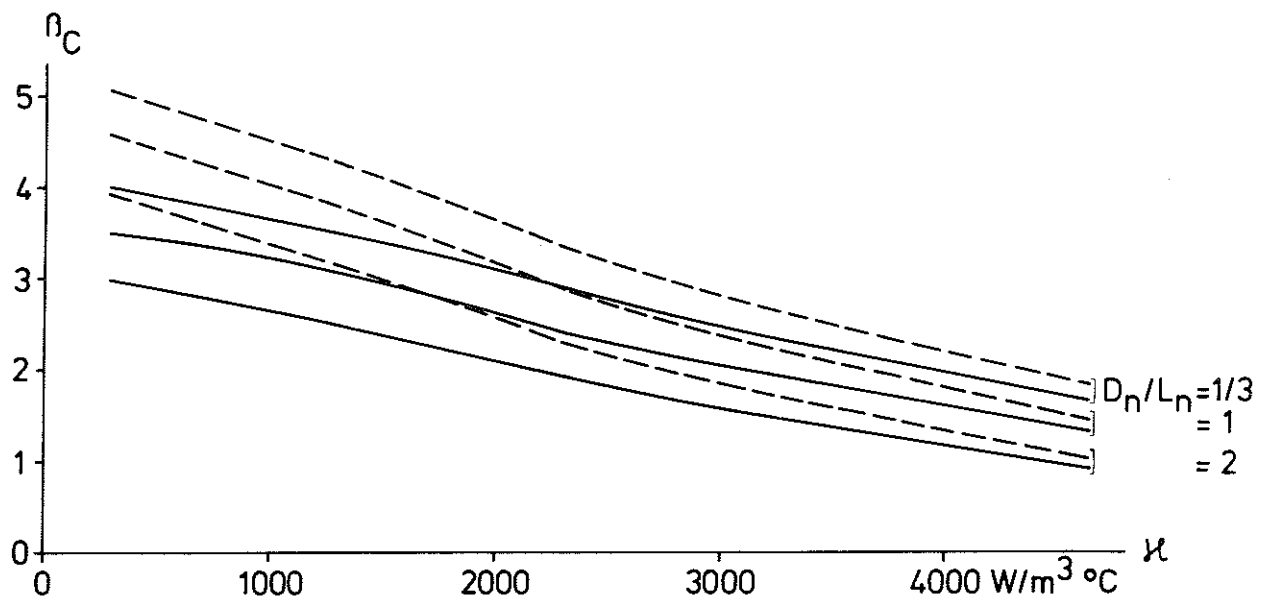


Figure 6.2b Variation of safety index β_C with insulation parameter κ_n and ratios D_n/L_n for a steel beam designed according to a standard fire endurance test. For comparison, the corresponding curves from Figure 4.3c are shown (-----). $A\sqrt{h}/A_t = 0.08 \text{ m}^{1/2}$

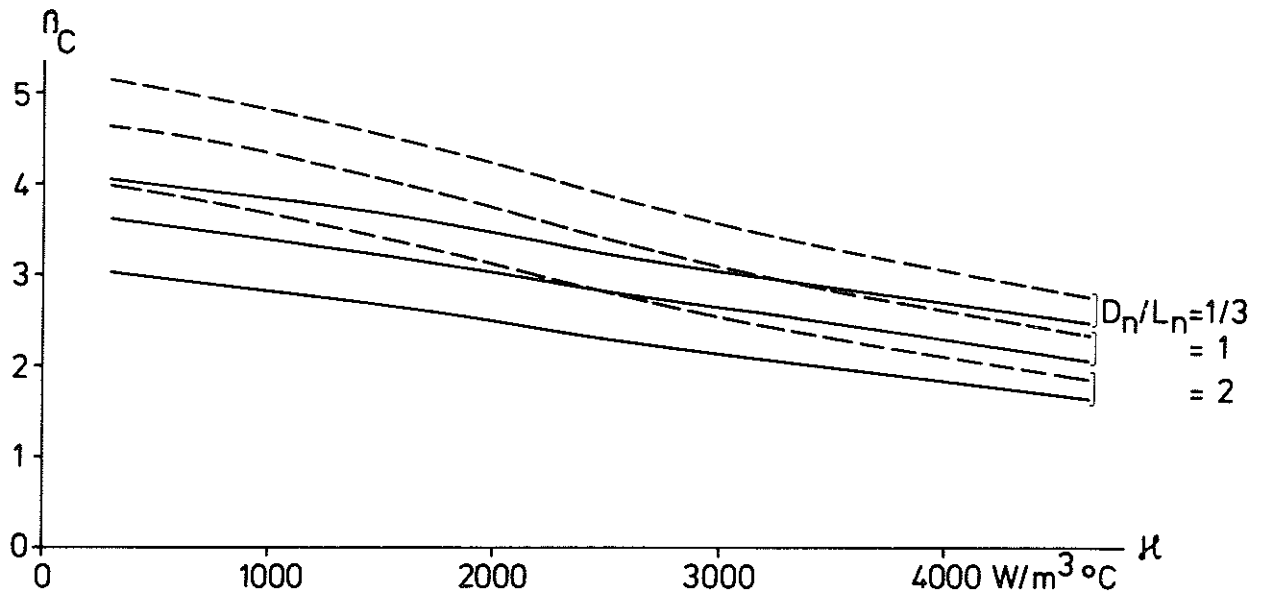


Figure 6.2c Variation of safety index β_C with insulation parameter κ_n and ratios D_n/L_n for a steel beam designed according to a standard fire endurance test. For comparison, the corresponding curves from Figure 4.3d are shown (-----). $A\sqrt{h}/A_t = 0.12 \text{ m}^{1/2}$

the β_C -value obtained from the new differentiated design method (see Table 6.1a), it is demonstrated how the versatility and flexibility of this latter method result in more consistent over-all safety levels. This fact becomes more conspicuous if the range of safety indices is transformed into range of failure probability P_f . In the differentiated design β_C varies, for the chosen design parameter space, within the range 1.66 - 2.84, corresponding to values of P_f between $5 \cdot 10^{-2}$ and $0.23 \cdot 10^{-2}$ with the ratio between minimum and maximum value ≈ 20 . For the beam just passing the 60 minute specification requirement, P_f would be in the range $4 \cdot 10^{-2}$ - $0.01 \cdot 10^{-2}$ with the corresponding ratio ≈ 400 . These figures presuppose that the random variate $R - S$ is normally distributed. The reasonableness of this assumption is discussed in chapter 4.

In practice, the difference between the two design methods is still larger. In the differentiated method, the variation of the resistance R with the following two factors is taken into account:

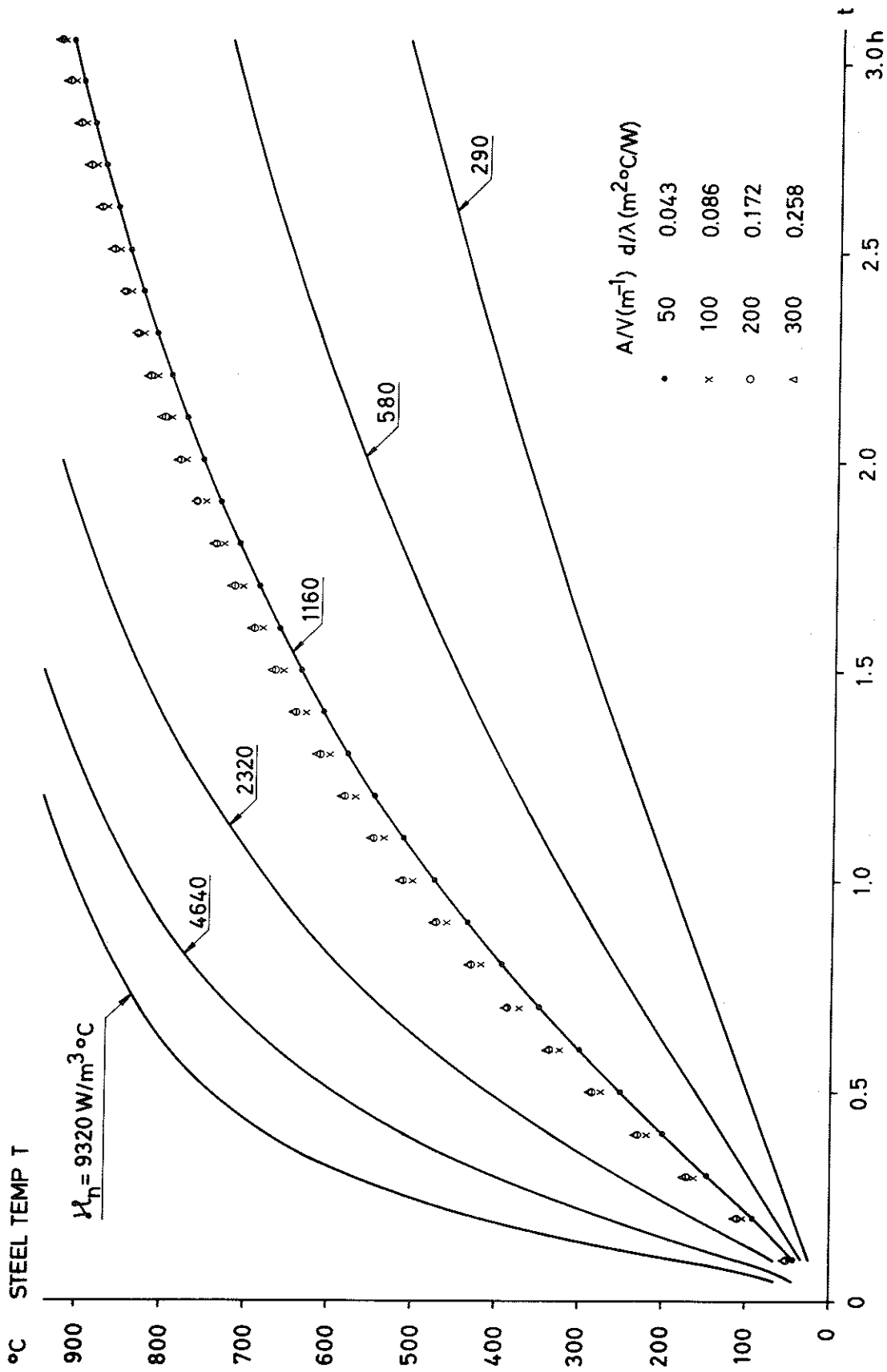


Figure 6.2d Computed steel temperature-time curves for structural steel members exposed to the standard endurance test as a function of insulation parameter κ . The different values for $\kappa = 1160 \text{ W/m}^3 \text{ }^\circ\text{C}$ illustrate the variation introduced by neglecting $1/\alpha$ in Eq. 1.3a

- combustible material in structural members (immobile fire load)
- the influence on the fire process of the thermal properties of walls, floor and ceiling (the factor k_f in Eq. 1.3b) /40/.

Table 6.1a shows that the new method is successful in reducing the variation in β_C due to changes in opening factor $A\sqrt{h}/A_t$ (this is of course a natural consequence of Eqs 3.2.2c-f) but, for the special structural element studied here, there is still a considerable dependence of β_C on the D_n/L_n -ratio. Chapter 7 will illustrate how known load factor design methods can be employed to minimize the dependence of derived reliability levels on the ratio D_n/L_n .

7. Evaluation of Load Factors in the Differentiated Design
Procedure for Fire-Exposed Structures

The nominal loads and load factors given in section 1.5.2 were chosen to give a design stress level that was equal to the same level prescribed for the standard fire endurance test, independent of the ratio D_n/L_n . The differing statistics of the load effect components S_D and S_L made the resulting failure probability dependent on the ratio D_n/L_n . By example it will be shown how statistically consistent load factors can be derived to match a predetermined safety level (safety index). The exemplifications will be based on the material computed in chapter 4 and may be seen as an attempt to apply the theories from the normal design field to the area of fire-exposed structures. Reference is made to /27/ and /28/.

7.1 Use of Linearization Function α

We start by repeating the design inequality equation, see Eq. 1.5.2a,

$$\phi R_{n,f} \geq \gamma_{D,f} D_{n,f} + \gamma_{L,f} L_{n,f} \quad (7.1a)$$

and assume that the value of $\beta_C = 2.16$ in Table 6.1a for $A\sqrt{h}/A_t = 0.08$ and with $L_n/D_n = 1$ is regarded by authorities as "socially acceptable". Using the de-coupling algorithm shown in section 2.4.7, we get

$$\bar{R} \geq \bar{S} + \beta_C \sqrt{\sigma_R^2 + \sigma_S^2} \quad (7.1b)$$

$$\bar{R} \geq \bar{S} + \beta_C \alpha_{RS} (\sigma_R + \sigma_S) \quad (7.1c)$$

$$\bar{R}(1 - \alpha_{RS} \beta_C V_R) \geq \bar{S}(1 + \alpha_{RS} \beta_C V_S) \quad (7.1d)$$

\bar{R} and σ_R are interpolated from Table 4.3b =

$$= (0.967, 0.265) L_e \quad (7.1e)$$

For \bar{S} and V_S we have

$$v_{S_D} = (v_D^2 + v_E^2)^{1/2} = (0.04^2 + 0.1^2)^{1/2} \approx 0.108 \quad (7.1f)$$

$$v_{S_L} = (v_L^2 + v_E^2)^{1/2} = (0.68^2 + 0.1^2)^{1/2} \approx 0.69 \quad (7.1g)$$

$$\bar{D} = \frac{2.0}{1.5 \cdot (2.0+2.0)} L_e = 0.33 L_e \rightarrow \sigma_{S_D} = 0.036 L_e \quad (7.1h)$$

$$\bar{L} = \frac{0.507}{1.5 \cdot (2.0+2.0)} L_e = 0.0845 L_e \rightarrow \sigma_{S_L} = 0.058 L_e \quad (7.1i)$$

$$\sigma_S = (\sigma_{S_D}^2 + \sigma_{S_L}^2)^{1/2} = 0.068 L_e \quad (7.1j)$$

(c.f. Table 4.3b)

Decomposing σ_S we get

$$\sigma_S \approx \alpha_{DL} (\sigma_{S_D} + \sigma_{S_L}) \quad (7.1k)$$

α_{RS} and α_{DL} can now be computed.

Exact values of α_{RS} and α_{DL} are 0.82 and 0.72.

Inserting these values leads to (c.f. Eq. 2.4.7i)

$$(1 - 0.82 \cdot 2.16 \cdot 0.27) \bar{R} \geq (1 + 0.82 \cdot 0.72 \cdot 2.16 \cdot 0.108) \bar{S} + (1 + 0.82 \cdot 0.72 \cdot 2.16 \cdot 0.69) \bar{S}_L \quad (7.1l)$$

or

$$0.52 \bar{R} \geq 1.14 \bar{S}_D + 1.88 \bar{S}_L \quad (7.1m)$$

Identifying with Eq. 7.1a yields (c.f. Eqs 2.4.7j-l)

$$\text{strength factor } \phi = 0.52 \cdot \frac{\bar{R}}{R_n} = 0.52 \cdot \frac{0.967}{0.65} = 0.77 \quad (7.1n)$$

$$\text{load factor } \gamma_{D,f} = 1.14 \quad (7.1o)$$

$$\text{load factor } \gamma_{L,f} = 1.88 \quad (7.1p)$$

Conventionally, the strength factor is put equal to unity, changing the values of the load factors to

$$\gamma_{D,f} = 1.48 \quad (7.1r)$$

$$\gamma_{L,f} = 2.44 \quad (7.1s)$$

Relations 7.1r-s suggest that values of $\gamma_{D,f} \approx 1.5$ and $\gamma_{L,f} \approx 2.5$ might be appropriate as load factors. Remembering Table 6.1a showing that the value of β_C in the differentiated design will change with the factor D_n/L_n , it must be investigated if these new values of $\gamma_{D,f}$ and $\gamma_{L,f}$ result in any improvement. Choosing $\gamma_{D,f} = 1.5$ and $\gamma_{L,f} = 2.5$ and applying the load factors on mean values of dead and live load, the degree of utilization of the cross-section will be $\approx 0.57, 0.72$ and 0.86 for $D_n/L_n = 1/3, 1$ and 3 respectively. The critical temperatures taken from Figure 7.1a are $\approx 540, 500$ and 420°C . Figure 7.1a is taken from the tables in the manual /5/ and shows design steel temperatures as function of κ for a design fire load density $q_n = 138.2 \text{ MJ/m}^2$ (see Eq. 1.5.1b). Design values κ_n of the insulation parameter κ will be approximately 3650, 3050 and 2050 $\text{W/m}^3 \text{ }^\circ\text{C}$. Table 7.1a gives the comparison between the values of the safety index β_C as compared with the values given by present nominal loads and load factors. It is emphasized that the load factors according to Eqs 7.1r-s are based on mean values of dead and live load.

7.2 Use of Mathematical Programming Methods

The load factors shown in Table 7.1a were derived by using approximate methods. The design parameters influencing the fire safety level for a given set of load factors are in the examined case primarily

- mean bay area
- opening factors $A\sqrt{h}/A_t$
- ratio D_n/L_n
- interaction with normal temperature design methods.

A given combination of these parameters or data variables will characterize a design case and may be denoted the data vector ω . For predetermined nominal loads and a load factor vector $\underline{\gamma}$ (con-

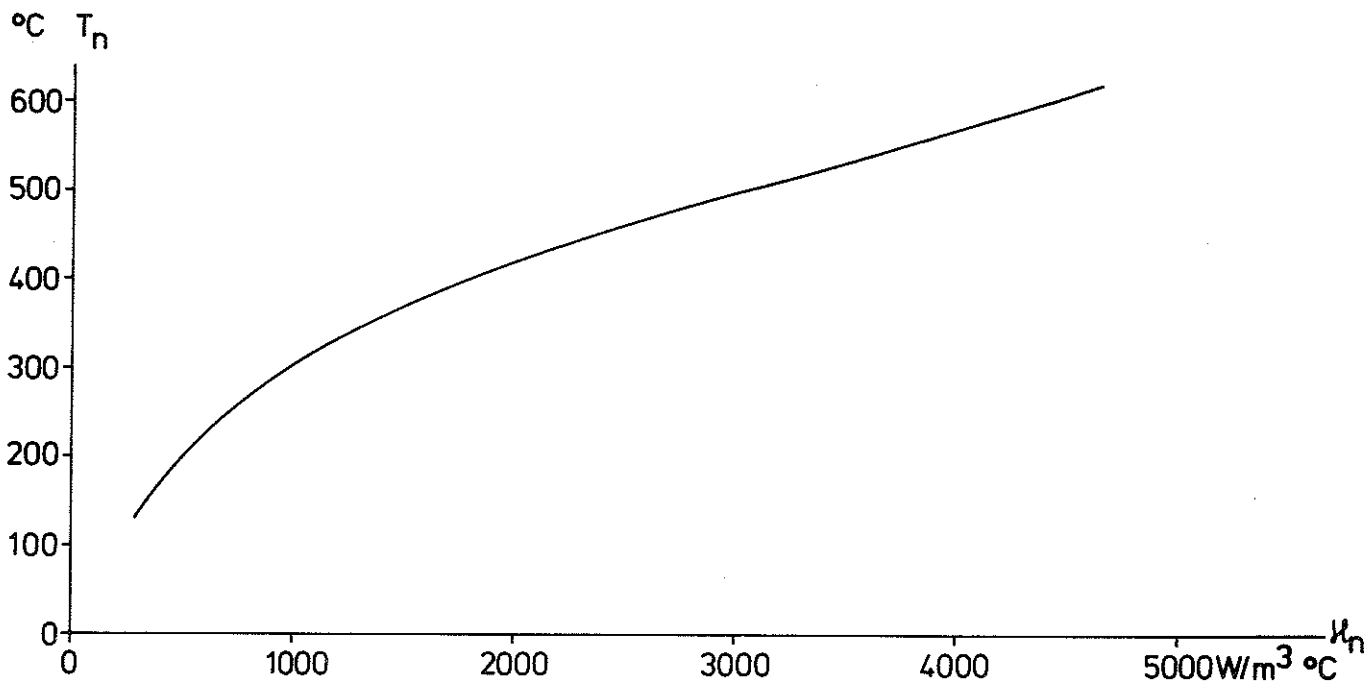


Figure 7.1a Maximum steel temperature in structural member with varying values of κ for a fire load density = q_n (138.2 MJ/m²)

taining the load factors applied to nominal values of fire load density, live load and dead load) the safety index will vary with the data vector \underline{w} , as has been exemplified. Let the preselected safety index be denoted by β_o . Use of standard mathematical programming techniques permits the evaluation of that particular load factor vector $\underline{\gamma}_o$, for which the difference between computed and preselected safety index value is minimized, taking all possible data vectors into account. The problem stated in mathematical terms could be formulated like this /32/:

Given the set of nominal loads \underline{P}_n , find $\underline{\gamma}$ such that the expression

$$\int_{\underline{w}} \left[1 - \beta(\underline{P}_n, \underline{\gamma}, \underline{w}) / \beta_o \right]^2 f(\underline{w}) d \underline{w} \quad (7.2a)$$

is minimized. The weight function $f(\underline{w})$ describes e.g. the relative frequency and economic importance of each particular structural component denoted by the vector \underline{w} . This is an unconstrained non-linear optimization problem, for which a number of solution algorithms have been suggested. In the case of Eq. 7.2a, a non-gradient technique will have to be employed. For a survey of available algorithms see /37/. Although the values of $\underline{\gamma}$ given in Table 7.1a are recognized not to be the optimum ones, no effort has been made to evaluate $\underline{\gamma}_o$.

8. Concluding Remarks

This last chapter will be used to summarily mention important influences and factors not previously touched upon.

8.1 Validity of Derived Safety Measures. Further Studies

Structural analysis of fire-exposed structures today is lagging behind the corresponding analysis for the normal temperature functions. The complexity in behaviour is largely due to factors like changing material properties and restraint forces. To the author's knowledge the first systematic research, validated by an adequate experimental basis, is given in /13/. Thus state-of-art today permits accurate analysis only of in-plane beam bending. For other types of structural elements, little is known of how restraint forces (moments, normal forces, torsional forces) and other perturbations like temperature gradients influence the load-carrying capacity.

The safety measures derived in this paper are primarily valid for a simply supported beam, uniformly loaded. The design diagrams given in /13/ for other support and loading conditions suggest that the proportional decrease in load-carrying capacity with increasing steel temperature is roughly constant for relevant temperature range ($T_{\max} < 450^{\circ}\text{C}$), indicating that the reliability levels computed in chapters 4 - 7 are approximately valid for a much larger class of structures.

Regarding the computational basis for a safety analysis of fire exposed steel columns, it might be mentioned that a research program is in progress at the Institute. The study comprises full scale tests of more than 30 columns with varying load levels, load eccentricity and degree of axial restraint. The experimental part of the project is correlated to a theoretical study, including a step by step computer simulation of the deformation process. Hopefully this work, when completed, will provide the input data and strength theory needed for a probabilistic analysis.

Substantial savings could be made by a reliability study solving the problem of determining which circumstances justify use of

unprotected steel members. Again, experimental data confirming existing compartment fire theories /38/ for very small fire load densities are not conclusive enough to serve as a basis for a reliability study. Consequently, a safety analysis will have to wait for this experimental verification.

8.2 Use of Temperature Criteria

As seen, there are still many design situations where, due to lack of knowledge, a theoretical structural analysis will have to be based on so many conservative approximations that the final result will be unrealistically on the safe side. In these cases there may be good economical reasons to perform a fire endurance test with the test assembly specified regarding restraint conditions, etc, so as to simulate the real fire behaviour. Choosing the testing load level so high that its exceedance in the actual service environment may be neglected, see e.g. Fig. 4.3e, a conservative lower bound of the reliability is now immediately given by comparing the experimental failure temperature with the statistics (mean and standard deviation) of the maximum steel temperature T_{\max} given in Tables 4.3a-c.

This problem is related to the question of connecting the vast amount of standard fire endurance tests results with reliability levels under service conditions. The transformation theories described in /7/ may constitute the deterministic foundation for such studies.

8.3 Consistent Structural Design

8.3.1 Gross Errors

The safety analysis performed does not take the occurrence of gross errors, such as unintended removal of fire protective material, into account. An unknown but potentially large proportion of structural failures due to fire-exposure are caused by such errors. This proportion increases with increasing structural integrity requirements, and may seem to imply that the probabilistic methods employed here are inconsequential. The conclusion is obviously a false one. A systematic use of these

methods will make more consistent and more economical safety level decisions possible. The profit may be used to increase the level of inspection and control and in this way minimize the total number of structural failures.

8.3.2 Passive and Active Fire Protection

To examine the possibility of making the structural fire protection design consistent with the safety level decisions made for other kind of loadings, a simple example will be taken. The more difficult problem of reliability optimization will be left aside, consideration will only be given to the problem of compatibility of different risks in an economic sense. Suppose that the non-fire design for the combination of live and dead load has been done with the safety index equal to a value β_{ER} using the Esteva-Rosenblueth formulation, see section 2.4.3. For this format /21/, a number of combinations of probability distributions of R and S give probabilities of failure that are approximated by the expression

$$P_F = 460 e^{-4.3\beta_{ER}} \quad (8.3.2a)$$

provided that P_F is of order of magnitude of 10^{-5} or less.

It is further assumed that the structural fire protection ensures that the risk of structural collapse during a fully-developed fire is defined by β_C with the resistance and load effect approximately normally distributed. Equating the loss potential, we get

$$460 e^{-4.3\beta_{ER}} = C \cdot \Phi(-\beta_C) \quad (8.3.2b)$$

The factor C expresses the different basis and consequences of the fire and non-fire failure. C can be written as the product of several factor $C_1 \dots C_n$, where e.g.

- C_1 = probability of a fully developed fire during the life time of the structure
- C_2 = probability that an installed sprinkler system will not work
- C_3 = ratio of economic consequences due to structural failure under fire exposure and due to structural failure for the other type of loading considered.

The formulation presupposes that all factors C_k are stochastically independent.

A qualitative basis for further work in this area is given by /35/.

Summary

A large amount of work is presently in progress regarding the optimum level, in an economic sense, of the overall fire protection of buildings. Structural damages can be prevented or limited by many measures, such as compartmentation, installation of detectors and sprinklers, reducing the attendance time of the fire brigade etc. Among those steps taken to reduce the fire damage, the oldest and most evident one is to increase the fire endurance of the individual structural member. For a high-rise building, the fire endurance must reach the level where the structural integrity of the building is maintained even during the most severe fire possible. For economic reasons, though, the fire endurance cannot be unlimitedly high. Some element of risk, however small, has to be accepted. Evidently, there is a need for a reliability analysis that makes it possible to identify this risk of structural collapse by fire and compare with the risks due to other kinds of catastrophic events.

In a recently published design manual a new approach to the design of fire-exposed steel structures is presented, complete with ready-to-use charts, diagrams and tables. The design method, authorized by the concerned Swedish authorities is a load factor design method based on the natural fire process, the decay period included. Unlike the traditional design method, defined by specification requirements measured as survival time in the standard fire endurance test, the new model permits the design to be made with the detailed characteristics of the fire process and structural member taken into account. The verification of a specific design solution may be made, in part or as a whole, by theoretical calculations. Via the gastemperature-time curve of the design fire process and the transient temperature fields arising in the structural element during fire exposure, deformation and strength calculations give the minimal value of load-bearing capacity for the complete fire process. As in any other design procedure, the choice of nominal loads (fire load density, live and dead load) and load factors will determine the final safety level.

The paper starts by describing and exemplifying the new design

method. An elementary survey of probabilistic methods (first-order, second moment theories) used in normal structural design is given. The safety analysis of fire-exposed structures begins with the procedure critical in every reliability evaluation; the assessment of underlying uncertainties. The paper presents a general systematized scheme for the identification and evaluation of the various sources and kinds of uncertainty possible for a fire-exposed building component. To get applicable and efficient final safety measures, the investigation comprises one specified structural element, an insulated simply supported steel beam of I-cross section as a part of a floor or roof assembly. The chosen statistics of dead and live load and fire load density are representative for office buildings. With the basic data variables selected, the different uncertainty sources in the design procedure are identified and dissembled in such a way that available information from laboratory tests can be utilized in a manner as profitable as possible. The derivation of the total or system variance $\text{Var}(R)$ in the load-carrying capacity R is divided into two main stages: variability $\text{Var}(T_{\max})$ in maximal steel temperature T_{\max} for a given design fire compartment, and variability in strength theory and material properties for known value of T_{\max} . Consecutively $\text{Var}(T_{\max})$ is decomposed into three parts: equation error in the theory of compartment fires and heat transfer from fire process to structural component, variability due to uncertainty in insulation material characteristics, possible difference between T_{\max} obtained in laboratory tests and in real service condition. In step number two, uncertainty in R for a given maximum steel temperature is, in the same way, broken down into three parts: variability in material strength, prediction error in strength theory and difference between laboratory test and a real life fire exposure. These uncertainty terms must be superimposed upon the basic variability due to the stochastic character of fire load density. Mean and variance of load effect S are evaluated using results from publications covering the non-fire loading case.

The component variances are quantified, whenever possible by comparing the design theory with experiments. System variance is evaluated in two ways: by Monte Carlo simulation and by use of a truncated Taylor series expansion. Employing the Monte Carlo pro-

cedure, the mean and variance of R and S have been computed for different values of ventilation factor of fire compartment, insulation parameter κ and ratio D_n/L_n , where D_n = nominal dead and L_n = nominal live load used in the normal temperature design. The second moment reliability as a function of these design parameters is evaluated by the Cornell and Esteva-Rosenblueth safety index formulations. The dependence of the final safety index value on variables such as

- uncertainty in knowledge of the thermal properties of fire-protective materials
- uncertainty in the relation fire load statistics - effective calorific contents

is shortly discussed. Especially the fundamental importance of differentiated and dependable fire load statistics is demonstrated.

The Taylor series expansion method is compared with the Monte Carlo method and demonstrated to give surprisingly good agreement. The mathematical structure of the partial derivatives method makes it natural to use it as a basis for a closer investigation of how the total uncertainty in e.g. load-carrying capacity R varies with the uncertainties arising from different sources. Such information is necessary in a systematic study of how to economically optimize the avoidance of a structural failure. From the introductory discussion performed in this paper it can e.g. be deduced that the measured variability in the design compartment fire and heat transfer theories (obtained by comparing design maximum steel temperatures with experimental values for 97 natural fire-exposed insulated steel columns) reduces to a factor of minor importance for the final safety index value.

The following section turns to the problem of comparing the reliability levels of the traditional and the new, differentiated design method. It is demonstrated how the flexibility of the new method, based as it is on the natural fire behaviour, results in drastically improved consistency for the failure probability P_f .

At the same time it is shown that the temporary nominal loads and load factors given by the manual do not result in reliabi-

lity levels that are independent of the ratio D_n/L_n . Using the linearization factor defined by Lind, it is exemplified how statistically more consistent load factors easily may be derived. Finally it is pointed out how mathematical programming algorithms may be employed to obtain load factors or partial safety factors that for a broader range of design parameters minimizes the difference between the demanded, preselected and the actual reliability level.

Summing up, this pilot study has demonstrated that a safety analysis, using probabilistic methods, of fire exposed structural steel components, is today well within the bounds of possibility. The implication is that one of the main components in the overall firesafety problem for the first time has been rationally assessed, thus opening the way for an integrated system approach with a reliability optimization as final objective.

Mean bay area (m ²)	1.1	1.4	2.4	5.2	14.0	31.2	58.0	111.2	192.2
Mean intensity (kN/m ²)	0.694	0.694	0.661	0.642	0.622	0.613	0.589	0.584	0.565
Standard deviation (kN/m ²)	0.886	0.766	0.646	0.527	0.426	0.345	0.302	0.263	0.215

Table 3.4a Mean and standard deviation of live load intensity levels for all floors, other than basement and ground floor, as a function of bay area /33/

Id. No.	\bar{T}_{\max} (°C)	$\sigma_{T_{\max}}$ (°C)	\bar{R} (L_e)	σ_R (L_e)	\bar{S} (L_e)	σ_S (L_e)	θ	β_{ER}	β_C	P_f $\cdot 10^4$	$\phi(-\beta_{ER})$ $\cdot 10^4$	$\phi(-\beta_C)$ $\cdot 10^4$
1131110	167	88	1.185	0.163	0.276	0.089	4.30	4.15	4.89	0	0.2	0.005
1131120	167	88	1.185	0.163	0.407	0.068	2.91	4.93	4.41	0	0.004	0.05
1131130	167	88	1.185	0.163	0.537	0.061	2.21	4.43	3.72	0	0.05	1.0
2131110	250	105	1.140	0.175	0.276	0.089	4.12	3.97	4.43	6	0.3	0.05
2131120	250	105	1.140	0.175	0.407	0.068	2.80	4.54	3.90	10	0.03	0.5
2131130	250	105	1.140	0.175	0.537	0.061	2.12	3.96	3.25	24	0.4	6
3131110	360	116	1.054	0.207	0.276	0.089	3.81	3.55	3.45	56	2	3
3131120	360	116	1.054	0.207	0.407	0.068	2.59	3.69	2.96	84	1	15
3131130	360	116	1.054	0.207	0.537	0.061	1.96	2.98	2.40	182	14	82
4131110	461	130	0.922	0.268	0.276	0.089	3.33	2.78	2.29	306	27	110
4131120	461	130	0.922	0.268	0.407	0.068	2.27	2.44	1.86	514	73	310
4131130	461	130	0.922	0.268	0.537	0.061	1.71	1.74	1.40	886	410	810
5131110	601	127	0.659	0.319	0.276	0.089	2.39	1.49	1.16	1458	680	1230
5131120	601	127	0.659	0.319	0.407	0.068	1.62	0.94	0.77	2408	1740	2210
5131130	601	127	0.659	0.319	0.537	0.061	1.22	0.41	0.38	3510	3410	3520

Table 4.3a Stochastically important quantities derived in a Monte Carlo simulation game of 5000 plays $A\sqrt{h}/A_t = 0.04 \text{ m}^{1/2}$

Id. No.	\bar{T}_{\max} ($^{\circ}\text{C}$)	$\sigma_{T_{\max}}$ ($^{\circ}\text{C}$)	\bar{R} (L_e)	σ_R (L_e)	\bar{S} (L_e)	σ_S (L_e)	θ	β_{HR}	β_C	P_F $\cdot 10^4$	$\phi(-\beta_{\text{HR}})$ $\cdot 10^4$	$\phi(-\beta_C)$ $\cdot 10^4$
123110	118	73	1.205	0.160	0.276	0.089	4.37	4.22	5.07	0	0.06	0.002
123120	118	73	1.205	0.160	0.407	0.068	2.96	5.08	4.59	0	0.002	0.02
123130	118	73	1.205	0.160	0.537	0.061	2.25	4.64	3.90	0	0.02	0.5
223110	175	90	1.181	0.164	0.276	0.089	4.27	4.14	4.85	0	0.2	0.006
223120	175	90	1.181	0.164	0.407	0.068	2.90	4.90	4.36	0	0.005	0.06
223130	175	90	1.181	0.164	0.537	0.061	2.20	4.41	3.68	0	0.05	1
323110	256	108	1.135	0.177	0.276	0.089	4.10	3.95	4.34	4	0.4	0.07
323120	256	108	1.135	0.177	0.407	0.068	2.79	4.49	3.84	14	0.03	0.6
323130	256	108	1.135	0.177	0.537	0.061	2.12	3.89	3.19	28	0.5	7
423110	351	129	1.055	0.218	0.276	0.089	3.81	3.50	3.31	88	2	5
423120	351	129	1.055	0.218	0.407	0.068	2.59	3.58	2.84	128	2	23
423130	351	129	1.055	0.218	0.537	0.061	1.97	2.87	2.28	254	21	113
523110	493	151	0.862	0.306	0.276	0.089	3.11	2.37	1.84	580	89	329
523120	493	151	0.862	0.306	0.407	0.068	2.12	1.91	1.45	984	281	735
523130	493	151	0.862	0.306	0.537	0.061	1.60	1.27	1.04	1524	1020	1492

Table 4.3b Stochastically important quantities derived in a Monte Carlo simulation game of 5000 plays $\sqrt{h}/A_t = 0.08 \text{ m}^{1/2}$

Id. No.	\bar{T}_{\max} (°C)	$\sigma_{T_{\max}}$ (L _e)	\bar{R} (L _e)	σ_R (L _e)	\bar{S} (L _e)	σ_S (L _e)	θ	β_{ER}	β_C	P_F .10 ⁴	$\Phi(-\beta_{\text{ER}})$.10 ⁴	$\Phi(-\beta_C)$.10 ⁴
133110	92	64	1.214	0.159	0.276	0.089	4.40	4.24	5.15	0	0.1	0.002
133120	92	64	1.214	0.159	0.407	0.068	2.98	5.14	4.67	0	0.002	0.01
133130	92	64	1.214	0.159	0.537	0.061	2.26	4.71	3.98	0	0.01	0.4
233110	129	79	1.201	0.161	0.276	0.089	4.34	4.21	5.03	0	0.1	0.003
233120	129	79	1.201	0.161	0.407	0.068	2.95	5.05	4.54	0	0.003	0.03
233130	129	79	1.201	0.161	0.537	0.061	2.24	4.59	3.86	0	0.02	0.6
333110	193	99	1.172	0.167	0.276	0.089	4.23	4.10	4.73	0	0.2	0.01
333120	193	99	1.172	0.167	0.407	0.068	2.88	4.81	4.24	0	0.007	0.1
333130	193	99	1.172	0.167	0.537	0.061	2.18	4.29	3.57	6	0.09	2
433110	273	122	1.119	0.192	0.276	0.089	4.04	3.84	3.98	26	0.6	0.4
433120	273	122	1.119	0.192	0.407	0.068	2.75	4.22	3.50	48	0.1	2
433130	273	122	1.119	0.192	0.537	0.061	2.09	3.58	2.89	84	2	19
533110	369	148	1.024	0.256	0.276	0.089	3.70	3.21	2.76	224	7	29
533120	369	148	1.024	0.256	0.407	0.068	2.52	3.07	2.33	360	11	99
533130	369	148	1.024	0.256	0.537	0.061	1.91	2.36	1.85	510	91	322

Table 4.3c Stochastically important quantities derived in a Monte Carlo simulation game of 5000 plays $\Delta h/A_t = 0.12 \text{ m}^{1/2}$

κ_n (W/m ³ °C)	C_o °C	C_T °C·m ² /MJ	$C_{\Delta\kappa}$ m ⁵ /(MJ·W)
1160	100	1.55	0.000905
2320	100	2.39	0.000823
4640	100	3.96	0.000411

Table 5.1a Values of C_o , C_T and $C_{\Delta\kappa}$ used in the approximate Taylor series expansion analysis for different nominal values of the insulation parameter κ_n . See Eq 5.1b. $A\sqrt{h}/A_t = 0.08$ m

	Nominal value of κ (W/m ³ °C)					
	1160		2320		4640	
	Taylor expansion	Simulated	Taylor expansion	Simulated	Taylor expansion	Simulated
\bar{T} (°C)	267	256	363	351	542	493
σ_T (°C)	97	108	131	129	181	151
\bar{R} (L _e)	1.10	1.14	1.03	1.06	0.839	0.862
σ_R (L _e)	0.182	0.177	0.215	0.218	0.356	0.306
\bar{S} (L _e)	0.418	0.407	0.418	0.407	0.418	0.407
σ_S (L _e)	0.068	0.068	0.068	0.068	0.068	0.068
β_C	3.53	3.84	2.73	2.84	1.16	1.45
β_{ER}	4.19	4.49	3.43	3.58	1.54	1.91

Table 5.1b Statistically important parameters for the reliability analysis of fire-exposed steel beam derived by using Monte Carlo simulation technique and by using a Taylor series expansion, truncated after the linear terms.

$$A\sqrt{h}/A_t = 0.08 \text{ m}^{1/2} \text{ and } D_n/L_n = 1$$

Variability in load-carrying capacity R due to	per cent of total variance
stochastic character of fire load density	36
uncertainty in insulation material properties	10
uncertainty in theory transforming fire load density into maximum steel temperature (theory of compartment fires and theory of heat transfer burning environment - structural steel component)	10
difference between laboratory test and an actual complete process of fire	2
uncertainty in yield strength of steel at room temperature	12
uncertainty in the deformation analysis giving the design capacity φ_n	11
difference between the impact of fire on R in laboratory test and under service conditions	19

Table 5.2a Decomposition of the total variance of load-carrying capacity into a sum of component variances for $\kappa_n = 3380 \text{ W/m}^3 \text{ } ^\circ\text{C}$

D_n/L_n =	$A\sqrt{h}/A_t =$					
	0.04 m ^{1/2}		0.08 m ^{1/2}		0.12 m ^{1/2}	
	$q_n =$		$q_n =$		$q_n =$	
	$q_{n,0}$	$q_{n,1}$	$q_{n,0}$	$q_{n,1}$	$q_{n,0}$	$q_{n,1}$
1/3	2.56	3.36	2.56	3.44	2.84	3.55
1	2.10	2.88	2.16	2.96	2.42	3.04
3	1.66	2.37	1.64	2.37	1.92	2.52

Table 6.1a Safety index β_C in the differentiated Swedish design model as a function of ratio D_n/L_n , opening factor $A\sqrt{h}/A_t$ and different values of nominal or design fire load density q_n

$q_{n,0}$ = as of now authorized value of $q_n = 138,2$ MJ/m² (Eq 1.5.1b)

$q_{n,1}$ = previously valid value of $q_n = 193.0$ MJ/m² (Eq 6.1a)

Fire endurance rating (min)	30	60	90	120
Required value of κ_{st} , (W/m ³ °C)	4080	1415	785	550
Range of variation in β_C	0.52-2.66	1.77-3.69	2.34-3.89	2.58-3.96

Table 6.2a Required value of insulation parameter κ_{st} and range of variation for safety index β_C implied in different fire endurance ratings according to the standard test

D_n/L_n	Value of β_C	
	Present	Exemplified
1/3	2.56	2.40
1	2.16	2.35
3	1.64	2.45

Table 7.1a Comparison of β_C -values obtained by using present nominal loads and load factors and obtained in a load factor design method with these values derived in a statistically consistent way

Notation

Main symbols used in this paper

A	=	area of vertical opening in fire compartment
A_f	=	fuel surface area
A_i	=	fire exposed surface area of steel member
A_t	=	total bounding surface area of fire compartment (walls, floor and ceiling)
$A\sqrt{h}$	=	air flow factor (ventilation factor)
$A\sqrt{h}/A_t$	=	opening factor
c.o.v.	=	coefficient of variation
D	=	dead load
D_n	=	nominal value of dead load intensity in non-fire structural design
$D_{n,f}$	=	nominal value of dead load intensity in fire structural design
d_i	=	thickness of steel member
d_u	=	uniformly distributed pseudo-random number
E	=	load effect prediction error factor
F	=	probability distribution function (= cumulative distribution function)
F_y	=	yield stress of steel at 20°C
f	=	probability density function (frequency distribution function), deflection of fire exposed steel beam
h	=	height of vertical opening in fire compartment
I_C	=	heat energy released per unit time during combustion

I_L	=	heat energy withdrawn per unit time from the compartment owing to the replacement of hot gases by cold air
I_R	=	heat energy withdrawn per unit time from the compartment by radiation through openings in the enclosed space
I_W	=	heat energy withdrawn per unit time from the compartment through wall, roof or ceiling, and floor structures
k_f	=	non-dimensional factor, describing influence of thermal properties of walls, floor and ceiling on computed gastemperature-time curves
L	=	live load intensity
L_e	=	uniformly distributed load level of a simply supported steel beam = $8 W Fy/l^2$, i.e. the elastic limit load
L_n	=	nominal value of live load intensity in non-fire structural design
$L_{n,f}$	=	nominal value of live load intensity in fire structural design
l	=	length of beam
M	=	material uncertainty factor
N	=	number of simulations, "plays" in each "game"
P_f	=	probability of failure
q	=	fire load density
R	=	resistance or load bearing capacity
S	=	load effect
T	=	steel temperature
T_n	=	nominal (design) value of maximal steel temperature
T_{max}	=	final value of maximum steel temperature
U	=	standardized safety margin

V	=	coefficient of variation (c.o.v.)
Var	=	variance
V_s	=	steel volume of structural member
W	=	heat value of fuel, elastic section modulus
Z	=	standardized safety factor
α	=	heat transfer coefficient, linearization factor
β_C	=	safety index according to Cornell
β_{ER}	=	safety index according to Esteva-Rosenblueth
γ_O	=	overall safety factor in allowable stress design
γ_D	=	load factor for dead load intensity in non-fire structural design
$\gamma_{D,f}$	=	factor corresponding to γ_D in structural fire design
Δq	=	uncertainty factor for fire load statistics
ΔT_1	=	uncertainty term defined by Eq. 3.2a
ΔT_2	=	uncertainty term defined by Eq. 3.2a
ΔT_3	=	uncertainty term defined by Eq. 3.2a
$\Delta \varphi_1$	=	uncertainty term defined by Eq. 3.3a
$\Delta \varphi_2$	=	uncertainty term defined by Eq. 3.3a
$\gamma_L, \gamma_{L,f}$	=	load factors for live load intensity
θ	=	central safety factor
κ	=	insulation parameter $(A_i/V_s \cdot \lambda_i/d_i)$, see Eq. 1.3c
σ	=	standard deviation
Φ	=	cumulative probability function of a standard normal variate

φ = resistance or load-carrying capacity of fire-exposed steel beam, defined by Figure 1.4a

ϕ = strength factor (capacity reduction factor)

Subscripts

d = design

f = fire

n = nominal

Superscript

\bar{D} = mean value of dead load, etc.

REFERENCES

- /1/ Magnusson, S.E., Probabilistic Analysis of Fire Safety. ASCE-IABSE International Conference on Planning and Design of Tall Buildings, Lehigh University Pa., August 21-26, 1972. Discussion No 3, Technical Committee 10
- /2/ Magnusson, S.E., Probabilistic Analysis of Structural Fire Safety. ASCE National Structural Engineering Meeting, San Fransisco, California, April 9-13, 1973
- /3/ Pettersson, O., Principles of Fire Engineering Design and Fire Safety of Tall Buildings. ASCE-IABSE International Conference on Planning and Design of Tall Buildings, Lehigh University, Pa., August 21-26, 1972, Summary Report of Technical Committee 8. - Slightly modified and published as Bulletin 31, Division of Structural Mechanics and Concrete Construction, Lund Institute of Technology, Lund, 1973
- /4/ Twilt, L. - Witteveen, J., Principles of Fire Engineering Design, Chapter 1, Fire Safety in Constructional Steelwork, Research Study, issued by Committee 3 of European Convention for Constructional Steelwork, October 1974
- /5/ Magnusson, S.E. - Pettersson, O. - Thor, J., Brandteknisk dimensionering av stålkonstruktioner (Fire Engineering Design of Steel Structures). Manual, issued by the Swedish Institute of Steel Construction, Stockholm, 1974. See also /28/
- /6/ Butcher, E.G. et al., The Temperature Attained by Steel in Building Fires, Fire Research Technical Paper No. 15, H.M. Stationary Office, London, 1966
- /7/ Pettersson, O., The Connection between a Real Fire Exposure and the Heating Conditions According to Standard Fire Resistance Tests, with Special Application to Steel Structures. Chapter 2, Fire Safety in Constructional Steelwork, Research Study, issued by Committee 3 of European Convention for Constructional Steelwork, October 1974

- /8/ Thomas, P.H. - Heselden, A.J.M. - Law, M., Fully Developed Compartment Fires - Two Kinds of Behaviour. Fire Research Station, Borehamwood, Herts, Technical Paper No. 18, 1967
- /9/ Magnusson, S.E., Thelandersson, S., Comments on Rate of Gas Flow and Rate of Burning for Fires in Enclosures. Bulletin No. 19, Division of Structural Mechanics and Concrete Construction, Lund Institute of Technology, Lund, 1971
- /10/ Harmathy, T.Z., A New Look at Compartment Fires. Fire Technology, Vol. 8, No. 3, August 1972, and No. 4, November 1972
- /11/ Magnusson, S.E. - Thelandersson, S., A Discussion of Compartment Fires. Fire Technology, Vol.10, No. 3, August 1974
- /12/ Batanero, J., Theme Report, ASCE-IABSE International Conference on Planning and Design of Tall Buildings, Technical Committee No. 19, Conference Preprints, Volume II-19, 1972
- /13/ Thor, J., Deformations and Critical Loads of Steel Beams under Fire Exposure Conditions. National Swedish Building Research, Document D16:1973, Stockholm
- /14/ Berggren, K. - Eriksson, V., Fire loads in Offices (Brandbelastning i kontorshus), Examination Work in Building Technics, Royal Institute of Technology, Stockholm, 1969
- /15/ Pettersson, O., Structural Fire Engineering Research Today and Tomorrow. Acta Polytechnica Scandinavica, Ci 33, Stockholm, 1965
- /16/ Esteva, L., ASCE-IABSE International Conference on Planning and Design of Tall Buildings, Summary Report, Technical Committee No. 10, Conference Preprints, Volume A, 1972, pp 181-204
- /17/ Structural Safety - A Literature Survey. Journal of the Structural Division, ASCE Vol. 98, No. ST4, April 1972
- /18/ Sentler, L. - Åkerlund, S. - Östlund, L., Några studier av säkerhetssystem (A Study of Safety Systems). Department of Structural Engineering, Lund Institute of Technology, 1973

- /19/ Ang, A. H.-S., Structural Risk Analysis and Reliability-Based Design. Journal of the Structural Division, ASCE, Vol. 99, No. ST9, September 1973
- /20/ Cornell, C.A., A Probability-Based Structural Code. ACI Journal, Proceedings Vol. 66, No. 12, December 1969
- /21/ Rosenblueth, E. - Esteva, L., Use of Reliability Theory in Building Codes, Conference on Application of Statistics and Probability to Soil and Structural Engineering, Hong Kong, September 1971
- /22/ Ditlevsen, O., Structural Reliability and the Invariance Problem, University of Waterloo, Solid Mechanics Division, Report No. 27, March 1973
- /23/ Hasofer, A.M. - Lind, N.C., Exact and Invariant Second Moment Code Format. Journal of the Engineering Mechanics Division, ASCE, Vol. 100, No. EM1, February 1974
- /24/ Lind, N.C., Consistent Partial Safety Factors. Journal of the Structural Division, ASCE, Vol. 97, No. ST6, June 1971
- /25/ Turkstra, C.J. - Shah, H.C., Assessing and Reporting Uncertainties, ASCE-IABSE International Conference on Planning and Design of Tall Buildings, Lehigh University, Pa., August 21-26, 1972. SOA-Report No. 1, Technical Committee No. 10, Conference Preprints: Reports Vol. 1b-10
- /26/ Ravindra, M.K. - Lind, N.C. - Siu, W., Illustrations of Reliability-Based Design, Modern Concepts of Structural Safety and Design. Journal of the Structural Division, ASCE, Vol. 100, No. ST9, September 1974
- /27/ Ravindra, M.K. - Heaney, A.C. - Lind, N.C., Probabilistic Evaluation of Safety Factors, IABSE Symposium on Concepts of Safety of Structures and Methods of Design, London 1969
- /28/ Magnusson, S.E. - Pettersson, O. - Thor, J., A Differentiated Design of Fire Exposed Steel Structures, Bulletin No. 44, Division of Structural Mechanics and Concrete Construction, Lund Institute of Technology, Lund, 1974

- /29/ Law, M., Analysis of Some Results of Experimental Fires. Paper 3, Symposium No. 2, Behaviour of Structural Steel in Fire, Boreham Wood, Herts., 24 January, 1967
- /30/ Bletzacker, R.W., Effect of Structural Restraint on the Fire Resistance of Protected Steel Beam Floor and Roof Assemblies, Building Research Laboratory, Final Report EES 246/266. Engineering Experiment Station, Ohio State University, Columbus, Ohio, September 1966
- /31/ Arnault, P. - Ehm, H. - Kruppa, J., Resistance au Feu des Poutres Isostatiques en Acier. Doc. CECM 3 - 74/2 F. Mars 1974
- /32/ Galambos, T.V. - Ravindra, M.K., Load Factor Design for Combination of Loads. Preprint 1940, ASCE National Structural Engineering Meeting, April 9-13, 1973, San Fransisco, California
- /33/ Mitchell, G.R. - Woodgate, R.W., A Survey of Floor Loadings in Office Buildings, Report 25, Construction Industry Research and Information Association, London, 1970
- /34/ Benjamin, J.R. - Cornell, C.A., Probability, Statistics and Decision for Civil Engineers, Mc Graw-Hill, 1970
- /35/ Baldwin, R. - Thomas, P.H., Passive and Active Fire Protection - The Optimum Combination. Fire Technology, Vol. 10, No. 2, May 1974
- /36/ Tall, L. - Alpsten, G.A., On the Scatter in Yield Strength and Residual Stresses in Steel Members. Vol. 4, IABSE Symposium on the Concepts of Safety of Structures and Methods of Design, London 1969
- /37/ Evans, D.J., Software for Numerical Mathematics, Academic Press, London and New York, 1974
- /38/ Nilsson, L., Experimental and Theoretical Investigations on Compartment Fires, Bulletin No. 37, Division of Structural Mechanics and Concrete Construction, Lund Institute of Technology, Lund 1974

- /39/ Bryl, S., Fire Loads in Office Buildings, Chapter III, Fire Safety in Constructional Steelwork, Research Study, issued by Committee 3 of European Convention for Constructional Steelwork, October 1974
- /40/ Magnusson, S.E. - Thelandersson, S., Temperature-Time Curves of Complete Process of Fire Development. Acta Polytechnica Scandinavica, Civil Engineering and Building Construction, Series No. 65, Stockholm 1970

